

**The Model Builder: A Multi-Fidelity Structural Modeling Tool for Seismic Hazard  
Analysis**

by

**Amedeo Thomas Hirata**

Bachelor of Science in Civil Engineering, University of Pittsburgh, 2018

Submitted to the Graduate Faculty of the  
Swanson School of Engineering in partial fulfillment  
of the requirements for the degree of  
Master of Science in Civil Engineering

University of Pittsburgh

2019

UNIVERSITY OF PITTSBURGH

SWANSON SCHOOL OF ENGINEERING

This thesis was presented

by

**Amedeo Thomas Hirata**

It was defended on

November 15, 2019

and approved by

Dr. Lev Khazanovich Ph.D, Professor, Department of Civil and Environmental Engineering

Dr. John Oyler Ph.D, Associate Professor, Department of Civil and Environmental Engineering

Thesis Advisor: Dr. Max Stephens Ph.D, Assistant Professor, Department of Civil and  
Environmental Engineering

Copyright © by Amedeo T. Hirata

2019

# **The Model Builder: A Model Generation Tool for Rapid Earthquake Analysis**

Amedeo Thomas Hirata, MS

University of Pittsburgh, 2019

Earthquakes affect millions of people across the earth. Earthquakes cause billions of dollars of damage and hundreds of thousands of deaths per year [1]. For these reasons that seismic resilience is a field of immense concern for government, stakeholders and researchers. As the field of earthquake engineering has advanced, higher levels of analysis have been developed, both in terms of fidelity and complexity, capable of capturing complex non-linear structural response. However, regional assessment frameworks, which estimate structural performance at regional scale, do not commonly use building-level structural modeling to capture structural response. Many of these frameworks instead use a fragility-based approach where seismic intensity measures (such as peak ground acceleration) are related to probabilistic levels of damage. The fragility functions used in this approach are based on the response of structural archetypes such as a steel moment frames or concrete shear walls. Thus, the response and damage estimations generated using these methodologies are not that of the actual structure in question, but rather that of an archetypical representation of the structure. While this approach can roughly predict the dominant characteristics of vulnerable structures subjected to seismic hazards, it is difficult to pinpoint critical deficiencies for immediate retrofit or evacuation and inspection.

The objective of this research is to develop a framework to provide building-specific nonlinear response predictions within regional structural simulation. First, existing regional response prediction frameworks for natural disasters and structural analysis are introduced. Next, the opensource finite element analysis software OpenSeesPy is introduced along with the multi-

fidelity *Model Builder* tool capable of rapidly developing building-level structural models using the software. This software uses the OpenSEES framework to create the models, apply ground motions, and assess levels of damage of the structural system. The Model Builder was then validated using several recorded structural response histories. Based on the findings here, the Model Builder can be applied to develop models for regional response simulation.

# Table of Contents

<b>Preface.....</b>	<b>xv</b>
<b>1.0 Introduction.....</b>	<b>1</b>
<b>1.1 Research Motivation .....</b>	<b>1</b>
<b>1.2 Research Objectives .....</b>	<b>2</b>
<b>1.3 Document Overview .....</b>	<b>2</b>
<b>2.0 The State of Practice on Earthquake Engineering and Analysis .....</b>	<b>4</b>
<b>2.1 HAZUS: Estimating Potential Losses from Disasters.....</b>	<b>4</b>
<b>2.1.1 The HAZUS Model Structure .....</b>	<b>7</b>
<b>2.1.2 HAZUS Analysis Methodologies: Basic and Advanced.....</b>	<b>10</b>
<b>2.1.3 HAZUS New Madrid Seismic Zone Catastrophic Case Study .....</b>	<b>13</b>
<b>2.2 PAGER: Prompt Assessment of Global Earthquakes for Response .....</b>	<b>15</b>
<b>2.2.1 PAGER Analysis Process .....</b>	<b>16</b>
<b>2.3 HAZ-Taiwan and the Taiwan Earthquake Loss Estimation System .....</b>	<b>17</b>
<b>2.4 RiskScape New Zealand.....</b>	<b>20</b>
<b>2.5 OpenSEES: The Open System for Earthquake Engineering Simulation .....</b>	<b>23</b>
<b>2.5.1 The OpenSEES Framework.....</b>	<b>24</b>
<b>2.5.2 The OpenSEES Finite Element Analysis Solution Procedure .....</b>	<b>25</b>
<b>2.5.3 OpenSEES Finite Element Analysis Validation Studies .....</b>	<b>27</b>
<b>2.5.4 Opensees Force-Based Element Formulations .....</b>	<b>30</b>
<b>3.0 The Model Builder: Multi Fidelity Modeling.....</b>	<b>32</b>
<b>3.1 Components of the Model Builder .....</b>	<b>33</b>

3.1.1	Ground Motion Library .....	33
3.1.2	Building Information Database .....	34
3.1.3	Python Code.....	35
3.1.4	Outputs.....	36
3.2	SDOF Modal/Maximum Spectral Acceleration Response Evaluation .....	36
3.2.1	Estimation of Fundamental Period.....	37
3.2.2	Creation of the Design Spectrum.....	37
3.3	MDOF Response History Evaluation .....	38
3.3.1	Information Transfer from the Building Database to the Model Builder ...	39
3.3.2	Model Types.....	40
3.3.2.1	Material Models .....	41
3.3.2.2	Elastic Modeling.....	42
3.3.2.3	Lumped Plasticity Modeling .....	43
3.3.2.4	Distributed Plasticity Modeling .....	45
3.3.3	Application of Mass and Gravity Loads .....	45
3.3.4	The Leaning Column .....	46
3.3.5	Gravity and Earthquake Analysis .....	47
4.0	Model Builder Validation Studies .....	48
4.1	The Wellington Building.....	48
4.1.1	Model Generation of the Wellington Building .....	49
4.1.2	Comparison of Recorded and Simulated Response History .....	51
4.2	The Van Nuys Holiday Inn .....	54
4.2.1	Model Generation of the Van Nuys Holiday Inn.....	55

4.2.2 Recorded versus Simulated Response History North / South Frame .....	55
4.2.3 Recorded versus Simulated Response History East / West Frame .....	58
4.2.4 Comparison Response History Between Frames in Both Directions .....	60
4.3 The E-Defense Building .....	61
4.3.1 Model Generation of the E-Defense Building .....	62
4.3.2 Comparison of Recorded and Simulated Response History .....	62
4.3.2.1 Kobe 25% Scaled Ground Motion .....	62
4.3.2.2 Kobe 50% Scaled Ground Motion .....	65
4.3.2.3 Kobe 100% Scaled Ground Motion .....	67
4.4 Results of the Validation Tests .....	69
5.0 Batch Analysis Time Study .....	70
5.1 Creation of the Building Index .....	71
5.2 Ground Motion Determination .....	71
5.3 Time Required for Analysis .....	72
5.4 Damage State Characterization .....	73
5.5 Methodologies for Real World Application and Optimization .....	76
6.0 Parametric Sensitivity Study .....	77
6.1 Mass and Load .....	78
6.2 Accounting for Miscellaneous Dead Loads .....	80
6.3 Leaning Column Loads .....	81
6.4 Cross Sections .....	83
6.5 Material Properties .....	85
7.0 Summary, Conclusions and Future Work .....	87

<b>Appendix A Model Builder Outputs for the Wellington Building .....</b>	<b>90</b>
<b>Appendix B Model Builder Outputs for the Van Nuys Holiday Inn.....</b>	<b>93</b>
<b>Appendix C Model Builder Outputs for the E-Defense Structure.....</b>	<b>99</b>
<b>Bibliography .....</b>	<b>108</b>

## List of Tables

<b>Table 1. Building Structure (Model Building) Types .....</b>	<b>8</b>
<b>Table 2 A Summary of Buildings used in the Time Study.....</b>	<b>70</b>
<b>Table 3. Analysis Times By Ground Motion .....</b>	<b>73</b>
<b>Table 4 Damage States Related to Maximum Story Drift.....</b>	<b>74</b>
<b>Table 5 Miscellaneous Dead Loads Incorporated.....</b>	<b>80</b>

## List of Figures

<b>Figure 1 Hazus Commercial Damage Output of the Golden Guardian 06 Project. [4]</b> .....	<b>6</b>
<b>Figure 2. A Standard Building Capacity Curve</b> .....	<b>11</b>
<b>Figure 3. Standardized Design Response Spectrum Shape</b> .....	<b>12</b>
<b>Figure 4. Hazus Damage Estimation Methodology.</b> .....	<b>13</b>
<b>Figure 5 Visualizing the PAGER analysis process [9]</b> .....	<b>15</b>
<b>Figure 6 The HAZ-Taiwan Methodology [13].</b> .....	<b>18</b>
<b>Figure 7 The Riskscape Framework [14]</b> .....	<b>22</b>
<b>Figure 8 The Main Abstractions in the OpenSEES Framework [19]</b> .....	<b>25</b>
<b>Figure 9 Classes within the OpenSEES framework [17]</b> .....	<b>26</b>
<b>Figure 10 Hysteretic Behavior of a Column Modeled Using OpenSEES [20]</b> .....	<b>28</b>
<b>Figure 11 Hysteretic Behavior of Bridge Columns Modeled with OpenSEES [21]</b> .....	<b>29</b>
<b>Figure 12 The Displacement-Based Element Solution Methodology.</b> .....	<b>30</b>
<b>Figure 13 The Force-Based Element Solution Methodology.</b> .....	<b>31</b>
<b>Figure 14. System Breakdown of The Model Builder.</b> .....	<b>33</b>
<b>Figure 15 Parameters Required for SDOF Analysis.</b> .....	<b>34</b>
<b>Figure 16 Information Required for the Model Builder.</b> .....	<b>34</b>
<b>Figure 17 The ASCE 7-10 Design Response Spectrum [26]</b> .....	<b>38</b>
<b>Figure 18 Model Structure Overview.</b> .....	<b>40</b>
<b>Figure 19 Concrete01 Example Material Model [24].</b> .....	<b>41</b>
<b>Figure 20 The Steel02 material model [25]</b> .....	<b>42</b>
<b>Figure 21 Elastic Model Versus Lumped Plasticity Model with Rigid Offset</b> .....	<b>44</b>

<b>Figure 22 The Leaning Column Methodology. ....</b>	<b>46</b>
<b>Figure 23 Elevation view of Sensor Locations within the Wellington Building [35]. ....</b>	<b>49</b>
<b>Figure 24 Elevation View of the Wellington Building Frame [35]. ....</b>	<b>50</b>
<b>Figure 25 Elastic Response History of the Wellington Building.....</b>	<b>51</b>
<b>Figure 26 Plasticity Model Response History of the Wellington Building. ....</b>	<b>53</b>
<b>Figure 27 Layout and Location of Accelerometers in the Van Nuys Holiday Inn.....</b>	<b>54</b>
<b>Figure 28 Elastic Response History of the N/S Van Nuys Holiday Inn.....</b>	<b>56</b>
<b>Figure 29 Plasticity Response History of the N/S Van Nuys Holiday Inn. ....</b>	<b>57</b>
<b>Figure 30 Elastic Response History of the E/W Van Nuys Holiday Inn. ....</b>	<b>58</b>
<b>Figure 31 Plasticity Response History of the E/W Van Nuys Holiday Inn.....</b>	<b>59</b>
<b>Figure 32 The Layout of the Two E-Defense Buildings [37].....</b>	<b>61</b>
<b>Figure 33 Elastic Response History of the E-Defense Structure (Kobe 25%).....</b>	<b>63</b>
<b>Figure 34 Plasticity Response History of the E-Defense Structure (Kobe 25%). ....</b>	<b>64</b>
<b>Figure 35 Elastic Response History of the E-Defense Structure (Kobe 50%).....</b>	<b>65</b>
<b>Figure 36 Plasticity Response History of the E-Defense Structure (Kobe 50%) ....</b>	<b>66</b>
<b>Figure 37 Elastic Response History of the E-Defense Structure (Kobe 100%).....</b>	<b>67</b>
<b>Figure 38 Plasticity Response History of the E-Defense Structure (Kobe 100%). ....</b>	<b>68</b>
<b>Figure 39 Chi-Chi Taiwan FEMA P695 121042 Scaled Ground Motion. ....</b>	<b>72</b>
<b>Figure 40 Time Study Batch Analysis. Left to Right: Elastic, LP Fiber, DP Fiber.....</b>	<b>75</b>
<b>Figure 41 Van Nuys Parametric Study: Changing Floor Load by <math>\pm 25\%</math>. ....</b>	<b>79</b>
<b>Figure 42 Parametric Study: Incorporating Miscellaneous Dead Loads. ....</b>	<b>81</b>
<b>Figure 43 Parametric study: Placing Loads on the Leaning Column Versus Frame.....</b>	<b>82</b>
<b>Figure 44 Beam Cross Section Details for the Van Nuys Holiday Inn.....</b>	<b>83</b>

<b>Figure 45 Parametric Study: Using Non-Typical Cross Sections.....</b>	<b>84</b>
<b>Figure 46 Parametric Study: Using Projected Actual Material Properties. ....</b>	<b>86</b>
<b>Appendix Figure 1 Wellington Building Floor Displacements: Distributed Plasticity. ....</b>	<b>90</b>
<b>Appendix Figure 2 Wellington Building Story Drifts: Distributed Plasticity. ....</b>	<b>90</b>
<b>Appendix Figure 3 Wellington Building Floor Displacements: Lumped Plasticity. ....</b>	<b>91</b>
<b>Appendix Figure 4 Wellington Building Story Drifts: Lumped Plasticity. ....</b>	<b>91</b>
<b>Appendix Figure 5 Wellington Building Floor Displacements: Elastic. ....</b>	<b>92</b>
<b>Appendix Figure 6 Wellington Building Story Drifts: Elastic.....</b>	<b>92</b>
<b>Appendix Figure 7 Van Nuys E/W Floor Displacements: Distributed Plasticity. ....</b>	<b>93</b>
<b>Appendix Figure 8 Van Nuys E/W Story Drifts: Distributed Plasticity.....</b>	<b>93</b>
<b>Appendix Figure 9 Van Nuys E/W Floor Displacements: Lumped Plasticity. ....</b>	<b>94</b>
<b>Appendix Figure 10 Van Nuys E/W Story Drifts: Lumped Plasticity. ....</b>	<b>94</b>
<b>Appendix Figure 11 Van Nuys E/W Floor Displacements: Elastic. ....</b>	<b>95</b>
<b>Appendix Figure 12 Van Nuys E/W Story Drifts: Elastic.....</b>	<b>95</b>
<b>Appendix Figure 13 Van Nuys N/S Floor Displacements: Distributed Plasticity.....</b>	<b>96</b>
<b>Appendix Figure 14 Van Nuys N/S Story Drifts: Distributed Plasticity.....</b>	<b>96</b>
<b>Appendix Figure 15 Van Nuys N/S Floor Displacements: Lumped Plasticity.....</b>	<b>97</b>
<b>Appendix Figure 16 Van Nuys N/S Story Drifts: Lumped Plasticity.....</b>	<b>97</b>
<b>Appendix Figure 17 Van Nuys N/S Floor Displacements: Elastic.....</b>	<b>98</b>
<b>Appendix Figure 18 Van Nuys N/S Story Drifts: Elastic. ....</b>	<b>98</b>
<b>Appendix Figure 19 E-Defense Floor Displacements: Kobe 25% Distributed Plasticity. ...</b>	<b>99</b>
<b>Appendix Figure 20 E-Defense Story Drifts: Kobe 25% Distributed Plasticity. ....</b>	<b>99</b>
<b>Appendix Figure 21 E-Defense Floor Displacements: Kobe 25% Lumped Plasticity.....</b>	<b>100</b>

<b>Appendix Figure 22 E-Defense Story Drifts: Kobe 25% Lumped Plasticity. ....</b>	<b>100</b>
<b>Appendix Figure 23 E-Defense Floor Displacements: Kobe 25% Elastic. ....</b>	<b>101</b>
<b>Appendix Figure 24 E-Defense Story Drifts: Kobe 25% Elastic.....</b>	<b>101</b>
<b>Appendix Figure 25 E-Defense Floor Displacements: Kobe 50% Distributed Plasticity. .</b>	<b>102</b>
<b>Appendix Figure 26 E-Defense Story Drifts: Kobe 50% Distributed Plasticity. ....</b>	<b>102</b>
<b>Appendix Figure 27 E-Defense Floor Displacements: Kobe 50% Lumped Plasticity.....</b>	<b>103</b>
<b>Appendix Figure 28 E-Defense Story Drifts: Kobe 50% Lumped Plasticity. ....</b>	<b>103</b>
<b>Appendix Figure 29 E-Defense Floor Displacements: Kobe 50% Elastic. ....</b>	<b>104</b>
<b>Appendix Figure 30 E-Defense Story Drifts: Kobe 50% Elastic.....</b>	<b>104</b>
<b>Appendix Figure 31 E-Defense Floor Displacements: Kobe 100% Distributed Plasticity.</b>	<b>105</b>
<b>Appendix Figure 32 E-Defense Story Drifts: Kobe 100% Distributed Plasticity. ....</b>	<b>105</b>
<b>Appendix Figure 33 E-Defense Floor Displacements: Kobe 100% Lumped Plasticity.....</b>	<b>106</b>
<b>Appendix Figure 34 E-Defense Story Drifts: Kobe 100% Lumped Plasticity. ....</b>	<b>106</b>
<b>Appendix Figure 35 E-Defense Floor Displacements: Kobe 100% Elastic. ....</b>	<b>107</b>
<b>Appendix Figure 36 E-Defense Story Drifts: Kobe 100% Elastic.....</b>	<b>107</b>

## **Preface**

The author would like to acknowledge the work of Dr. Minjie Zhu, whose work in creating the OpenSEES Python conversion has been critical to the creation of the Model Builder tool. The author would also like to acknowledge the members of the committee to whom the author owes much of his knowledge and success as a future engineer. Finally, the author would like to acknowledge the Civil Engineering Department of the University of Pittsburgh to whom the author attributes their understanding and deep appreciation of the field of engineering.

## **1.0 Introduction**

### **1.1 Research Motivation**

Earthquakes affect millions of people across the earth, causing billions of dollars of damage and hundreds of thousands of deaths per year [1]. For these reasons, seismic resilience is a field of immense concern for governments, stakeholders and researchers. As the field of earthquake engineering has advanced, higher levels of analysis have been developed, both in terms of fidelity and complexity, which are capable of capturing complex non-linear structural response. However, regional assessment frameworks, which estimate structural performance at regional scale, do not commonly use building-level structural modeling to capture structural response. Many of these frameworks instead use a fragility-based approach where seismic intensity measures (such as peak ground acceleration) are related to probabilistic levels of damage. The fragility functions used in this approach are based on the response of structural archetypes such as a steel moment frames or concrete shear walls. Thus, the response and damage estimations generated using these methodologies are not that of the actual structure in question, but rather that of an archetypical representation of the structure. While this approach can roughly predict the dominant characteristics of vulnerable structures subjected to seismic hazards, it is difficult to pinpoint critical deficiencies for immediate retrofit or evacuation and inspection. Further, hidden and unexpected vulnerabilities, as was discovered in concrete moment frame structures in the 2016 Kaikoura earthquake [7], may not be captured or quantified. However, developing structural response models for structures at a regional scale is time-consuming and impractical.

## **1.2 Research Objectives**

The objective of this research is to overcome this deficiency by developing a framework to provide building-specific nonlinear response predictions within regional structural simulations. This framework is based on identifying and indexing key infrastructures so that models can be rapidly generated and analyzed after an earthquake occurs to aid in disaster relief efforts. The framework requires an end user to supply minimal information for each structure in order to create and analyze simplified structural systems which are used to estimate the response of actual structures.

## **1.3 Document Overview**

This thesis presents the development and validation of a numerical framework for rapid finite element model development and simulation which provides building-level response predictions for regional performance evaluation. The components of the research were as follows: (1) perform a comprehensive literature review...

Chapter 2 reviews existing regional frameworks and methodologies implemented for natural disasters and structural analysis, highlighting their capabilities and the levels of analysis they provide. This chapter also introduces the opensource structural analysis software OpenSEES, including the structure of the software and validation studies which have used experimental data to validate the various parameters such as the finite element procedure and material and element formulations.

Chapter 3 introduces, a multi-fidelity model generation tool capable of rapidly developing building-level structural models will be introduced. This software, named the *Model Builder*, uses the opensource framework OpenSEES to create the models, apply ground motions, and assess levels of damage of the structural system. The goal of the Model Builder is to provide a higher fidelity estimation of response than current methodologies without having to manually develop a detailed model. The framework of the Model Builder will be shown, breaking down each component of the system.

Chapter 4 compares numerical results generated using the model builder against recorded data in order to validate the results of the Model Builder. Chapter 6 introduces a time study that was performed to determine the applicability of the Model Builder as a post-event disaster relief tool. Chapter 7 presents a parametric study which was conducted to determine which factors most affect the results when building a structural model. Finally, Chapter 8 summarizes conclusions drawn from this work and recommends opportunities for future work and continued improvement of the framework.

## **2.0 The State of Practice on Earthquake Engineering and Analysis**

The current state of practice of earthquake engineering has seen a paradigm shift toward performance-based design. By targeting specific structural performance objectives, an engineer can design much more efficient structures. One important aspect of performance-based design is the ability to characterize structural damage and downtime following an event. Fragility functions and multi-fidelity numerical modeling are new tools that engineers can use to assess structural damage in the modern era. Despite this, there are currently no methods to apply high fidelity models at a regional scale. In this literature review, several of the most widely used frameworks such as FEMA's Hazus and Taiwan's TELES will be introduced and discussed to better understand the current state of earthquake engineering and analysis in terms of regional damage assessment.

### **2.1 HAZUS: Estimating Potential Losses from Disasters**

Hazus is a free tool that was developed by FEMA The Federal Emergency Management Agency (FEMA) that can model and estimate structural losses at a regional scale due to earthquakes, floods, and hurricanes. The Hazus framework has several features which allow end users to estimate losses.: Geographic Information Systems (GIS) technology for accurate geolocation, graphical illustration of identified high-risk areas, and spatial viewing of assets [2]. Hazus has applications in both pre-event damage mitigation as well as post-event recovery efforts. Government agencies, city officials, and emergency responders can use Hazus for scenario

planning, mitigation planning, and post-event assessment and recovery. Hazus quantifies loss in three ways [2]:

- Physical damage to residential and commercial buildings, schools, critical facilities, and infrastructure;
- Economic loss, including lost jobs, business interruptions, repair, and reconstruction costs;
- Social impacts, including estimates of shelter requirements, displaced households, and population exposed to scenario floods, earthquakes, and hurricanes, and tsunamis;

The Hazus earthquake model, as it specifically pertains to buildings and infrastructure, can be used to estimate damage and loss in buildings from both scenario and probabilistic earthquakes. The damage estimates include ground shaking and ground failure, damage to buildings, estimation of casualties, associated costs [3].

Hazus has been extensively used to simulate events and prepare post-event planning on a large scale. The “Golden Guardian ‘06” project was a live 36 hour exercise in which Hazus was used to simulate the San Francisco Bay Area being subjected to the 1906 San Francisco earthquake, the outputs of which can be seen in Figure 1. A Hazus simulation of the entire San Francisco bay region was performed including all counties within the region. The analysis yielded several key results following the 1906 event: over \$120 billion in building losses, 463,254 buildings damaged, 37,025 buildings deemed total losses, 60,000 to 120,000 persons requiring short-term shelter, and 3,332 deaths [4].

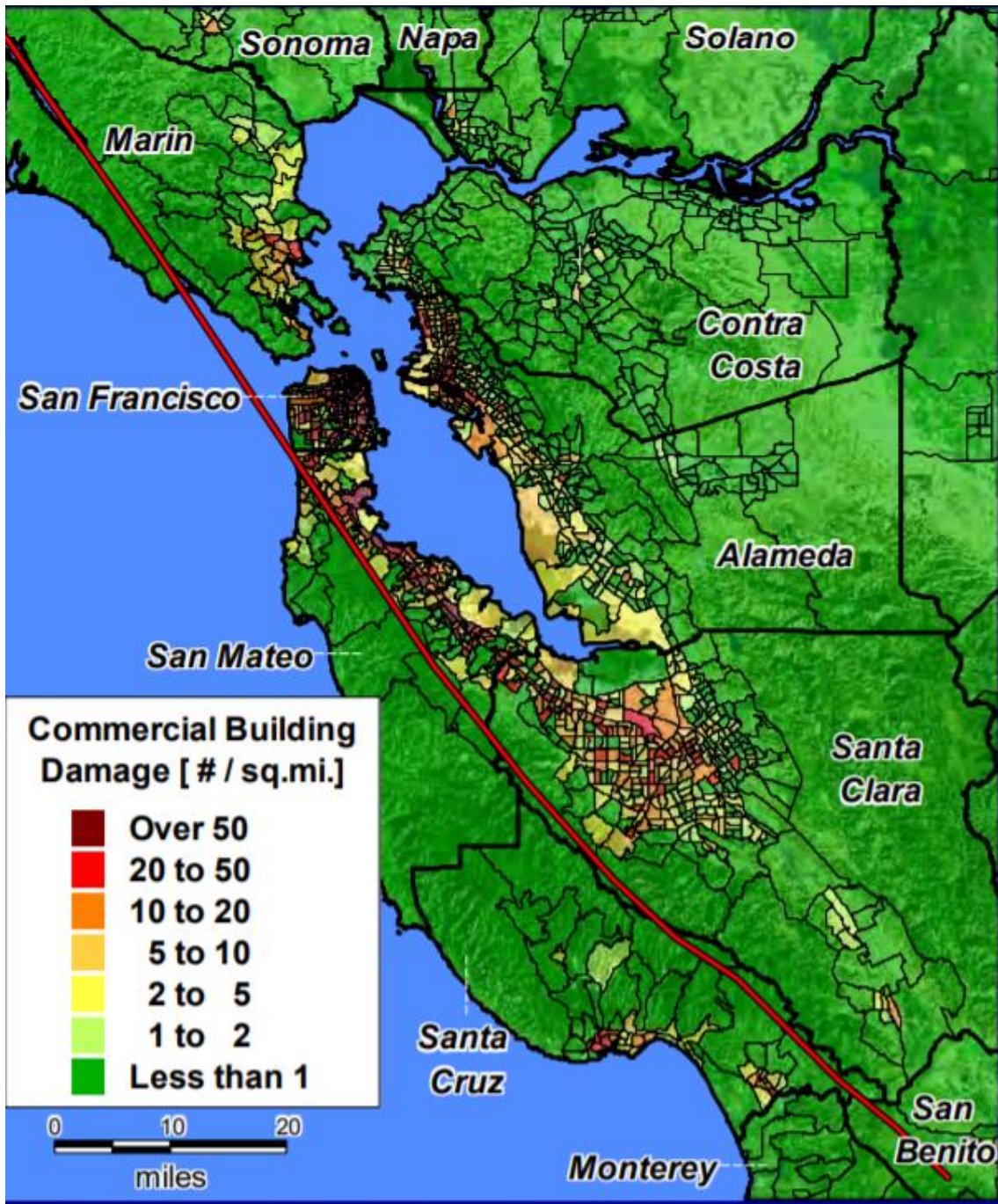


Figure 1 Hazus Commercial Damage Output of the Golden Guardian 06 Project. [4]

### **2.1.1 The HAZUS Model Structure**

Hazus is composed of six distinct and interdependent modules: potential earth science hazard, inventory and exposure data, direct damage, induced damage, direct losses, and indirect losses. The first module is the Potential Earth Science Hazard (PESH) module. This module estimates both ground motion (spectral acceleration, SA, and peak ground acceleration, PGA) as well as ground failure (landslides, liquefaction, and surface fault rupture). Ground motions are estimated based on geographic location, size, type of earthquake, and local geology [5].

The Inventory and Exposure Data (IED) module is a national-level database which includes information that can supplement a preliminary analysis where refined site-specific information may not yet be available. The database shown in Table 1 includes information on archetypical buildings classified by occupancy, and by model building type [6].

**Table 1. Building Structure (Model Building) Types**

No.	Label	Description	Height			
			Range		Typical	
			Names	Stories	Stories	Feet
1	W1	Wood/ Light Frame ( $\leq 5,000$ sq.ft)		1-2	1	14
2	W2	Wood, Commercial and Industrial (>5,000 sq. ft.)		All	2	24
3	S1L	Steel Moment Frame	Low-Rise	1-3	2	24
4	S1M		Mid-Rise	4-7	5	60
5	S1H		High-Rise	8+	13	156
6	S2L	Steel Braced Frame	Low-Rise	1-3	2	24
7	S2M		Mid-Rise	4-7	5	60
8	S2H		High-Rise	8+	13	156
9	S3	Steel Light Frame		All	1	15
10	S4L	Steel Frame with Cast-in-Place Concrete Shear Walls	Low-Rise	1-3	2	24
11	S4M		Mid-Rise	4-7	5	60
12	S4H		High-Rise	8+	13	156
13	S5L	Steel Frame with Unreinforced Masonry Infill Walls	Low-Rise	1-3	2	24
14	S5M		Mid-Rise	4-7	5	60
15	S5H		High-Rise	8+	13	156
16	C1L	Concrete Moment Frame	Low-Rise	1-3	2	20
17	C1M		Mid-Rise	4-7	5	50
18	C1H		High-Rise	8+	12	120
19	C2L	Concrete Shear Walls	Low-Rise	1-3	2	20
20	C2M		Mid-Rise	4-7	5	50
21	C2H		High-Rise	8+	12	120
22	C3L	Concrete Frame with Unreinforced Masonry Infill Walls	Low-Rise	1-3	2	20
23	C3M		Mid-Rise	4-7	5	50
24	C3H		High-Rise	8+	12	120
25	PC1	Precast Concrete Tilt-Up Walls		All	1	15
26	PC2L	Precast Concrete Frames with Concrete Shear Walls	Low-Rise	1-3	2	20
27	PC2M		Mid-Rise	4-7	5	50
28	PC2H		High-Rise	8+	12	120
29	RM1L	Reinforced Masonry Bearing Walls with Wood or Metal Deck Diaphragms	Low-Rise	1-3	2	20
30	RM1M		Mid-Rise	4+	5	50
			High-Rise			
31	RM2L	Reinforced Masonry Bearing Walls with Precast Concrete Diaphragms	Low-Rise	1-3	2	20
32	RM2M		Mid-Rise	4-7	5	50
33	RM2H		High-Rise	8+	12	120
34	URML	Unreinforced Masonry Bearing Walls	Low-Rise	1-2	1	15
35	URMM		Mid-Rise	3+	3	35
36	MH	Mobile Homes		All	1	10

The four building inventory groups are: general building stock, essential and high potential loss facilities, transportation systems, and utilities. To set up an accurate model, the infrastructure of the study area must be categorized with the standardized classification tables and accurate quantities determined following Hazus methodology [5].

The direct damage module estimates damage for each of the inventory groups based on several factors. The vulnerability and level of exposure of the structure determine the potential damage seen at various ground motion intensities. The potential structural damage is based on fragility curves in combination with site specific response spectra. Non-structural damage is not subject to the same methodology and is calculated separately based on drift and acceleration. Damage, defined in terms of probabilities of occurrence of specific damage states, is finally assigned based on a five-state methodology: none, slight, moderate, extensive, and complete [5].

Beyond immediate structural impacts, HAZUS incorporates models that can predict secondary effects such as social and economic. The induced damage module defines and estimates any damage which is considered a secondary consequence of the event. Damages that are tracked include: fire, debris, dam/levee inundation potential, and hazardous materials release [5].

The direct losses module estimates losses in terms of both economic and social impact. Economic losses are losses which pertain to the impact that damaged structures have on the economy: relocation costs, business inventory losses, capital-related losses, income losses, and rental losses. Any form of economic loss due to the loss or damage of a structure are accounted and estimated here. Social losses are characterized in terms of casualties, displaced households, and short-term shelters. Shelter needs are based on the number of structures that are uninhabitable [5].

The last module, indirect losses determines long-term effects on the study area's economy due to the earthquake losses. The results in this section include employment and income changes due to the previously stated losses [5].

### **2.1.2 HAZUS Analysis Methodologies: Basic and Advanced**

Hazus analyses come in two basic forms: basic and advanced. A basic analysis can be generated based on national databases incorporated into the Hazus software. This analysis type is used when site-specific information cannot be obtained or if site-specific information is lacking and needs to be supplemented. In a basic analysis, the default library of values is used in lieu of more site-specific information to generate estimates of damage. The advanced analysis allows for much more accurate loss estimates when site-specific information is included. Information that is required for an advanced analysis includes: local hazard conditions, accurate local inventories of buildings, essential facilities and other infrastructure, geological and hydrological map data, and GIS information [7].

The same methodology of analysis is performed in both forms. Based on the building type and general characteristics such as height, capacity and demand curves are generated. The capacity curve is a plot of a structure's lateral resistance as a function of lateral displacement. In order to compare it to the demand curve the plot is generated in terms of spectral acceleration and spectral displacement. Capacity curves as shown in Figure 2 are defined by three control points describing the modeled building capacity: the design capacity, yield capacity, and ultimate capacity. The design capacity represents the strength dictated by current seismic code provisions. The yield capacity represents the "true" strength of the structure by taking into consideration redundancies

in design, the conservative nature of design codes, and true material strengths. The ultimate capacity represents the structure in a fully plastic state.

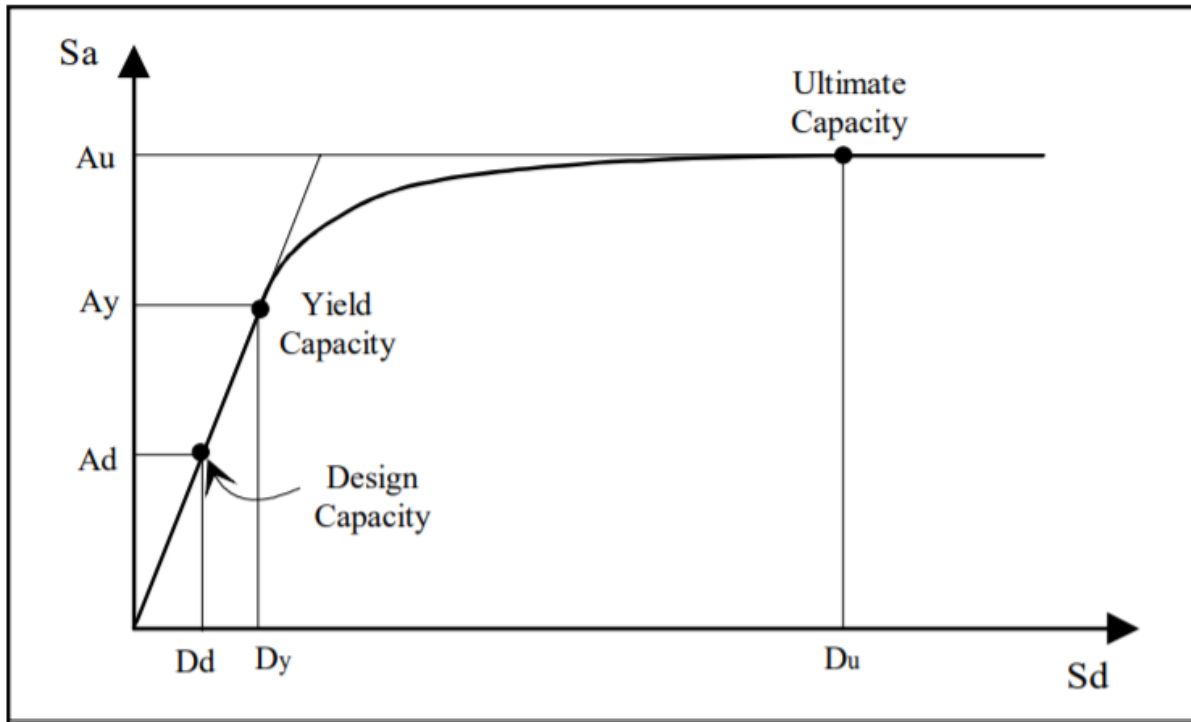


Figure 2. A Standard Building Capacity Curve

The design response spectrum as shown in is generated using the PESH module within Hazus and consists of four parts: peak ground acceleration (PGA), a region of constant spectral acceleration at periods from zero seconds to  $T_{AV}$  (seconds), a region of constant spectral velocity at periods from  $T_{AV}$  to  $T_{VD}$  (seconds) and a region of constant spectral displacement for periods of  $T_{VD}$  and beyond [6].

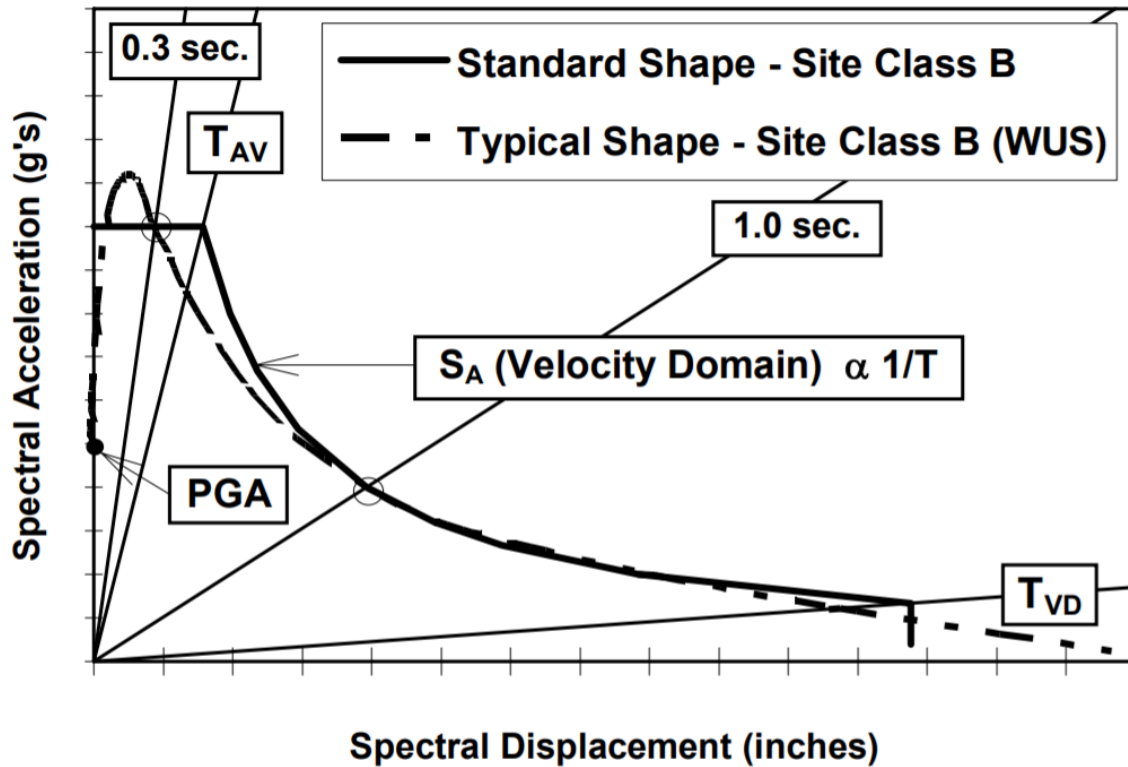


Figure 3. Standardized Design Response Spectrum Shape

Structural fragility curves are determined and evaluated for spectral displacement and acceleration defined by the intersection of the capacity and demand curves. Each of these curves describes the cumulative probability of being in, or exceeding, a set damage state. Five damage states exist within Hazus: none, slight, moderate, extensive, and complete. Figure 4 displays the methodology Hazus uses to assess damage states. Based on the spectral displacements and accelerations determined by comparing capacity and demand curves, a percentage distribution of probable damage state can be assigned based on the fragility curves.

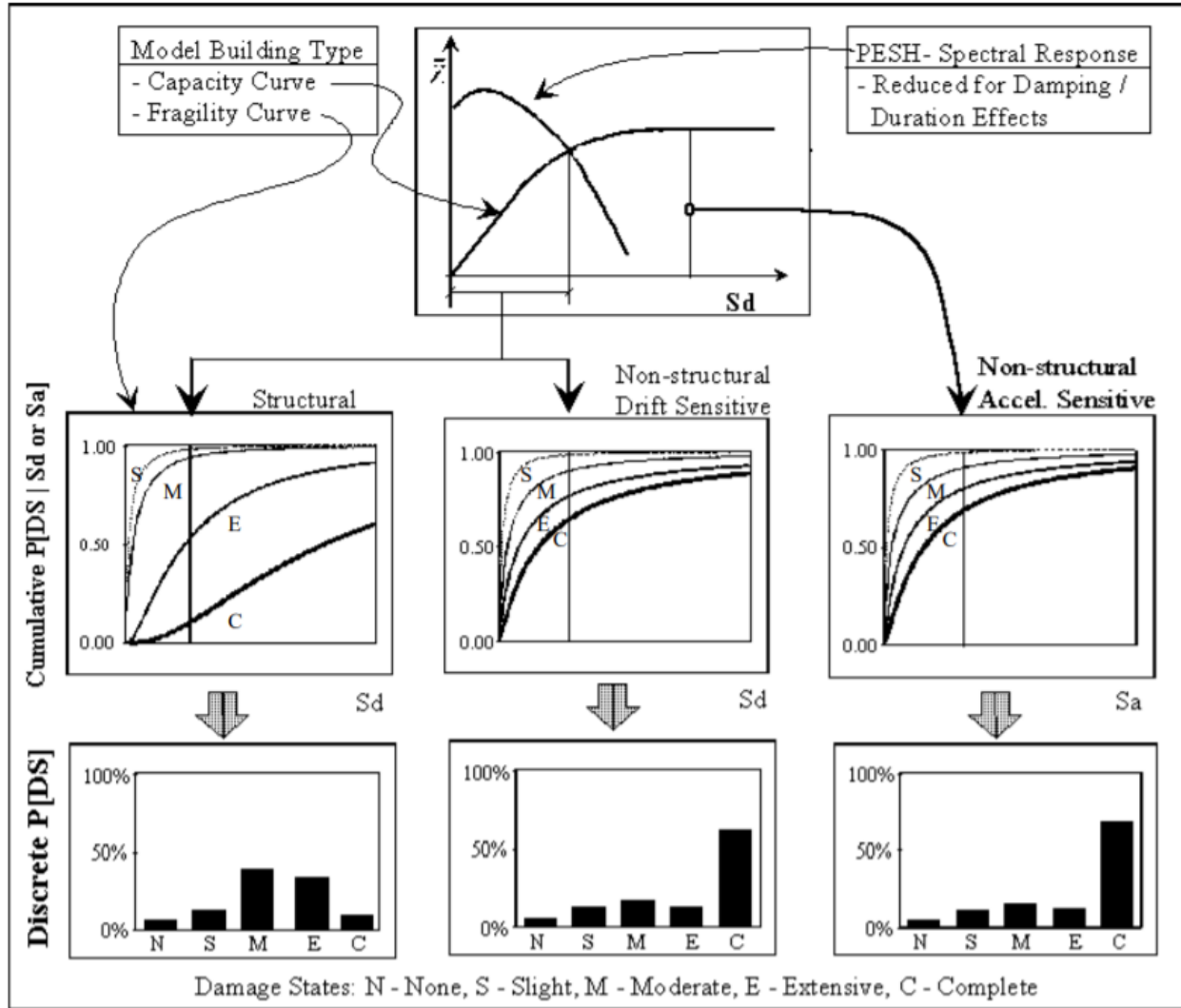


Figure 4. Hazus Damage Estimation Methodology.

### 2.1.3 HAZUS New Madrid Seismic Zone Catastrophic Case Study

FEMA developed a joint study through the assistance of the eight states comprising the New Madrid Seismic Zone (NMSZ) in the central United States to analyze and develop earthquake response plans. The eight states that comprise the NMSZ are: Alabama, Arkansas, Illinois, Indiana, Kentucky, Missouri, Mississippi and Tennessee. The NMSZ initiative used scenario planning to provide a preliminary analysis of 230 counties in the NMSZ. Both basic and advanced

analyses were performed as a sensitivity study to the national building index as provided within Hazus, more specifically three analyses are performed: basic, improved basic, and advanced analyses. The basic analysis used the default values within Hazus and did not require any input from the user, as a result the accuracy of this solution is low and should only be used as a benchmark for more refined analyses. The improved basic analysis applied ground motions while considering local geography, however the basic Hazus building inventory and structural components are still used. Finally, the advanced analysis looks at an additional set of parameters including: liquefaction susceptibility, pipelines inventory and building fragilities. For this study the parameters were developed by the Mid-America Earthquake Center (MAE) for Memphis, Tennessee and adjusted to fit the entire region of study [8].

A total of 3.8 million structures resided within the region of analysis. The predominant general building type being wood frame construction followed by low-rise unreinforced masonry and mobile homes [8]. Fragility functions were used to analyze the various building systems on a regional level (as described above). This is advantageous as it allows for a rough damage estimation of potentially millions of structural systems in a reduced timeframe. However, this isn't without its drawbacks as it severely simplifies and lowers the resolution to an archetypical structural system and compares it to the estimated ground motion accelerations within a county. This effectively reduces the "resolution" of Hazus to the size of a county rather than direct analysis of individual and discreet framing systems; however, analysis with that resolution on the scale of the New Madrid analysis would require too much computational time and setup information to be feasible.

## 2.2 PAGER: Prompt Assessment of Global Earthquakes for Response

The United States Geological Survey (USGS) developed a regional response estimation tool similar to FEMA's Hazus. This tool, known as the Prompt Assessment of Global Earthquakes for Response (PAGER), is a worldwide system which provides fatality and economic loss impact estimates in a post-earthquake zones. PAGER is an automated system maintained by the USGS that monitors and produces data regarding the impact of earthquakes at a global scale. PAGER assesses the earthquakes and estimates economic loss and fatalities based on historical data, shaking intensity, and stored models [9]. The estimates range on a color-coded spectrum: no response needed (green), local/regional (yellow), national (orange), or international (red). PAGER provides real time alert notifications based on the various levels of damage [10]. In addition to the notification system, PAGER identifies key building archetypes that would be vulnerable in the region, exposure and fatality reports from previous earthquakes which occurred in the region, and a summary of site-specific secondary hazards that may occur. Examples of secondary hazards include landslides, tsunamis, and soil liquefaction [10]. While PAGER results are available within a short period of an event, usually within 30 minutes of a significant earthquake, refined estimates can be generated once the extents of the event as well as refined intensities are incorporated.

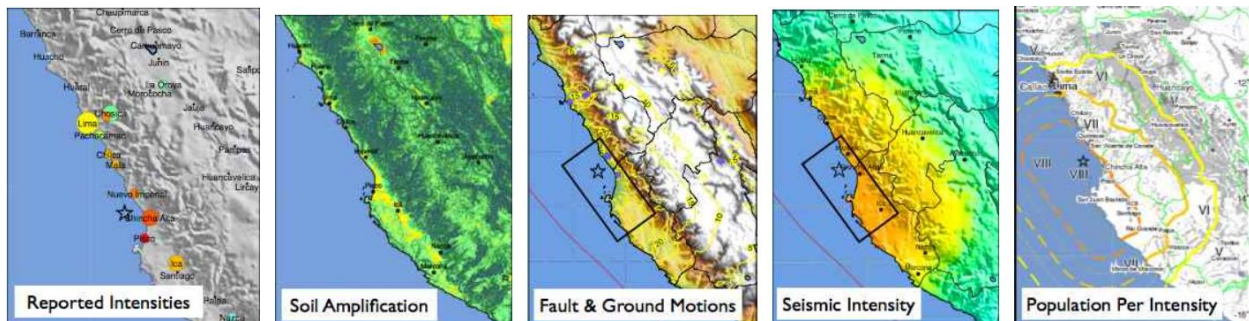


Figure 5 Visualizing the PAGER analysis process [9].

### 2.2.1 PAGER Analysis Process

The PAGER process involves 7 key steps summarized in Figure 5. When an event is triggered, the USGS logs a ground motion and determines its location and magnitude. These variables are used by PAGER to estimate the ground shaking using the ShakeMap methodology whereby mapping of the earthquake ground motion produces distributions of shaking severity [11]. ShakeMap then generates a site-specific ground motion amplification map based on topographic slope and site-specific soil characteristics. This map accounts for the soil characteristics effects on amplifying or transmitting the energy of the earthquake. As the information of the fault geometry and size are determined they are added to the ShakeMap. Once incorporated, the ShakeMap system produces contour estimates of regional ground shaking intensity. These contour maps incorporate the reported intensities based on the USGS “Did you Feel It?” system [12], the site-specific ground motion amplification map, and wave attenuation functions [9]. Once incorporated, ShakeMap then converts the estimated ground motions into a map of seismic intensity. This map incorporates anecdotal data (USGS “Did you Feel It?”), soil amplification data, and fault information to determine a geographic mapping of intensity throughout a region. This map, in combination with population mapping databases provided by the Oak Ridge National Laboratory, are used to then estimate the number of people exposed to shaking at each intensity level. Finally, the total number of lives lost is calculated based on the number of people exposed to each intensity level of shaking. Economic models that are incorporated within PAGER are used to estimate economic losses [10].

### 2.3 HAZ-Taiwan and the Taiwan Earthquake Loss Estimation System

The HAZ-Taiwan project is an initiative that was founded in 1998 to identify a systematic approach to seismic hazard mitigation. The Taiwan Earthquake Loss Estimation System (TELES) is the software that incorporates the HAZ-Taiwan framework into a program which can be implemented for regional impact assessment. The framework of the HAZ-Taiwan program includes analysis, risk assessment and estimates of socioeconomic loss due to an event. This includes simulation of seismic events, creation of a decision support system and response plans for governmental agencies after a hazardous event, and risk analysis of civil infrastructure. The HAZ-Taiwan program follows the methodology of FEMA's Hazus framework, however it is specially tailored to Taiwan's environment and engineering practices. The HAZ-Taiwan incorporated many of the steps in Hazus however it was developed with the following criteria in mind [13]:

- Standardize data classification system and analysis methodology;
- Provide user-friendly application software;
- Accommodate various user needs and different levels of funding;
- Use modular approach and balance the input/output accuracy;
- Utilize state-of-the-art analysis models and parameters, which are non-proprietary;

The HAZ-Taiwan methodology is broken into three main sectors as seen in Figure 6: Potential Earth Science Hazard (PESH) analysis, physical damage assessment, estimation of social and economic losses. These three sectors are all interdependent however are distinct modules within HAZ-Taiwan. This allows for estimates to range from full models using all modules to simplified models using stock data, akin to the basic/advanced Hazus analysis. The HAZ-Taiwan

methodology was broken into these modules as it allows for studies to be limited to areas of interests which may include singular loss types if budgets or inventories are limited.

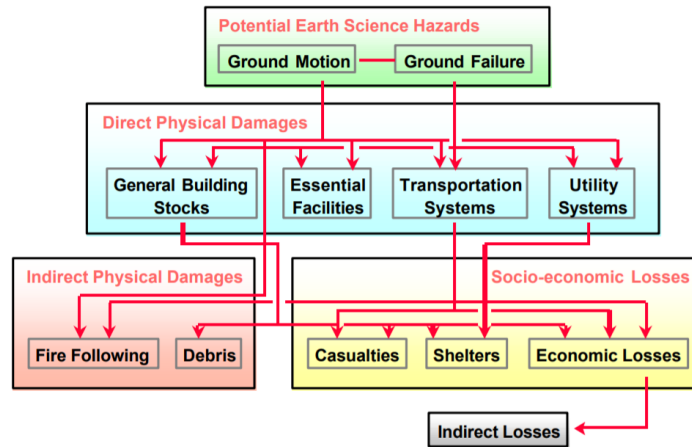


**Figure 6 The HAZ-Taiwan Methodology [13].**

The PESH module in HAZ-Taiwan is geared toward estimating both ground motion and ground failure. Ground motion demands defined in terms of response spectra and peak ground acceleration/velocity are determined based on scenario earthquakes and local geological conditions. As compared to Hazus, the HAZ-Taiwan framework does not consider other related earth science hazards such as tsunamis and flooding. The incorporation of GIS technology allows the framework to define the site-specific shaking parameters to obtain estimates of damage and loss in the scenario region. In order to obtain the estimates of ground shaking intensities a user can take either a deterministic approach, probabilistic approach, or provide a seismic ground shaking map such as the ones created by ShakeMap. The deterministic approach obtains the ground shaking intensities by using historical events and/or existing seismic sources. The probabilistic approach uses contour maps of spectral response for different levels of return period to generate estimates of damage and loss. Once the ground shaking intensities are determined they are further modified by soil site characteristics which can account for amplification or other soil-based ground effects [13].

Physical damage modeling in HAZ-Taiwan is performed using fragility function analysis like Hazus. HAZ-Taiwan groups buildings into archetypes based on structural type and building rise: low (L), medium (M), and high rise (H). The full breakdown of the disparate models are as follows: wood (L), steel (L, M, H), light steel (L), reinforced concrete (L, M, H), pre-cast concrete (L), reinforced masonry (L, M), un-reinforced masonry (L), and steel reinforced concrete (L, M, H) buildings. Further still, buildings are divided into high-code, moderate-code, low-code, and pre-code. In order to analyze buildings on a large scale, the following analysis regime was implemented for the building archetypes [13]:

1. Based on the structural characteristics and local design codes, the incremental pushover curve, representing nonlinear capacity of a building, is computed.
2. The site-specific elastic response spectra (ADRS curve), generated by the PESH module, are modified to account for the effects of both increased damping at higher response levels and system degradation upon long duration of ground shaking.
3. The modified site-specific response spectra are overlaid on the capacity curve of building to determine the performance point. The intersection point defines the expected building response in terms of spectral displacement and spectral acceleration.
4. For the expected building response, structural and nonstructural fragility curves are evaluated to determine damage state probabilities.
5. The damage state probabilities are modified to account for site-specific probable ground failure. Based on the level of damage, loss-of-function estimate, expressed as a percentage of full capacity, and restoration-time estimate, needed to recover to full capacity, are computed.

Using the models of structural damage, estimates of economic and social loss can be calculated using socioeconomic and social statistics incorporated into the application software. The HAZ-Taiwan project also plans to incorporate probabilistic seismic hazard analysis into TELES and may have opportunities to integrate applications that would work in identifying seismic insurance policies by region [13].

## **2.4 RiskScape New Zealand**

New Zealand is vulnerable to a wide range of hazards including tsunamis, earthquakes, volcanoes and large storms. In the effort to maintain their communities, New Zealand has undergone several avenues to create models with which community risk and loss can be both modeled and estimated. In 2004 the Foundation for Research, Science and Technology (FRST) provided funding to develop a tool that would utilize existing hazard information for scenario planning to estimate damage and replacement costs, casualties, disruption and number of people that could be affected [14]. The Riskscape program identified the need for a tool that: (1) was affordable and not reliant on expensive software licenses, (2) was easy to learn and use, (3) was designed to be extended to a wide range of users, and (4) was able to incorporate the large number of hazards in New Zealand [15]. Riskscape is a relatively new initiative and has been developed for the scope and application of New Zealand's landscape; including using up-to-date GIS data to allow for the generation of building archetypes specific to New Zealand. Riskscape has identified key aspects of previous solutions and follows a similar yet distinctly unique framework [14]:

- Establish the how large and how often each natural hazard is expected to occur
- Use a form of attenuation function to compute the intensity of the resulting action across the region of interest.
- Compute the damage to each set of inventory assets under consideration by reference to the damage state/intensity relationship for the various inventory classes.
- Establish the impact such damage may have on full operational capability and
- Ascertain the resulting levels of performance that result from that damage (disruption) and the likely costs of repair to reinstate the damage incurred.
- When damage exceeds certain thresholds, injuries are to be anticipated and in extreme cases (when a building may have perhaps experienced either partial or complete collapse) then loss of life is to be expected. The extent of injury is a function of the demographics of those people (known to be significant in ascertaining their ability to recover from either injury or neighborhood disruption) and their distribution across the various classes of inventory with a nocturnal and seasonal variation included where appropriate.
- Establish anticipated recovery expectations from the extent of damage and injury incurred
- Spatially distribute the losses in accordance with the geographic location of the assets and their damage state from the particular hazards being considered.
- Prepare a suitable graphical interface that will present the damage distribution data in a manner suitable for decisions relating to rescue, response or recovery.

Three main modules comprise the Riskscape software as shown in Figure 7. the user interface, the software engine, and the building inventory. The building inventory database is a disparate module not contained within the software engine consisting of the structures within the hazard zone. Structures are not analyzed at the individual level; they are instead analyzed at the meshblock level, with a meshblock being the smallest geographic unit for which statistical data is collected and processed by Statistics New Zealand. Meshblocks are geographic areas that range in from sections of city blocks to large swaths of rural land. The entirety of New Zealand is broken down into meshblocks to form a network that is used to define electoral district and local authority boundaries [16]. Meshblocks were chosen as they represent a good compromise between aspect ratio and computation requirements. Additionally, crucial data such as the geological classification, elevation and typical terrain can be pulled from GIS data for each meshblock. To develop archetypical properties to be used for the meshblocks, several sites were surveyed at random to develop characteristic architectural and structural details to attribute to the meshblocks.

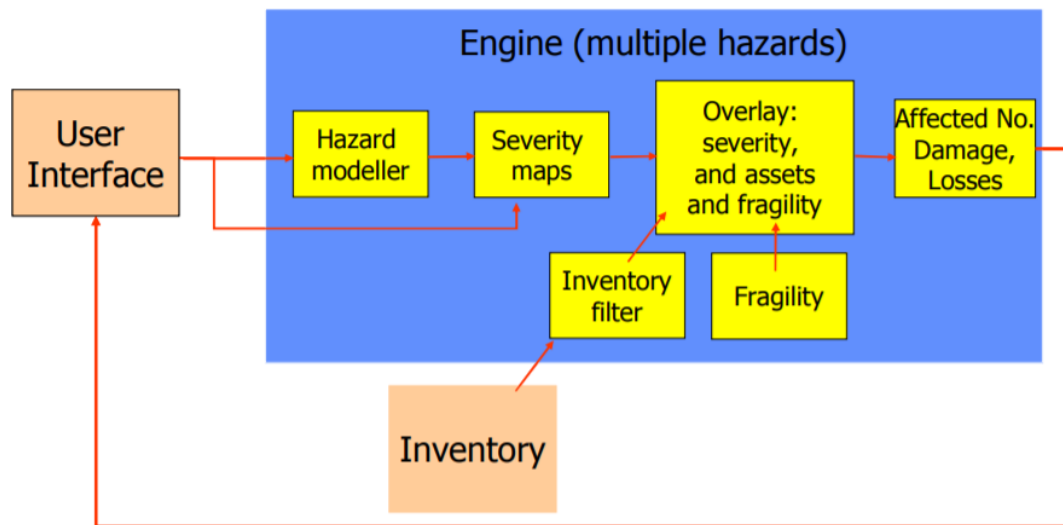


**Figure 7 The Riskscape Framework [14].**

The Riskscape software earthquake analysis comes in two models: level 1 modelling and level 2 modelling. Level 1 modelling consists of determining earthquake losses through direct Modified Mercalli (MM) intensity/distance relationships derived through the study of damage from historical New Zealand earthquakes. The MM relationships are intensity scales which provide a correlation between the intensity of a ground motion and the damage ratio of a structure. From the damage ratio, a cost of repair or replacement can be estimated. Level 2 modelling as outlined previously uses design spectra and determines damage state, losses, and cost of repair. Level 2 analysis is more refined and potentially allows for single building analysis however it currently works on archetypical systems [14]. Building system classification is broken in to two primary classes: residential and workplace. Each of these classes is further broken down into subgroups based on their age, materials, height, and presence of structural deficiencies. Each subgroup is assigned a fragility class based on the conglomerate effects of the specified parameters. After an earthquake analysis, Riskscape utilizes the direct loss module to transcribe damage into repair costs and community losses for both level 1 and level 2 analyses.

## **2.5 OpenSEES: The Open System for Earthquake Engineering Simulation**

As the field of earthquake engineering develops, more refined analysis methods are being introduced and used. The OpenSEES framework is one such solution to the needs of current engineers and researchers as a finite-element software for use in dynamic non-linear analysis. Being a code-based program, OpenSEES allows for the easy development of parametric and reliability studies. OpenSEES also gives the user a large amount of control over materials, element formulations, and solution algorithms not available in commercial formulations.

With the proliferation of research into the development of performance-based design strategies, a need has arisen for high-fidelity non-linear modelling software. Currently implemented structural engineering software such as SAP2000 do not have the capability for full scope modelling to incorporate effects due to substructure soil interactions, fire, and other secondary loadings. And while there currently exist several robust and proven finite-element software such as ABAQUS, MSC Nastran, and LS DYNA, none of these frameworks were built dedicated structural engineering finite-element software. While current finite element programs can incorporate high fidelity material models and perform dynamic analysis, materials in the real world are highly variable. An engineer can use finite element reliability methods to encapsulate a level of uncertainty in their models. This is done by allowing the engineer to input material parameters as random variables and approximate probabilistic methods to encapsulate the response of nonuniformity associated with real world materials. OpenSEES was developed from the start as a fully encompassing structural engineering FEM and FE reliability software for the future of earthquake engineering [17].

### **2.5.1 The OpenSEES Framework**

OpenSEES is an object-oriented software framework which allows the creation of finite element models that simulate the response of structural systems. OpenSEES was developed by Frank McKenna and Gregory Fenves through the Pacific Earthquake Engineering Center (PEER) with funding from the National Science Foundation (NSF) [18]. Designed as a flexible and modular system, OpenSEES has several advantages that non dedicated structural finite element programs do not have. One such advantage is that classes within OpenSEES are abstract.

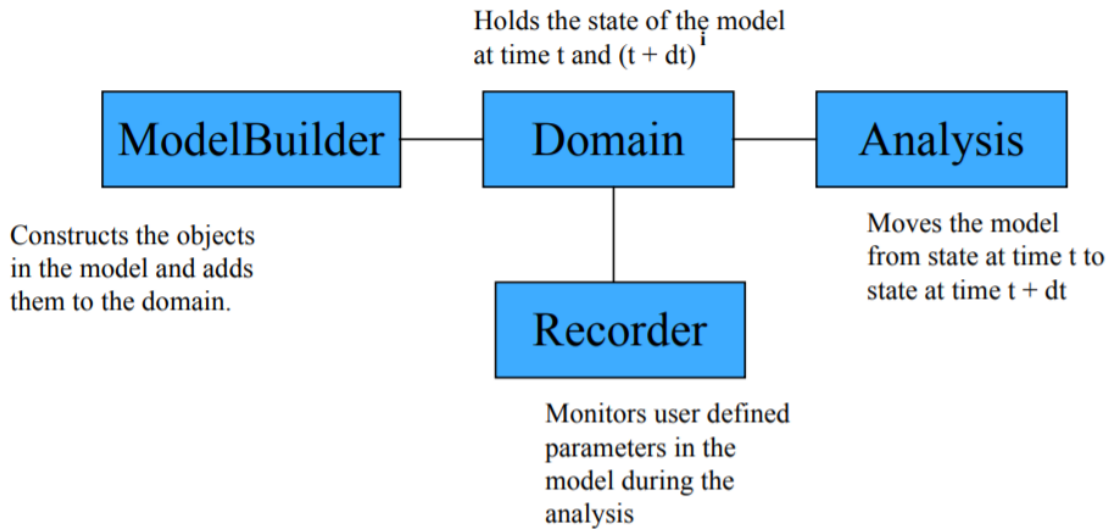


**Figure 8 The Main Abstractions in the OpenSEES Framework [19].**

Abstraction of key modules shown in Figure 8 allows users the ability to provide their own subclasses within these modules to modify the application. This has direct benefits in earthquake engineering as it allows engineers to use the most cutting-edge algorithms and integration schemes for high fidelity analysis [17].

### **2.5.2 The OpenSEES Finite Element Analysis Solution Procedure**

OpenSEES follows a standard finite element analysis procedure. The governing partial differential equations are discretized into a system of nonlinear ordinary differential equations (ODE's) and solved at each time increment. Solutions are completed within OpenSEES through an object composition approach whereby the analysis procedure is constructed through the joining of objects from other classes as shown in Figure 9; each representing a fundamental step in the solution process.

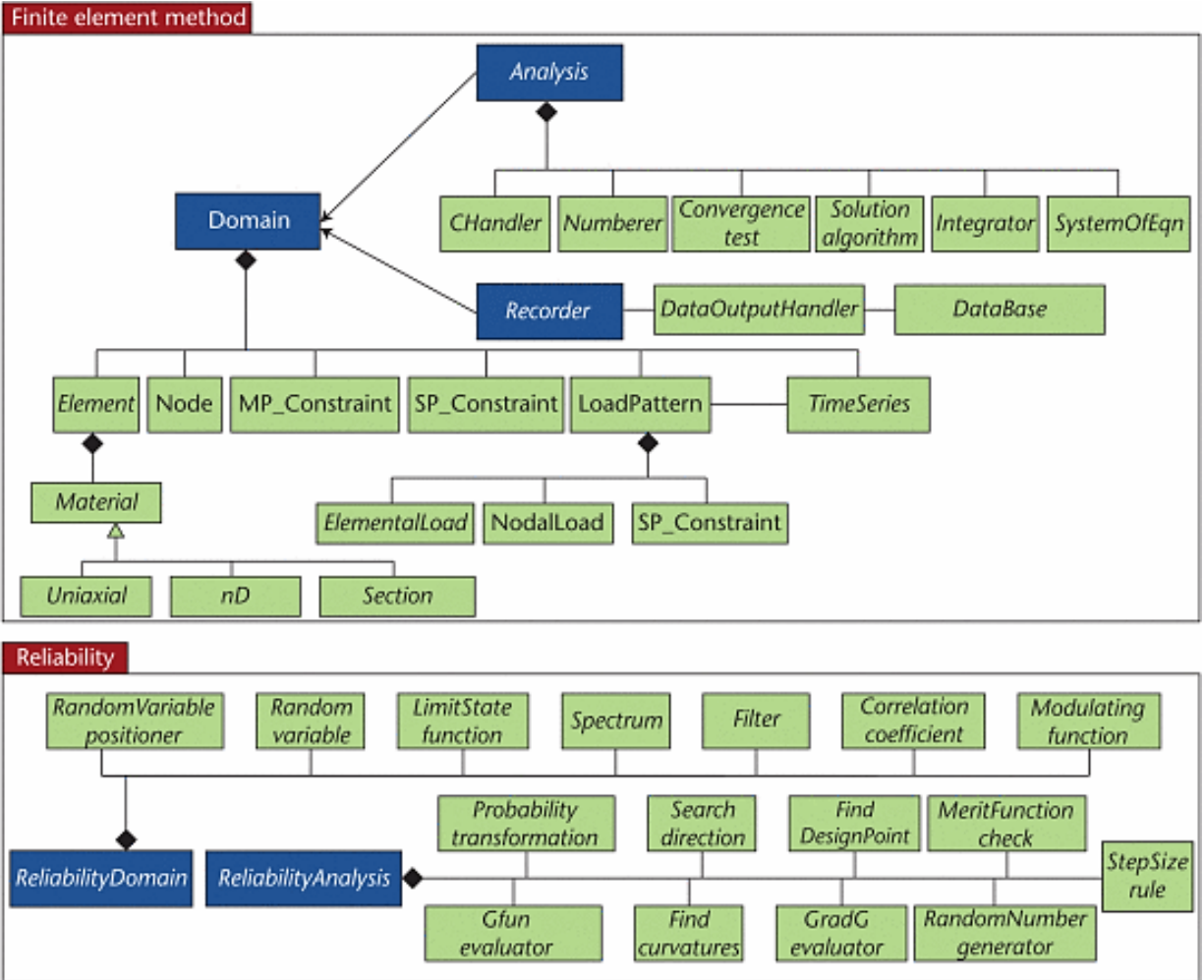


Figure 9 Classes within the OpenSEES framework [17].

The first step in the process is to set up the constraints handler object. The constraints handler object determines how the constraint equations are enforced in the analysis. Constraint equations can either enforce a specific value for a given degree of freedom or a relationship between degrees of freedom. Once the constraints of the system are determined, the numberer object is created. This object determines the mapping between equation number and degrees of freedom in the system. Following the mapping of equations, the system object is used to construct a linear system of equations and linear solver objects to store and solve the system of equations in the analysis. As stated earlier, one of the advantages of OpenSEES is that these modules are abstract, and thus can allow users to implement their own unique solution methods, as a result

several exist: BandGeneral, BandSPD, ProfileSPD, SuperLU, UmfPack, FullGeneral, SparseSYM, PFEM, and MUMPS [18]. Each of these system objects, aside from the FullGeneral system, attempt to condense and simplify the system of equations per their unique sets of rules. Once the system of equations is condensed, a solution method is implemented through the algorithm command. This command constructs the solution algorithm object, which determines the sequence of steps to solve the various equations. Ten solution methods exist within OpenSEES, however as the algorithm class is abstract, users can use one of the pre-loaded solution methods such as linear or Newton algorithms, or they can specify their own. After the solution method is specified, the integrator object is created. This object determines several things: the predictive step for the next time increment, the tangent matrix, the residual vector at any iteration, and the corrective step based on the displacement increment based on what type. The type of integrator used in the analysis is dependent on whether the analysis is static or transient. Finally, the analysis object is created, and the analysis is performed. This final set of stages determines the type of analysis, static or transient, and the time and number of increments to analyze. At each analysis step the composition of all prior steps is used to solve the set of differential equations and ensure continuity at all degrees of freedom.

### **2.5.3 OpenSEES Finite Element Analysis Validation Studies**

Numerous studies have been conducted to validate the finite element procedure that OpenSEES uses. Vecchio et. Al (2013) performed several experiments which compared hysteretic behavior of reinforced concrete columns from the PEER Column Test Database in both numerical and experimental testing. One of the goals of the testing was to determine if OpenSEES could provide an adequate simulation of the hysteretic behavior of concrete in a non-linear cyclic seismic

loading regime. The experiments compared analytical results of several models: fiber elements in OpenSEES, frame elements in VecTor5 and continuum elements in VecTor2. These models were all compared to full scale experimental tests conducted on the requisite column details. The models were compared against a cantilevered column with a flexural failure mode.

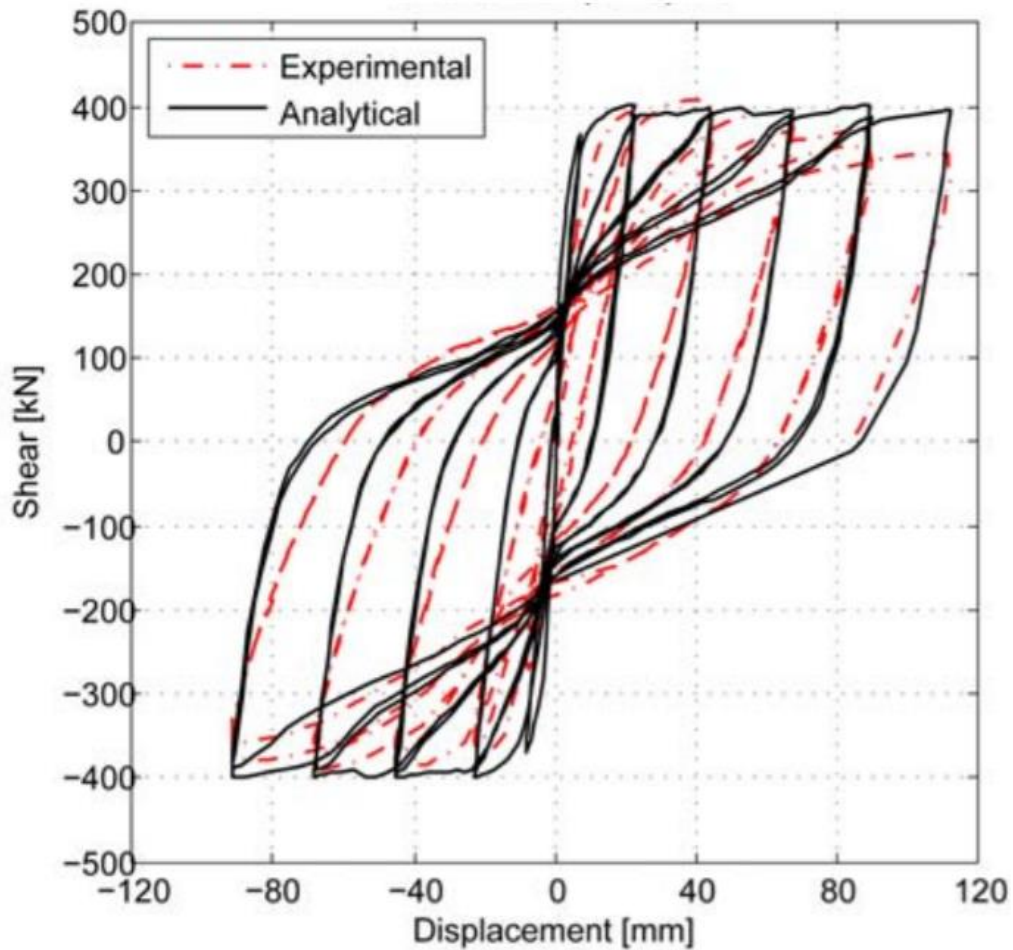


**Figure 10 Hysteretic Behavior of a Column Modeled Using OpenSEES [20].**

The OpenSEES analyses adequately modeled strength, deformability, and pinching to an acceptable degree. The simulated hysteresis shown in Figure 10 displayed a higher initial stiffness as compared to the experimental data however this response may be related to the fact that bar slippage was not accounted for in the analytical model. Both the fiber and lumped plasticity models used accurately predicted the overall characteristics and response of the experimental data.

Berry et. Al 2008 used OpenSEES as a method for developing accurate column-modeling under seismic loading. The study aimed to determine whether OpenSEES would be able to accurately model global and local forces, deformations, and the progression of damage [21]. Both lumped plasticity models and distributed plasticity models were generated based on the cross sections of eight full scale reinforced concrete columns tested by Lehman and Moehle (2000).

Results indicated that the OpenSEES models shown in Figure 11 accurately classified column behavior at lower ductilities and low cycles for both the distributed plasticity and lumped plasticity models. While it was determined that the OpenSEES models were applicable for lower ductility applications, the particular models were set up without a method to capture degradation due to repeated deformations at high ductility [21].

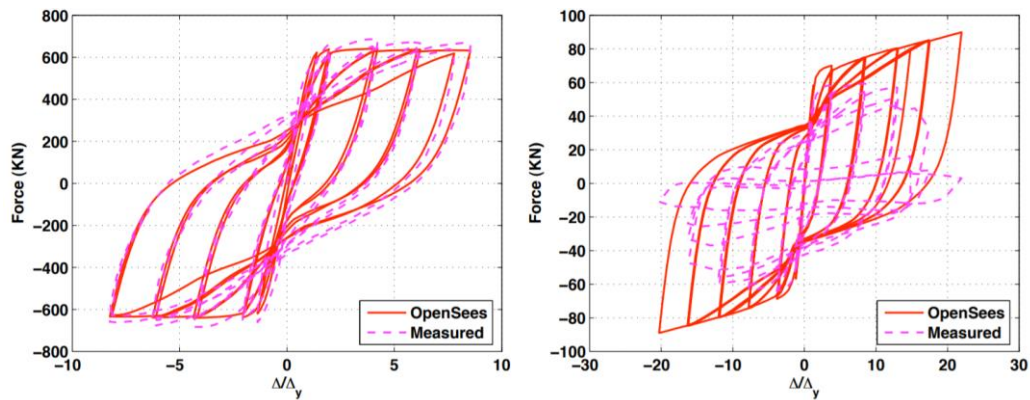


**Figure 11 Hysteretic Behavior of Bridge Columns Modeled with OpenSEES [21].**

The authors concluded that without a zero-length bond-slip section or an added shear-deformation component the cyclic response of the column depended on the cyclic response of the material constitutive models. This fact, in combination with the material models chosen (Steel 02, Concrete01) which do not model degradation due to repeated deformations at high ductility displays that the models used portrayed accurate results according to how they were setup. The OpenSEES models generated data which, while not matching the experimental data, matched the theoretical output based on the model type.

## 2.5.4 Opensees Force-Based Element Formulations

The main type of element used to model plasticity in the Model Builder is the force-based beam column element. A force-based beam column element differs from a traditional displacement-based beam column element in several ways. Force based beam column elements assume constant axial force along the element with a linear moment distribution as compared to constant axial strain and a linear curvature distribution in a displacement-based element [22]. Displacement-based elements follow a standard finite element formulation whereby section deformations are interpolated from an approximate displacement field. The principle of virtual displacements (PVD) is used to form the element equilibrium relationship at all integration points along the element. Nonlinearity is approximated using constant axial deformation and linear curvature along the element length. Figure 12. shows how displacement-based element solve for displacements exactly at nodes and approximates forces and moments [23].

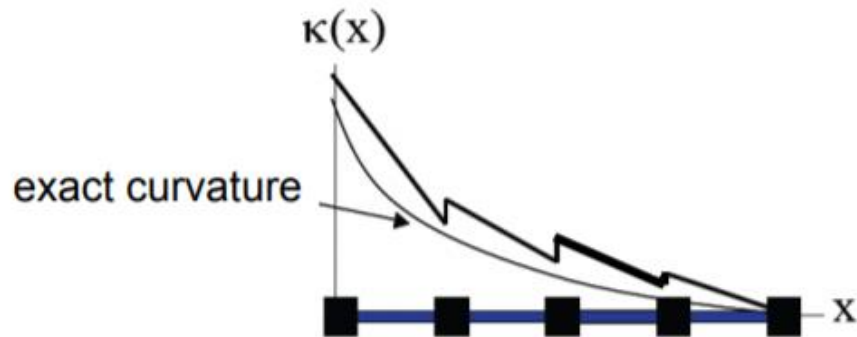


**Figure 12 The Displacement-Based Element Solution Methodology.**

The force-based element necessitates an intra-element solution to determine sectional strains and curvatures to satisfy compatibility equations, however in a nonlinear environment a displacement-based methodology requires many more elements in order to accurately capture nonlinearity; and thus degrees of freedom are much greater than a force-based element

methodology. For applications of structural frames undergoing seismicity, a force-based element approach will overall reduce the number of degrees of freedom within the system and result in an overall smaller computational load. Figure 13. shows how force-based element solve for forces exactly at nodes and approximates displacements [23].

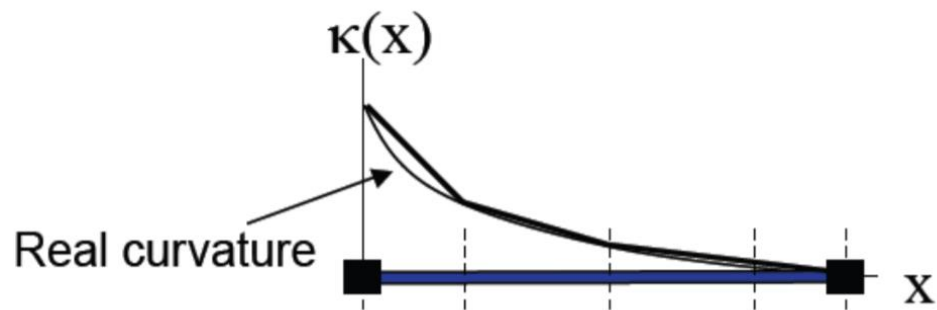


**Figure 13 The Force-Based Element Solution Methodology.**

### **3.0 The Model Builder: Multi Fidelity Modeling**

As the field of earthquake engineering advances, a need for a higher level of analysis within regional response estimation frameworks is apparent. Fragility functions of archetypical structural systems are only applicable if structures conform to their archetype. For critical infrastructures such as governmental buildings and hospitals, an ideal solution would be to develop detailed structural models for every building. In a large city which may have hundreds if not thousands of these critical infrastructures, this is currently not feasible. The multi-fidelity model builder provides an efficient method for generating structural models for building-level response prediction.

The Model Builder uses the opensource code language Python [24] and the recently developed opensource structural analysis software OpenSeesPy [25] for model development, structural analysis and response evaluation. These platforms were selected to allow for ease of user modification and widespread distribution as well as end-to-end data analysis and visualization. The Model Builder relies on building design information in existing structural databases and can easily be modified for common database structures including Excel, SQL and many others for model development and response evaluation. Model fidelities range from linear SDOF modal-maximum spectral acceleration evaluations through non-linear MDOF response history analyses. The resolution of individual structural models can be selected by the user, however model fidelity is limited by the amount of structural design information available for any given structure in the database. The following sections provide detailed information on the modeling and response evaluation methodologies available in the Model Builder.

### 3.1 Components of the Model Builder

The Model Builder is comprised of four disparate systems as shown in Figure 14: A library of ground motions and ground motion response spectra given by the end-user, the building information database, The Model Builder code itself, and the outputs generated by the tool.

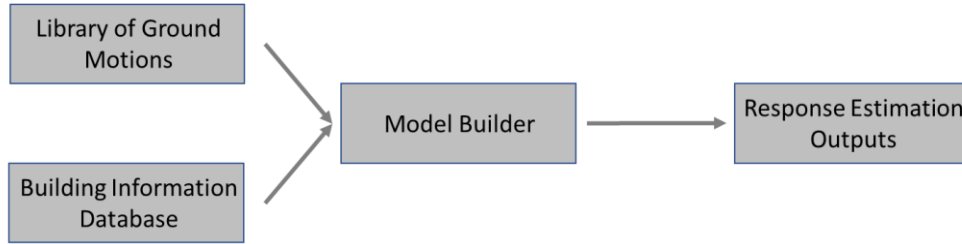


**Figure 14. System Breakdown of The Model Builder.**

In order to use the Model Builder, the end-user is required to have a library of buildings which have been catalogued in the building information database as well as ground motion demand data. For one dimensional analysis, recorded spectral acceleration response spectra are supplied by the end user. For two-dimensional analysis, recorded or synthetic acceleration histories are required. The Model Builder code consists of the executable file in the main folder as well as all its separate sub-routines within the functions folder.

#### 3.1.1 Ground Motion Library

The ground motion library is a folder which contains all an end-user's specified ground motions and response spectra. Ground motions and response spectra can have any file extension and naming format as specified by the end-user but should have only a single column of data representing the raw ground motion data. Timesteps and number of data points are not required in the ground motion files and are specified in the building information database.

### 3.1.2 Building Information Database

The structural parameters required for analysis depend upon the type of analysis selected by the end user. The one-dimensional (1D) analysis follows ASCE7-10 section 12.8.2.1 in addition to ASCE 7-10 section 11.4.4 [23] to calculate the fundamental period of the building structure and compare the values of the recorded response spectrum versus the design response spectrum. Figure 15 details the requirements the end user must specify to perform the analysis.

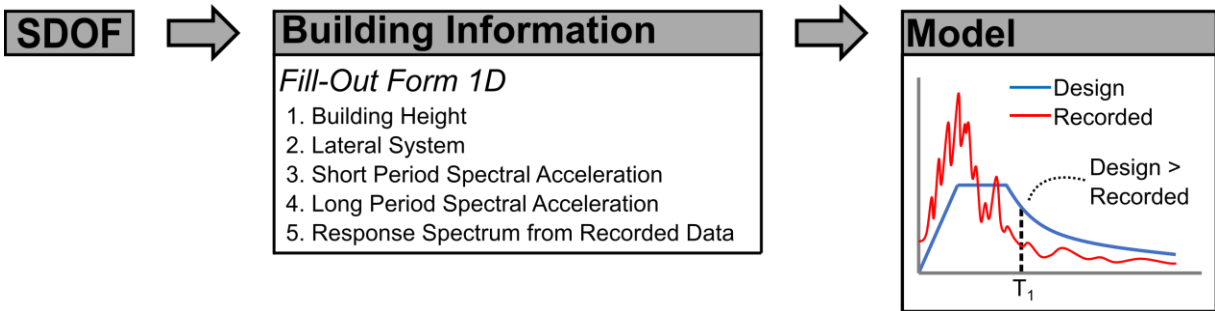


Figure 15 Parameters Required for SDOF Analysis.

The two-dimensional (2D) analysis constructs and subjects a two-dimensional lateral system such as a frame or wall to a ground motion using OpenSEES. In order to create this model, four main areas of information are required as summarized in Figure 16: setup information, column details, beam details, and material properties.

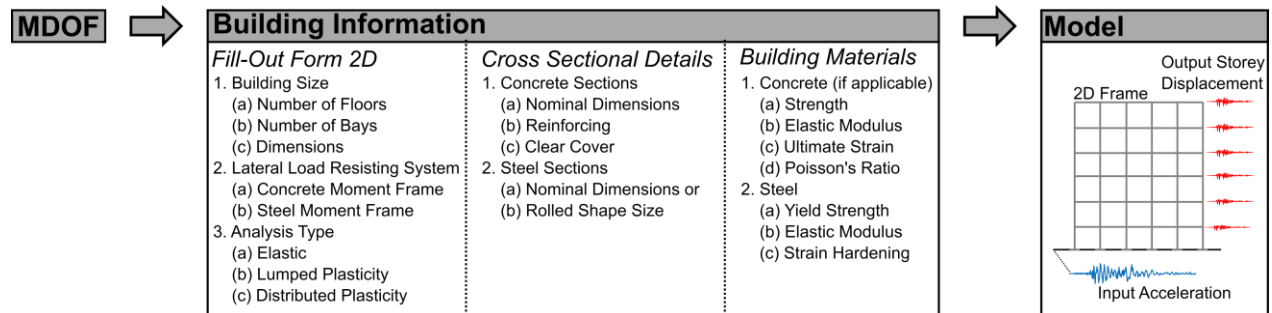


Figure 16 Information Required for the Model Builder.

The setup information provides the Model Builder with several key features: the details of the ground motion being used, the general size of the building (bays and floors), the column and beam types as specified by the user, and the type of analysis that the user wishes to perform. The column and beam detail sections are used to specify the cross sections of the respective elements. Several types of elements are available such as reinforced concrete circular and rectangular columns in addition to standard steel I shapes. Lastly, the material properties are required. The properties specified are used to generate typical material response curves such as Concrete01, Steel02 and Confined Concrete 01.

### **3.1.3 Python Code**

The Model Builder is compiled with a download-and-run functionality such that no end-user modification of the code is required. This allows users to run the Model Builder from any location on their computer and all inputs and outputs are stored within the main folder. Upon running the Model Builder, the user is prompted for either single or batch analysis. In instances of prioritized analysis, users can perform single analyses on critical buildings. If a single analysis is not chosen, a full library analysis will be performed. This creates and analyzes models for every building that has a building information spreadsheet.

### **3.1.4 Outputs**

The last section of the Model Builder software is the outputs folder. All results generated from any analyses performed will be placed in the outputs folder upon completion of the analysis. While the analysis can be back-end configured to generate whatever data the user would like to generate, the current iteration of the Model Builder software outputs an excel spreadsheet with a tab detailing a full response history of the column drifts as well as a tab for floor nodal displacements.

### **3.2 SDOF Modal/Maximum Spectral Acceleration Response Evaluation**

ASCE 7-10 has a method for both approximating the fundamental period of a structure and generating the design seismic hazard response spectrum. ASCE 7-10 Chapter 12: Seismic Design Requirements for Building Structures prescribes procedures used in seismic analysis and design of structures. Section 12.8.2 of the design guide details a method for estimating the fundamental period of a structure. This method takes into consideration structural properties such as lateral load resisting system and the height of the structure.

Following the estimation of the fundamental period, ASCE 7-10 Chapter 11: Seismic Design Criteria prescribes provisions to determine the design seismic hazard response spectrum based on the short and 1-s period [27]. As noted in the ASCE 7-10, these analyses are permitted to determine seismic loading in lieu of more detailed analyses, however they are conservative estimates of the true response.

The 1D analysis used in the Model Builder is based off ASCE 7-10 Chapter 11 and Chapter 12 [26]. The approximate fundamental period of the structure is calculated using the method as prescribed by ASCE 7-10 Section 12.8.2 “Period Determination”. The design spectrum is created using ASCE 7-10 section 11.4 “Seismic Ground Motion Values”. Both the actual and design spectrum responses are indexed at the approximate period and a prognosis is generated based on which value is higher. For any building structure which has a higher actual response compared to its design response a rating of “Unsafe” is given.

### **3.2.1 Estimation of Fundamental Period**

The period is determined as per ASCE 7-10 Section 12.8.2. This method establishes the fundamental period as the product of the structural characteristic coefficient and the height of the building. The structural characteristic coefficient is based on the structural type where values of  $C_t$  and  $x$  are determined for several structural archetypes: steel moment-resisting frames, concrete moment-resisting frames, eccentrically braced steel frames, and all other structural systems.

### **3.2.2 Creation of the Design Spectrum**

The design spectrum as shown in Figure 17 is created to compare against the recorded spectral acceleration. ASCE 7-10 section 11.4.5 is used to create the design spectrum based on a simplified analysis [26]. The design spectrum is broken into a series of four segments which define the overall response spectrum. These curves are determined using both the short and 1-second design spectral response acceleration parameters  $S_{DS}$  and  $S_{D1}$  respectively.

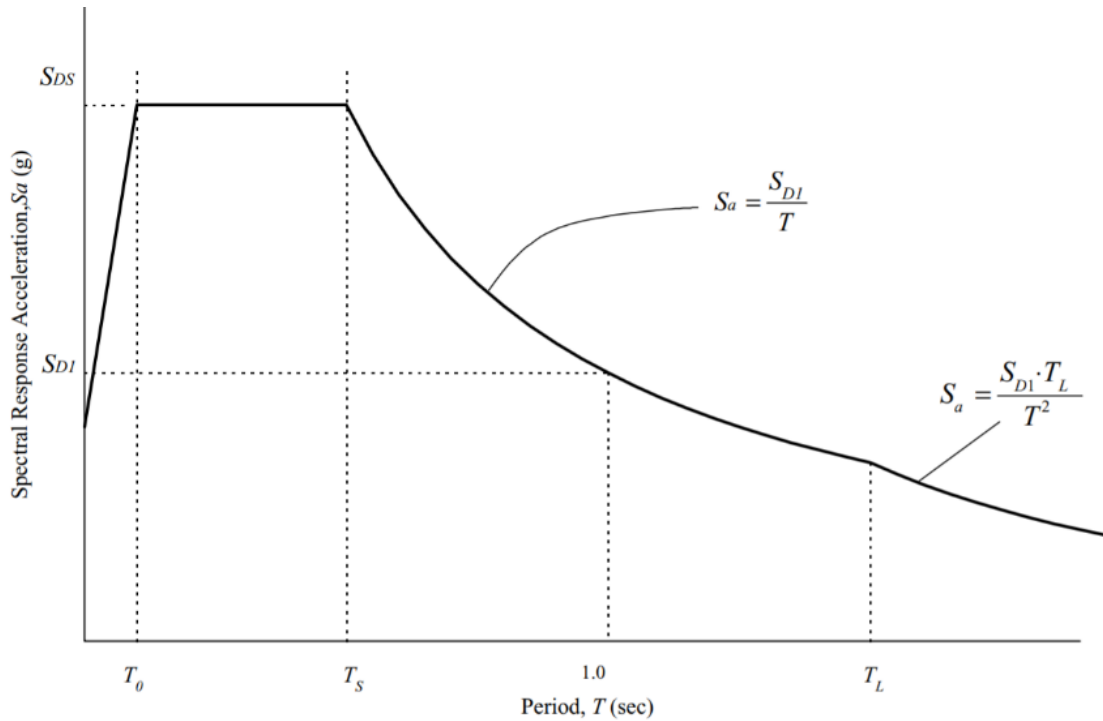


**Figure 17 The ASCE 7-10 Design Response Spectrum [26].**

### 3.3 MDOF Response History Evaluation

The 2D analysis implements OpenSEES for dynamic and structural analysis. OpenSEES was chosen as the software framework due to it being a robust open-source framework which has shown capabilities in several fields of analysis. Recent efforts have created an interpreter of OpenSEES (OpenSEES.py) which allows this framework to be used in Python, another open-source software. OpenSEES.py was implemented in the Model Builder due to its ease of use and continued development.

The model-building process entails the creation of materials, sections, building geometries, nodes, and elements in addition to the application of masses, loads, and ground motions. A leaning column is also applied to capture any additional loads on the structure that are assumed by interior gravity-only columns. Once the structure is created, a full static gravity is performed so that initial stresses and strains can be induced before the application of the ground motion. After imposing gravity loads, the building is subjected to a transient time-history analysis of the associated ground motion. From this analysis inter-story drifts and nodal floor displacements are recorded and output to an excel file for end-user analysis.

### **3.3.1 Information Transfer from the Building Database to the Model Builder**

In order to begin the model building process, the data is required to be transferred from the building library into python. Current versions of the Model Builder use Microsoft Excel spreadsheets to detail and catalogue buildings due to its understandable structure and ease of end-user use however the Model Builder uses pandas, a library within python which allows for the reading of various types of data structures such as xlsx, SQL, and others. All the data that was specified in the end-user specified building information section is read into python to be used in future steps of the model building process.

### 3.3.2 Model Types

Following the reading of data into the Model Builder, the creation of the model is dictated by the type of analysis requested by the end-user. Currently, three types of 2D analysis are available: elastic, lumped plasticity with fiber elements, and full distributed plasticity fiber elements. The latter two analysis types use a rigid offset model which further increases the fidelity of the model by incorporating rigid joints at the intersection of beam and column elements to mimic the functionality of real-world beam column interfaces. Figure 18 displays the overall model structure, highlighting the differences between the three model types. In the event of a single building analysis, the user is prompted to choose their model type. If a full library analysis is chosen, the model type will be determined as specified in each building's individual file.

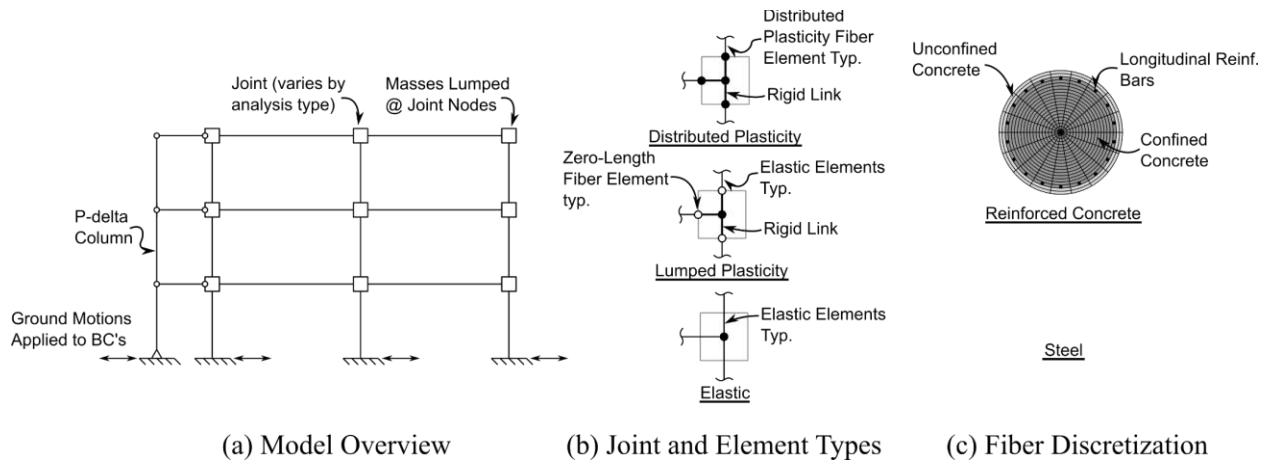


**Figure 18 Model Structure Overview.**

### 3.3.2.1 Material Models

Several material models are used in the lumped plasticity and distributed plasticity models. Concrete01 is the main concrete model used for reinforced concrete sections. Concrete01 was chosen as the main concrete material model as it represents the simplest material model for concrete, with degraded linear unloading/reloading stiffness and zero tensile strengths. In order to define its behavior as shown in Figure 19, the 28-day strength, maximum strain, crushing strength, and strain at crushing are required [28]. While the exclusion of tensile strength does represent inaccuracy in material fidelity, neglectation of concrete tensile strength greatly reduces computational expenditure and only affects the stiffness of models with relatively small elastic deformations.

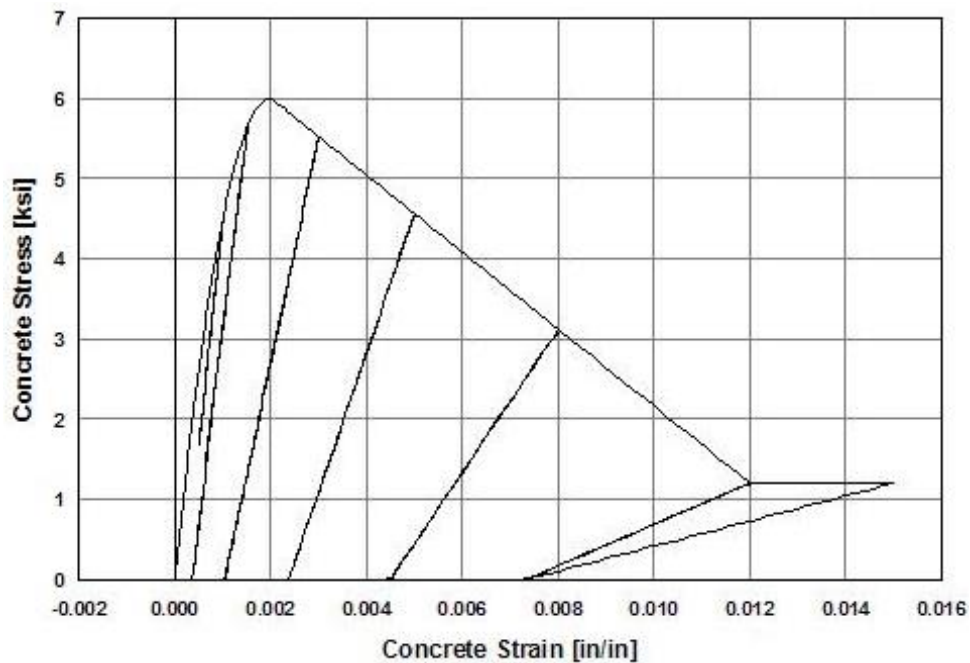


Figure 19 Concrete01 Example Material Model [24].

For all instances of reinforcing steel and steel used for wide flange sections the material model Steel02 is used. The Steel02 material model shown in Figure 20 consists of a uniaxial material with isotropic strain hardening. Values of yield strength, Young’s modulus, strain hardening ratio are used to define its behavior.

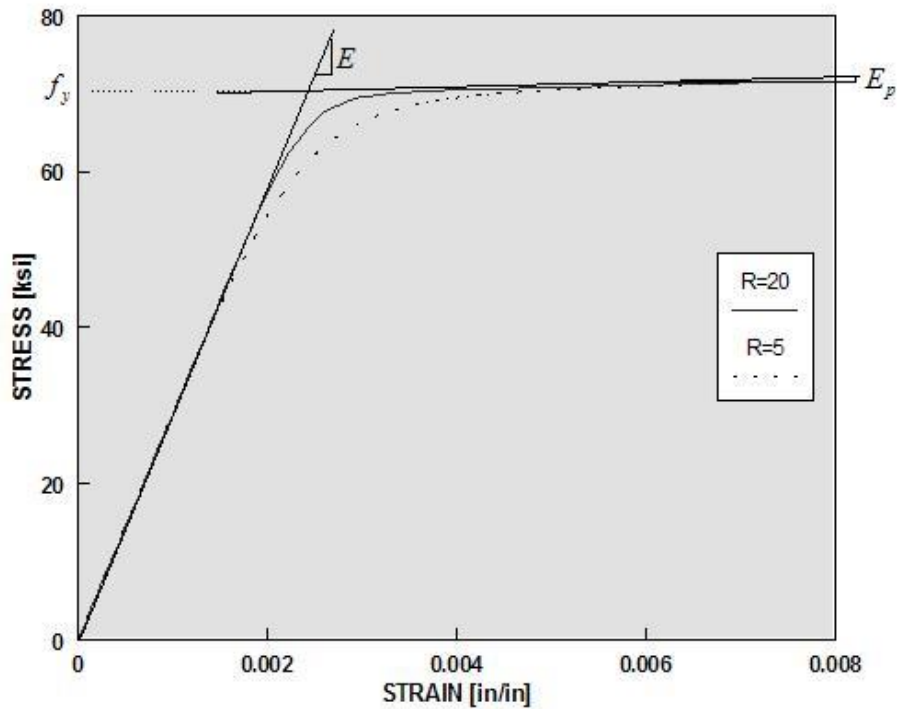


Figure 20 The Steel02 material model [25].

### 3.3.2.2 Elastic Modeling

The elastic model is the simplest and least computationally expensive model. In the elastic model nodes and elements are assigned based on the floor heights and bay widths. No rigid offset model is present in this analysis type and elements are fully elastic with section properties based on the area, Young’s modulus, and moment of inertia of the sections. Material models are not implemented in this model type as the only required material parameters are Young’s modulus.

For reinforced concrete elements the moment of inertia of the section is modified in accordance with ACI 3-18: 6.6.3.1.1(a) to account for the reduction in moment of inertia due to cracking [30].

### **3.3.2.3 Lumped Plasticity Modeling**

The lumped plasticity fiber model is one of the two model types which relies on fiber sections and the rigid offset joint type. Unlike elastic elements, the lumped plasticity and distributed plasticity models require element cross sections to be defined by sectional details and material models rather than just geometric properties. This necessitates the use of a fiber section. The fiber section is used to represent force-deformation relationships at the integration points along an element. The fiber section discretizes a cross section into subsections which each have their own assigned material and size. The conglomeration of all these subsections represents the overall fiber section which is then used for analysis.

In this model each node on the equivalent elastic model is replaced by a 5-node, 4-element module with dimensions equal to that of the full depth of the beam and width of the column as shown in Figure 21. The rigid offset is used to model beam column joints by placing a rigid zone in the area where the beam and column interfaces. By adding in a rigid offset, the locations of plastic deformation are pushed outward from the center of the node to where the face of the beam or column would protrude from the joint. The elastic model was deemed to not need the beam column joint as the elastic model is inherently lower fidelity does not see plastic deformation.

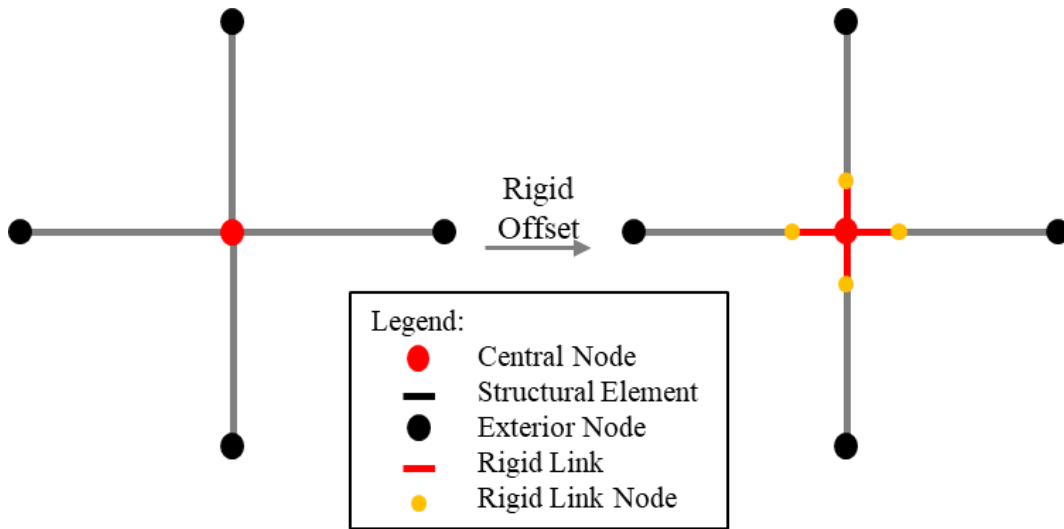


**Figure 21 Elastic Model Versus Lumped Plasticity Model with Rigid Offset.**

The lumped plasticity model employs zero length elements at the ends of the rigid offsets and elastic elements with the equivalent properties in between. The zero-length element have their moment-rotation relationship derived from a specified fiber cross section.

The lumped plasticity fiber in addition to the distributed plasticity fiber models are both models which take advantage of the creation of fiber-based sections. The sections are created based on materials and geometries specified in the building library. For general concrete applications, the simplified Kent-Scott-Park concrete01 material with degraded linear unloading and reloading stiffness is used [31]. For all rebar and steel sections, the Giuffre-Menegotto-Pinto steel material with isotropic strain hardening model is used [32]. Once the column and beam cross sections are created, geometric coordinate transformations and beam integration commands are implemented. Columns have five integration points across the elements and capture second order P-Delta effects whereas beams have 10 integration points and capture linear effects.

#### **3.3.2.4 Distributed Plasticity Modeling**

The distributed plasticity fiber model is the second model type to incorporate both force-based fiber elements and the rigid offset mechanism, however the elements joining the node clusters are fully fiber section elements. The benefit to a distributed plasticity model type is the ability to develop plasticity throughout the length of the element. A lumped plasticity model assumes beams and columns will have plasticity develop at the ends of the elements where the fiber section is specified, however for elements such as beams with high dead loads, plasticity can also occur at the center of the element and spread outward. The benefit to the distributed plasticity model is an increased ability for plasticity and frame growth. This model type currently represents the highest fidelity 2D model and is correspondingly much more computationally expensive.

#### **3.3.3 Application of Mass and Gravity Loads**

Masses and gravity loads are applied to the building structure in order to induce stresses, inertias, and deflections. Masses are assigned in two forms: elemental unit length masses which are representative of the self-weight of beams and columns, and point masses at nodes which represent the individual tributary areas multiplied by the assumed dead load of the structure. Loads are applied as nodal point loads and are equivalent in magnitude to the masses multiplied by gravity. The total mass and load on the lateral system represents only mass and load within the tributary area of the frame. For a building system which has interior gravity-only columns, the load associated with these columns induces the need for a leaning column.

### 3.3.4 The Leaning Column

After the loading of the building structure, a leaning column is attached to the structure to incorporate any additional loads due to the presence of internal gravity-only columns. While the leaning column is generated for each model, if there are no internal gravity-only columns, there will be no loads placed on the column. Loads that are applied on the leaning column are representative of the total load on interior gravity columns per floor, the model simplifies this by taking the total load as the total tributary area of interior gravity columns multiplied by the assumed distributed load.

The leaning tower shown in Figure 22 is constructed in a similar fashion to previous Opensees models [33]. The column is displacement-fixed, rotation-free at its base and consists of very stiff elastic elements coupled with rotational zero-length springs to create a set of rigid, pinned links. The rotational zero-length springs are required for model convergence. The column is tied to the main structure using very stiff truss elements which do not impart rotation.

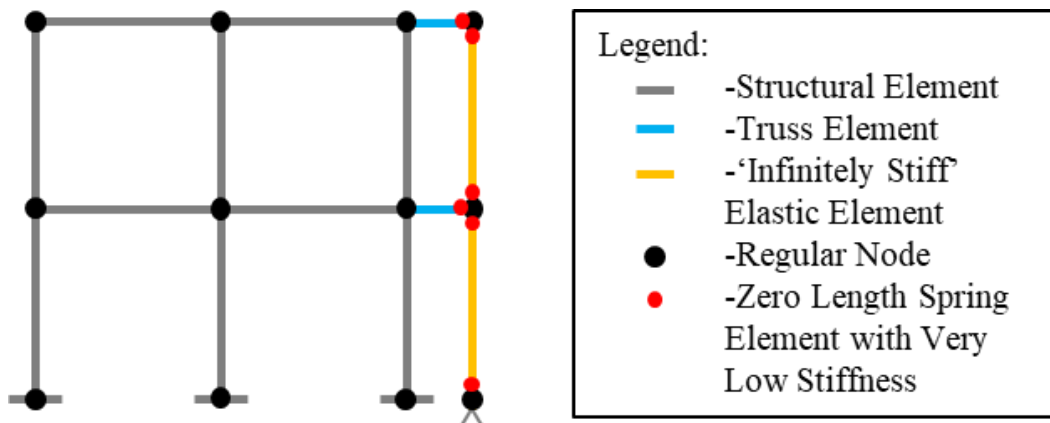


Figure 22 The Leaning Column Methodology.

### **3.3.5 Gravity and Earthquake Analysis**

Before subjecting the finished structure to a ground motion, a static gravity analysis is performed to determine initial stresses and deflections within the structure. This analysis is conducted in a static manner in a 100-step incremental loading with a linear analysis algorithm. Once the gravity analysis has been performed, the building is subjected to the specified ground motion.

The ground motion analysis is a transient analysis which constructs a convergence test that uses the norm of the right-hand side of the matrix equation to determine if convergence has been reached [34]. There are several nested convergence tests used the first of which is a Newton-Raphson solution algorithm that has a maximum of 10 iterations per timestep. If this solution algorithm fails to converge, a 100 step Modified-Newton algorithm which uses the tangent at the initial guess to iterate, instead of the current tangent. During each time step of the analysis, nodal recorders capture the nodal displacements of the leaning column. Interstory drifts as well as nodal displacements are calculated and logged in an output file as specified by the end user.

## **4.0 Model Builder Validation Studies**

Three full scale instrumented buildings were used to evaluate the accuracy of models developed using the Model Builder. The structures included a concrete moment frame building in Wellington, New Zealand (herein referred to as The Wellington Building), the Holiday Inn in Van Nuys California, and a full-scale concrete moment frame building tested on the E-Defense shake table in Japan. For each structure, three separate 2DOF models were created: elastic, fiber section based lumped plasticity, and full distributed plasticity. These models were subjected to ground motions for which measured instrumentation data was available, and the measured and numerical results were compared.

### **4.1 The Wellington Building**

The Wellington building was a 5-story reinforced concrete moment frame structure which was damaged in the 2016 Kaikōura earthquake. This building was comprised of three distinct modules which were tied together using rigid trusses on several floors to create a single structure. The modules themselves consisted of exterior moment frames with precast hollow core floor slabs spanning the interior 17m clear span as shown in Figure 23. The building was instrumented using both accelerometers and displacement transducers in several key locations within the building structure. The southernmost module of the building was fit with accelerometers in the ceiling cavity of each floor. These accelerometers measured accelerations in both directions of the frame.

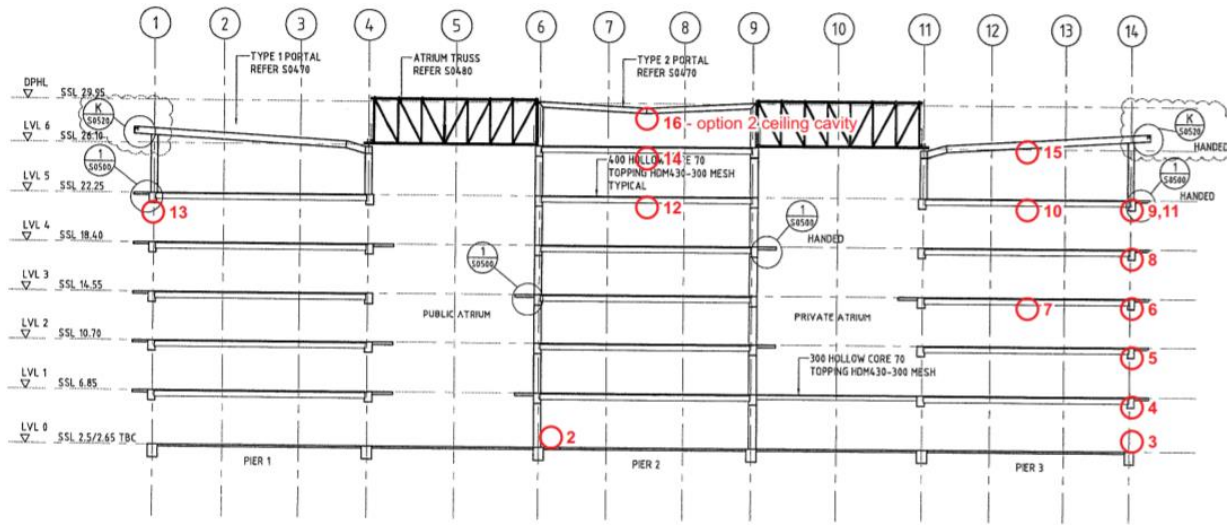
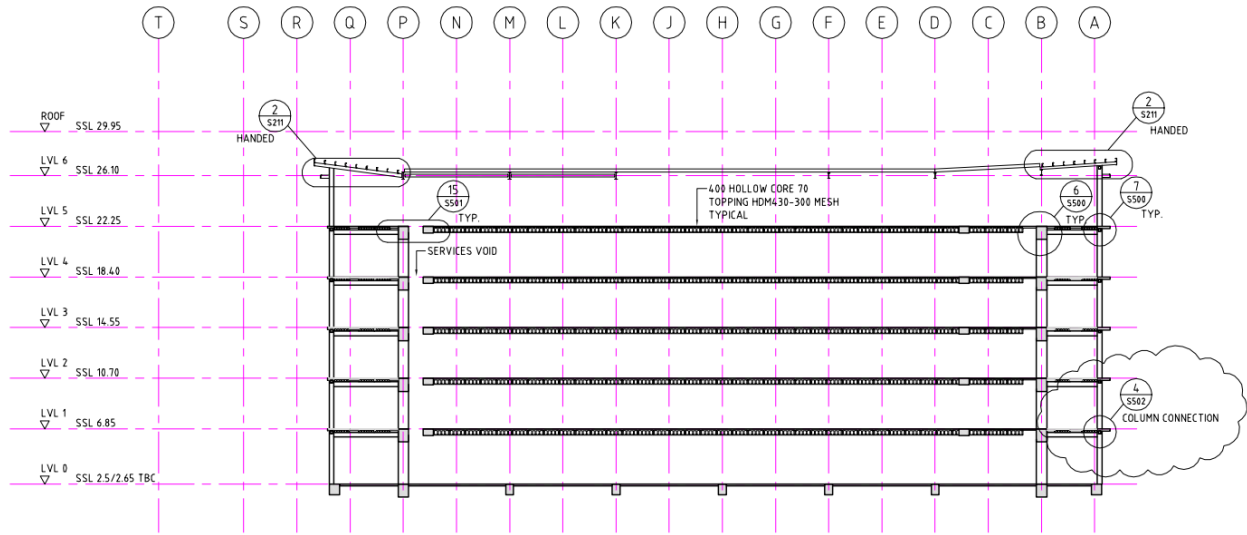


Figure 23 Elevation view of Sensor Locations within the Wellington Building [35].

#### 4.1.1 Model Generation of the Wellington Building

Due to the module-style design of the Wellington building, only the direction without the trusses was selected for the validation study. This direction was selected because individual frames connected with trusses could not be readily built using the model builder. Although the building itself was designed such that the individual modules were self-supporting and self-bracing, the linking of the modules via trusses added in additional support which couldn't be justifiably accounted for by adjusting the typical sections in a single frame within the builder.



**Figure 24 Elevation View of the Wellington Building Frame [35].**

The longitudinal moment frame modeled for this study consisted of a 5 story, 7 bay layout with a typical interior-moment frame column on column lines P, M, K, H, F, D, and B as well as a larger exterior column on line A which had strong axis orientation in the transverse direction. The simplified version of this model consisted of the same 5 stories and 7 bays, however the typical interior moment frame column was assumed for all columns including the exterior columns.

The dead load associated with the Wellington building was assumed to comprise of the sum of the weight of all concrete components: #400 Precast hollow core floor system with a 70mm screeded coating, beams, and columns. Due to the layout of the building structures, all mass and loads were applied to the frame as there were no interior gravity columns; no load was applied to the leaning column.

### 4.1.2 Comparison of Recorded and Simulated Response History

The numerical and recorded top-floor displacements are split for visual clarity between the linear elastic model and the nonlinear lumped plasticity and distributed plasticity models shown in Figure 25 and Figure 26 respectively. Top floor displacements were chosen for review as they represented the largest magnitude displacements and reflect the overall building response more accurately than the lower stories as the top floor displacements incorporate the stiffness of the entire structure. Displacement and story-drift response-histories can be found for all floors in the appendix. Periods for all structures were also calculated based on model type. Periods for the elastic, lumped plasticity, and distributed plasticity models were 1.22, 1.10, and 1.10 seconds respectively.

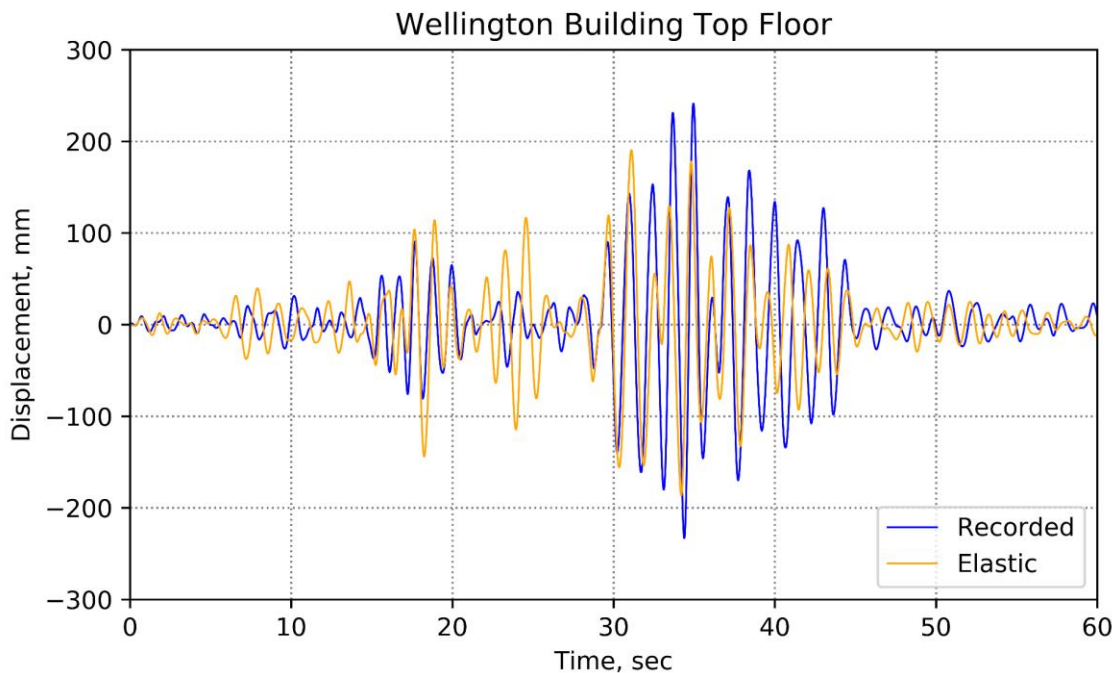


**Figure 25 Elastic Response History of the Wellington Building.**

The recorded data displays a peak displacement of 241mm at roughly 35 seconds with consistent peaks during the primary period of shaking of anywhere between 100 to 200mm as indicated in both figures. The elastic, lumped plasticity and distributed plasticity models all display relatively good fit to the recorded data. The overall magnitude of the analytical results closely matches that of the recorded response history. The maximum displacements of the elastic, lumped plasticity, and distributed plasticity analytical models are 190mm, 272mm, and 224mm respectively. The elastic model displayed spikes of over 100mm displacement in the time period between 20 and 30 seconds which was not present in the recorded data. These spikes may be due to the “cracked concrete” reduced moment of inertia assumption present in the elastic model where the actual structure was uncracked and therefore much stiffer than the analytical model. The peak displacement for the elastic model occurred before the recorded data at roughly 32 seconds, however, both the shape and magnitude of the peaks within the main displacement time period (between 30 and 45 seconds) is agreeable.

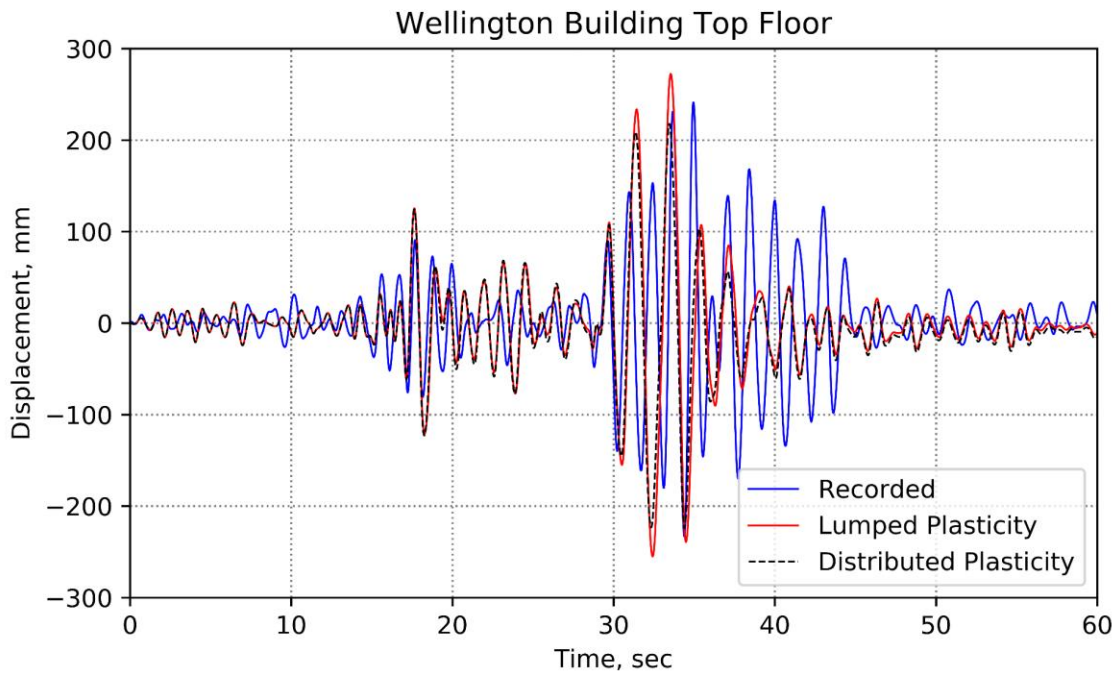


**Figure 26 Plasticity Model Response History of the Wellington Building.**

The lumped plasticity and distributed plasticity models displayed slightly different behavior as compared to the elastic model. The displacements occurring in the analytical models between 20 and 30 seconds is not as pronounced as the elastic model which would suggest that the cracked assumption is the cause of the large elastic deformations. Both plasticity models have peak displacements at the same time period occurring right before the recorded data peak. While the peak displacements align much more with the recorded data, the post peak behavior occurring between 30 and 45 seconds is much more damped as compared to the elastic model, with displacements quickly dropping off after the initial peaks. It is worth noting that while the lumped plasticity model had a significantly higher peak displacement, the response history closely matched that of the distributed plasticity model where disparities in displacements only occurred mostly at peaks.

## 4.2 The Van Nuys Holiday Inn

The Van Nuys Holiday Inn is a seven-story reinforced concrete structure. The building consists of two reinforced concrete moment frames with 8-bays spanning 150' 0" in the East-West direction and 3-bays spanning 61' 0" in the North-South direction. The structure suffered extensive damage in the 1994 Northridge earthquake resulting in being red-tagged after inspection [36]. The building was instrumented using both accelerometers and displacement transducers on several floors within the building structure. Sensors placed in the eastern stairwell of the building recorded data in both the North-South direction (short direction) as well as the East-West direction (long direction) on floors 1, 2, 5, and 7 as indicated in Figure 27.

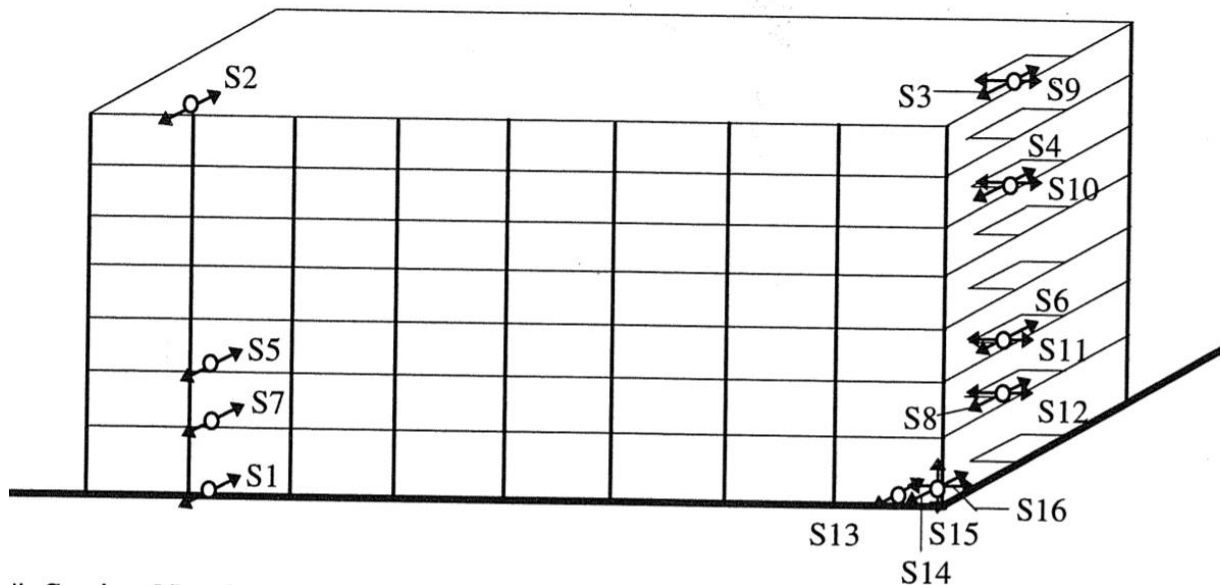


Figure 27 Layout and Location of Accelerometers in the Van Nuys Holiday Inn.

#### **4.2.1 Model Generation of the Van Nuys Holiday Inn**

The Van Nuys Holiday Inn is a very regular structure, and as such the Model Builder can quickly and easily analyze both directions of frames. The East-West moment frame consisted of a 7 story, 8 bay layout with a typical column and two beam details consisting of a unique section for the second floor and a typical section for all other floors. The model consisted of the typical column and beam details, simplifying the second-floor beams as the typical sections. The North-South moment frame utilized the same column and beam details however it was a 7 story, 3 bay layout. The bays were sized at 20' 1", 20' 8" and 20' 1" respectively for an overall length of 61' 0". The model generated distributed the 61' 0" span evenly across all three bays for three equal span lengths of 20' 4".

The dead load associated with the Van Nuys Holiday Inn was assumed to comprise of the sum of the weight of all concrete components: Cast in place flat slab, beams, and columns.

#### **4.2.2 Recorded versus Simulated Response History North / South Frame**

The frame in the North / South direction was the smaller of the two frames, consisting of three bays with uniform column and beam cross sections throughout all floors. Periods for the structure were also calculated based on model type. Periods for the elastic, lumped plasticity, and distributed plasticity models were 2.78, 2.84, and 2.84 seconds respectively. These periods greatly exceed the period estimated at 0.79 seconds [36]. It should be noted that the frame in the North / South direction has the same typical cross sections for both beams and columns as the frame in the East / West direction although less than half as many bays. This would indicate that the frame in the North / South direction, which is responsible for carrying the same mass and load as the frame

in the opposite direction, should have a much larger period than the frame in the East / West direction. The reported structural periods were 0.79 seconds and 0.88 seconds in the North / South direction and East / West direction respectively which does not appear to reflect the drastically different stiffnesses of the two frames.

Recorded response-history data was plotted against the elastic model and fiber models separately for clarity and can be seen in Figure 28 and Figure 29 respectively.

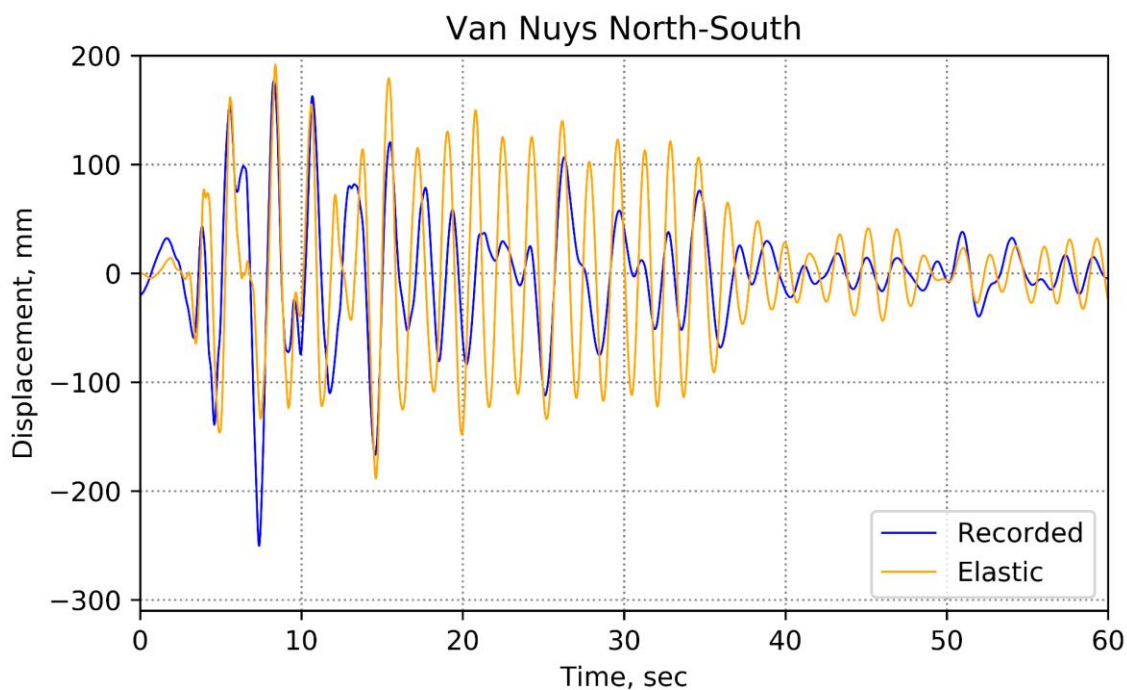


**Figure 28 Elastic Response History of the N/S Van Nuys Holiday Inn.**

All three models aligned acceptably both in terms of overall magnitude with the recorded data as well as alignment of peaks. Despite this, the overall response history of the elastic model is overly conservative as compared to the recorded data. The maximum displacement occurs at roughly 7 seconds which is shared across all models and the recorded data. The maximum displacement at this peak was 250mm for the recorded data, 191mm for elastic, 299mm for the lumped plasticity model, and 302mm for the distributed plasticity fiber model. While the peak of

the elastic model was not as high as expected, the elastic model did show much less stiffness as its post-peak vibrations were much higher than all other models and recorded data.

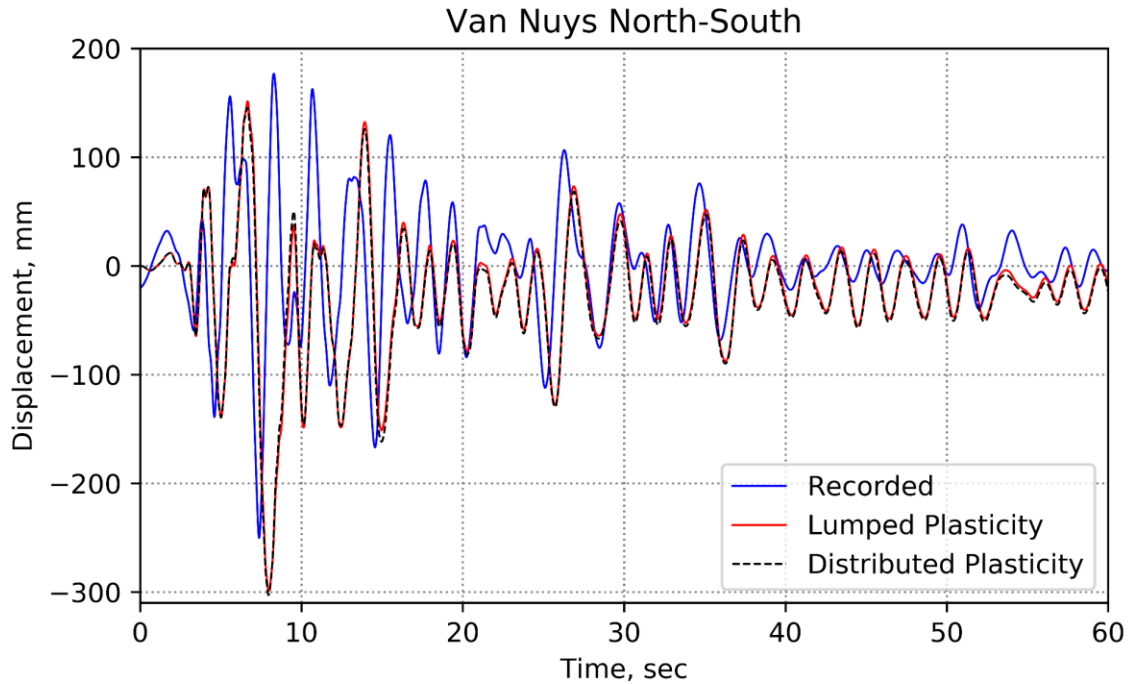


**Figure 29 Plasticity Response History of the N/S Van Nuys Holiday Inn.**

The lumped plasticity and distributed plasticity models shared nearly identical response histories throughout the entire event indicating that the formulation of the lumped plasticity model accurately portrays the response of a full fiber model for events with small amounts of residual plastic deformation. Overall, the response of the frame is inadequately modeled using an elastic analysis, however the results of both the lumped plasticity and distributed plasticity models are much closer to the recorded response.

### 4.2.3 Recorded versus Simulated Response History East / West Frame

The frame in the East / West direction consisted of seven bays with uniform column and beam cross sections throughout all floors. Periods for the structure were also calculated based on model type. Periods for the elastic, lumped plasticity, and distributed plasticity models were 1.71, 1.83, and 1.83 seconds respectively. These periods greatly exceed the period estimated at 0.88 seconds [36]. Despite doubling the reported periods, when compared to the modeled periods of the frame in the North / South direction the reduced periods reflect the much stiffer frame in the East / West direction.

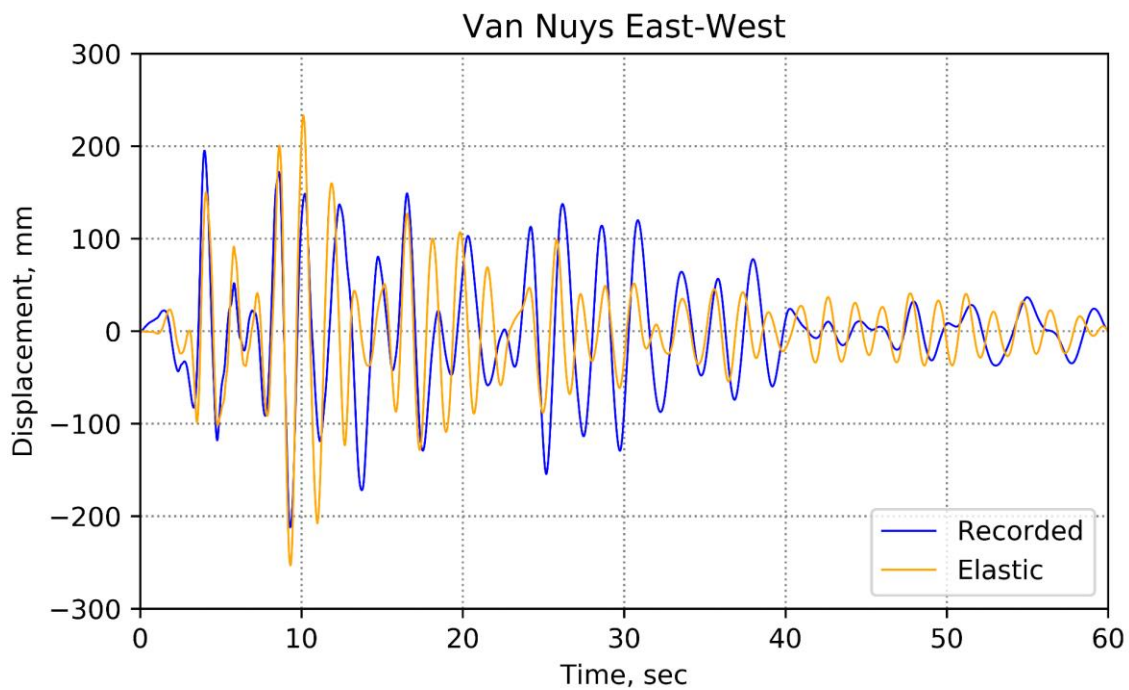
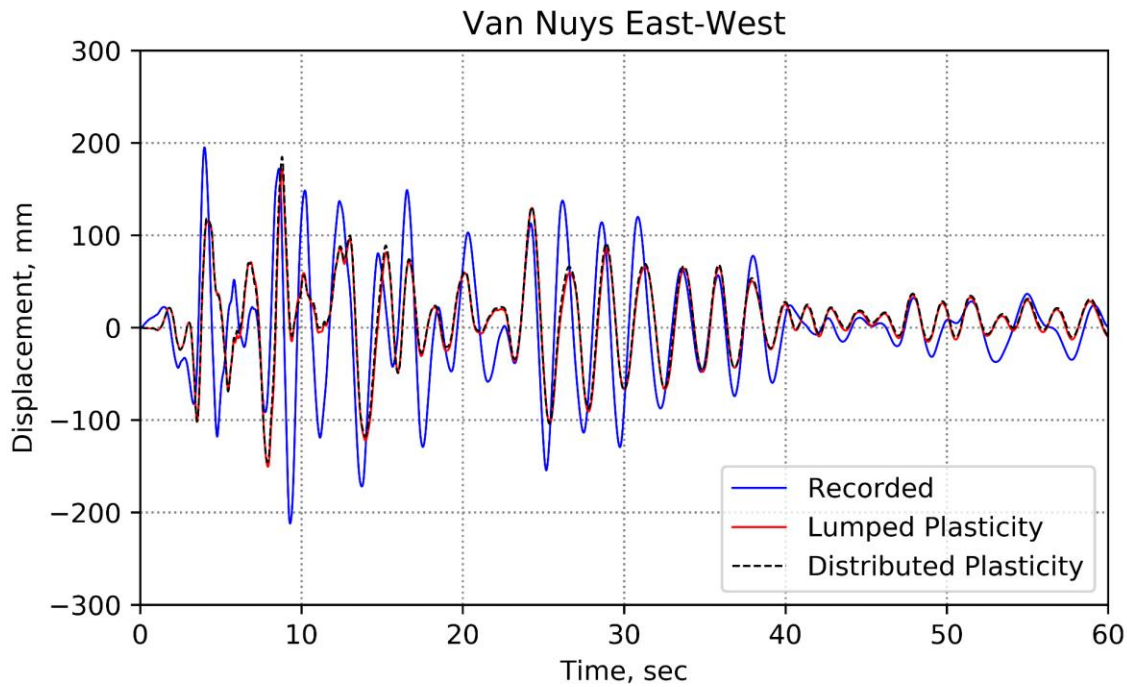


Figure 30 Elastic Response History of the E/W Van Nuys Holiday Inn.

The response of the East / West frame wasn't predicted as accurately as the North / South frame using the three modeling approaches. The recorded data displays a peak overall displacement at roughly nine seconds into the response history. This peak in the recorded data is only captured in the elastic model; the lumped plasticity and distributed plasticity models displayed a different response to the ground motion. After the positive displacement peak occurring at roughly eight and a half seconds, the recorded data and the elastic model both rebound into the overall maximum magnitude displacement peak in the negative direction.



**Figure 31 Plasticity Response History of the E/W Van Nuys Holiday Inn.**

The lumped plasticity and distributed plasticity models do not display this behavior, indicating that either the stiffness of these models was different than the actual stiffness of the frame, or the default 5% damping used in all models did not accurately represent the actual structural damping. The maximum displacement was 212mm for the recorded data, 253mm for elastic, 171mm for the lumped plasticity model, and 184mm for the distributed plasticity fiber

model. It should be noted that the maximum displacements for both the lumped plasticity model and the distributed plasticity model occurred at the same peak of roughly 8.5 seconds, the peak immediately preceding the peak that the recorded and elastic models share. The recorded model also displays a significant amount of post peak vibration occurring between 20 and 40 seconds in the response history. While all three models also displayed this, none of the models displayed displacements as large as displacements measured in the recorded data, indicating that perhaps the load takeoff performed under accounted for mass and subsequent loads.

#### **4.2.4 Comparison Response History Between Frames in Both Directions**

While both frames share the same exact column and beam sections, the frame in the East / West direction has over twice as many bays (7 versus 3) than the frame in the North / South direction. With both frames being required to support the same amount of seismic mass and load, it is posited that the displacement response history of the frame in the East / West direction should have peak displacements roughly half that of the frame in the North / South direction, assuming limited inelastic behavior. With a maximum peak displacement of 212mm in the East / West direction and 250mm in the North / South direction, the overall peak displacement of East / West frame is only 15% lower than that of the substantially less stiff North / South direction.

Periods generated by the Model Builder were in excess of two times higher than the reported periods. Despite this, the reported periods were marginally different, which does not align with the drastically different stiffness in the two frames. The relationship between frame stiffness and period aligns much better with Model Builder results. Despite this, the overall magnitude of the periods generated by the Model builder are significantly higher than engineering judgement, and basic period estimations, would dictate as acceptable.

### 4.3 The E-Defense Building

Two, full-scale, four-story buildings were constructed as part of a shake table test conducted in December 2010 at the E-Defense facility in Japan [37]. The buildings consisted of a 2-bay moment frame in one direction and a shear wall in the other shown in Figure 32. One of the buildings tested was a non-prestressed conventional reinforced concrete structure, while the other was post-tensioned; the conventional reinforced concrete structure is used as the validation case-study here. The buildings were subjected to a series of 5 ground motions which were based on the 1995 Kobe earthquake and the Takatori record. The first three ground motions were the 25% scaled Kobe, 50% scaled Kobe and the full 100% unscaled Kobe earthquake. These three tests were followed by the 40% scaled Takatori record, and finally the 60% scaled Takatori record. Severe damage developed in the traditional reinforced concrete building after the 100% Kobe ground motion, and as a result the comparison between recorded and the Model Builder does not include the 40% Takatori nor the 60% Takatori records due to the large loss in stiffness in the experimental run.



Figure 32 The Layout of the Two E-Defense Buildings [37].

### **4.3.1 Model Generation of the E-Defense Building**

The East-West moment frame of the E-Defense building consisted of a 4 story, 2 bay layout with the same column and beam cross sections at each floor. The generated model consisted of these same column and beam section details; no simplifications were required. It should be noted that the North-South shear wall consisted of a 2.5m x 0.25m thick wall that is centered within the 7.2m bay. The shear wall was not accounted for in the modelling of the moment frame, and despite it being oriented perpendicular to the moment frame, its presence may have impacted the outputs of the recorded response history of the moment frame.

### **4.3.2 Comparison of Recorded and Simulated Response History**

#### **4.3.2.1 Kobe 25% Scaled Ground Motion**

The first analysis performed was the Kobe ground motion scaled to 25% peak ground acceleration. The recorded response history of the structure saw small displacements on the order of only +/- 20mm in either direction as indicated by the top story displacement history plotted in Figure 26. The top story displacement exhibited seven peaks of roughly 20mm each in the timespan occurring between 4 and 6 seconds. After this, the structure did not experience any displacements exceeding 15mm with displacements quickly trailing off under 10mm in either direction. Results from the elastic, lumped plasticity, and distributed plasticity models do not align well with the recorded data for the 25% Kobe event. While the peak displacements occurred roughly at the same time, the magnitude of all three analytical responses are on the order of two to three times the recorded response throughout the entire response history.

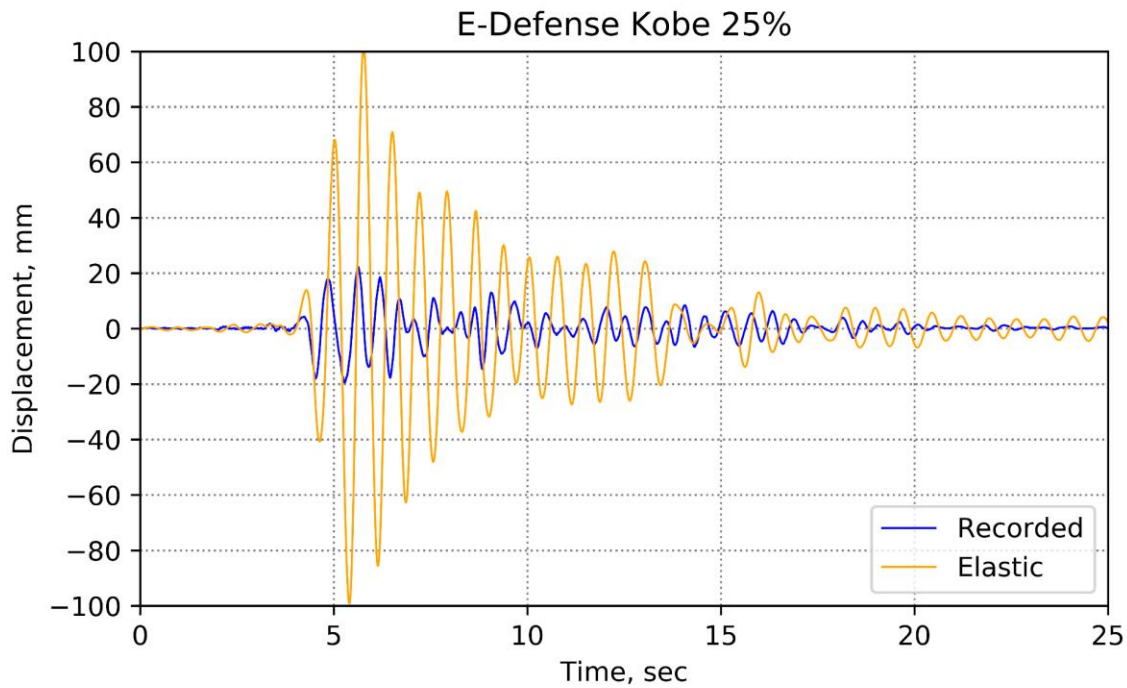


**Figure 33 Elastic Response History of the E-Defense Structure (Kobe 25%).**

Periods for the structure were also calculated based on model type. Periods for the elastic, lumped plasticity, and distributed plasticity models were 0.74, 0.61, and 0.61 seconds respectively as compared to the reported 0.3 second period. For a structure of this scale, the reported period seems much more in line with expected values. Despite the large disparity of magnitudes in the analytical versus experimental results, there are several key features which are also of interest. The overall period and shape of the modeled result indicates much less stiffness than the recorded results, this is evident both in the magnitude of the displacement, but also the period of vibration (0.74 seconds and 0.61 seconds versus 0.3 seconds).

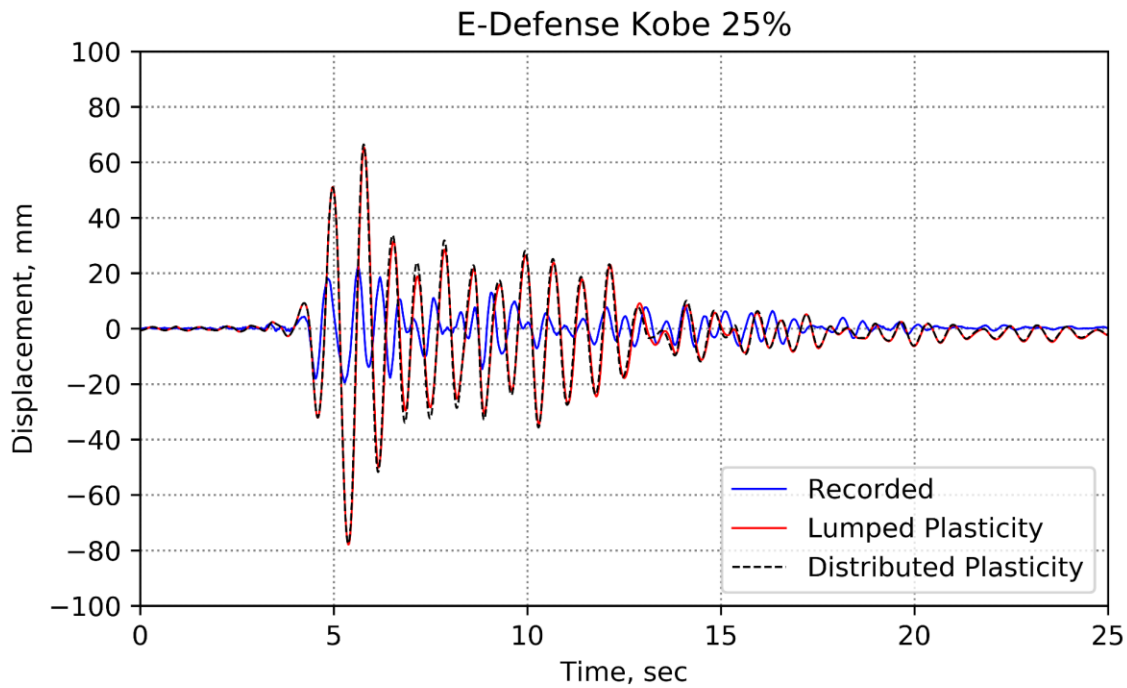


**Figure 34 Plasticity Response History of the E-Defense Structure (Kobe 25%).**

The analytical results all had much higher periods than the recorded response, and all three analytical results went out of sync with the recorded result early into the response history. Despite this, all three analytical results line up well with respect to each other, this would suggest that the experimental setup had additional stiffness that the model builder was incapable of capturing. Since the E-Defense structure had typical cross sections for the columns and beams, no compromise was made in terms of modeling cross sections, therefore it is of the opinion of the author that the tensile strength of the concrete, which is not accounted for in the Concrete01 material mode, greatly contributed to the overall stiffness of the structure, fundamentally changing the response of the moment frame. In the elastic model, the included assumption of a reduced moment of inertia due to cracked concrete for beams and columns is also not applicable for a response history that is completely linear elastic.

#### 4.3.2.2 Kobe 50% Scaled Ground Motion

The second analysis performed was the Kobe ground motion scaled to 50% the peak recorded ground acceleration. The displacement vs. time plot for the top story was again split between elastic elements and fiber elements and is shown in Figure 35 and Figure 36. Doubling the intensity of the ground motion (in terms of PGA) caused a large increase (over six-times that of the 25% ground motion) in recorded peak displacement. As with Kobe 25%, peak displacements occurred within the timeframe of 4 to 6 seconds with the maximum recorded displacement being -141mm occurring just after five seconds.

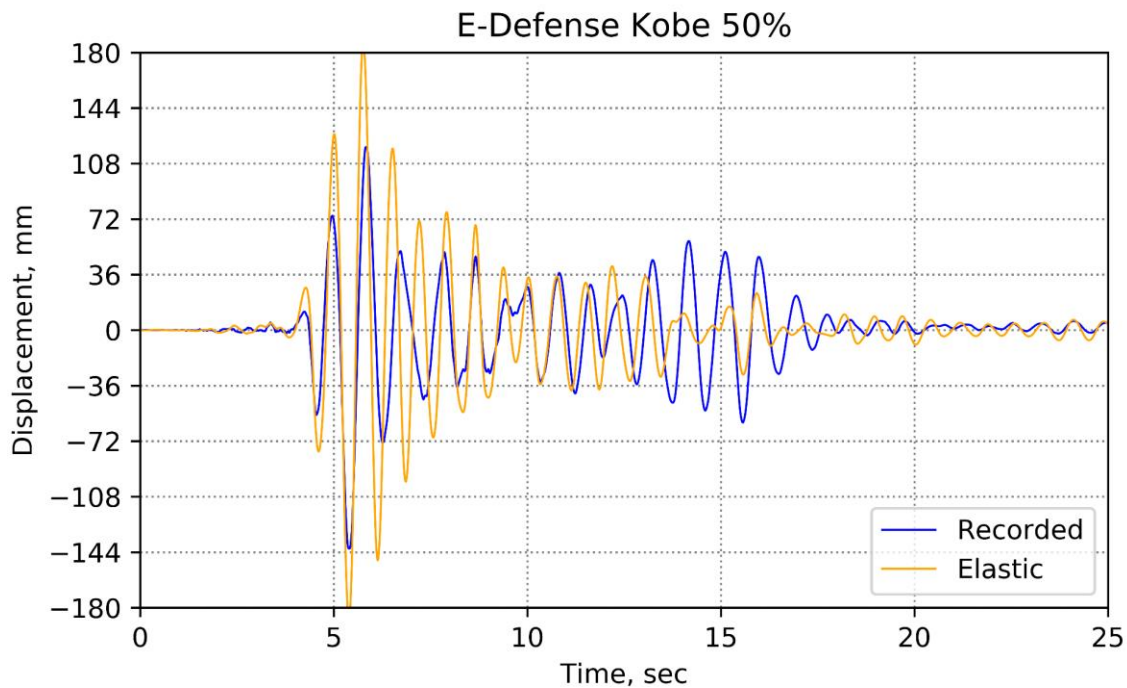


**Figure 35 Elastic Response History of the E-Defense Structure (Kobe 50%)**

The overall response of the analytical models shows much better fitment with the recorded data. Peak displacements all occurred at the same peak (which was the same peak as the recorded displacements), and the overall maximums are relatively similar. The maximum displacement was 141mm for the recorded data, 187mm for elastic, 159mm for the lumped plasticity model, and

160mm for the distributed plasticity fiber model. As opposed to the Kobe 25% run, all three models for the Kobe 50% run displayed good fitment both in terms of magnitudes, but also in alignment of the peaks and troughs of the analytical data lining up well with the recorded data. The period between 13 and 17 seconds is the only area where displacements between analytical and experimental do not fit well.

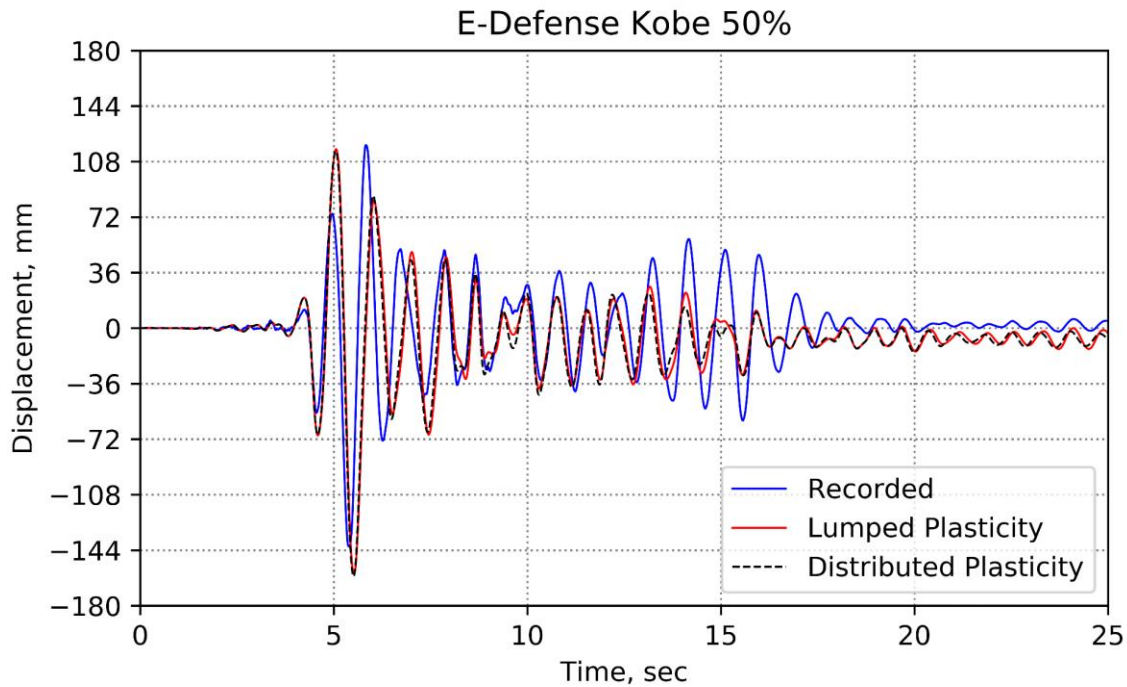


**Figure 36 Plasticity Response History of the E-Defense Structure (Kobe 50%)**

The experimental data shows a not-unsubstantial amount of secondary displacements which wasn't captured in any of the analytical models, the reason for this disparity is currently unknown. Despite this, the Model Builder was able to successfully model the response of the structure under the Kobe 50% ground motion, matching both peak displacements as well as overall response history.

### 4.3.2.3 Kobe 100% Scaled Ground Motion

The final response history evaluated for the E-Defense building was the Kobe ground motion at 100% scale relative to the recorded peak PGA. It should be noted that due to the testing regime of the E-Defense structure, cracking had already occurred due to both the Kobe 25% and Kobe 50% motions having been run prior. This disparity was not captured in the Model Builder and may be a cause for disparities in the comparison between analytical and experiment data.

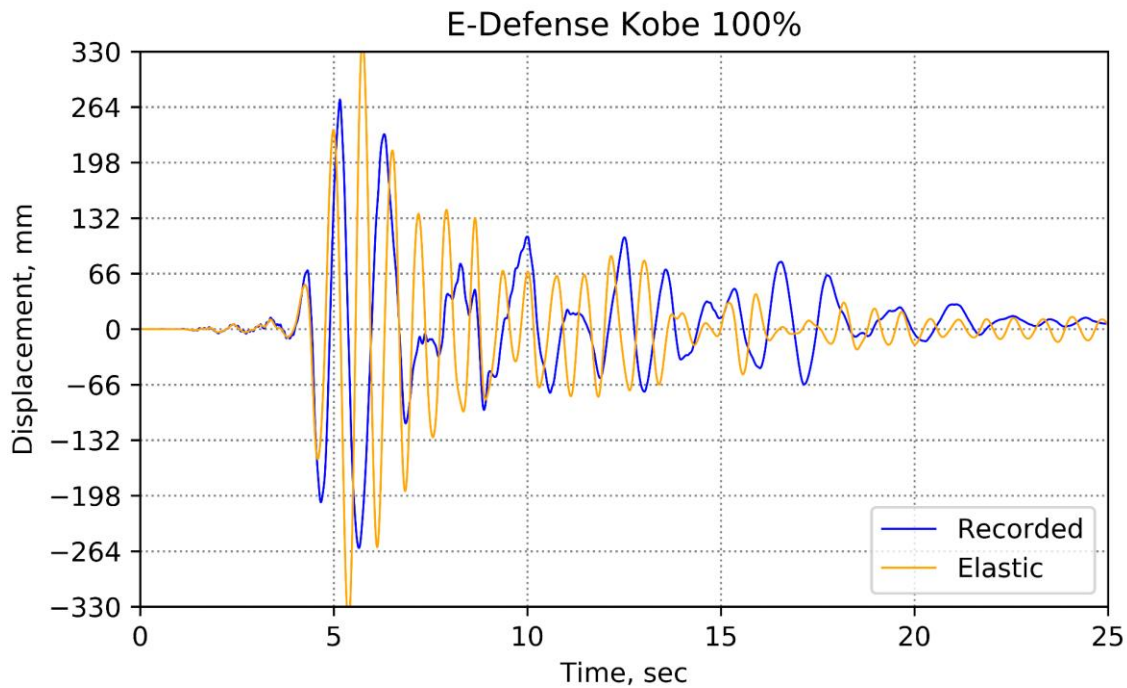


**Figure 37 Elastic Response History of the E-Defense Structure (Kobe 100%).**

The analytical response for both elastic (Figure 37) and fiber models (Figure 38) compares moderately well with the experimental data. Peaks are aligned with the recorded response indicating a similar period, however the overall magnitude of the displacements for the lumped plasticity and distributed plasticity models underpredict the recorded data throughout. The experimental data recorded a peak displacement of 270mm occurring just past five seconds. This peak displacement occurred at the same time step as the same peak of the lumped plasticity and

fiber models having 218mm and 223mm of displacement respectively. The elastic model displayed much higher displacements with maximum drifts exceeding 330mm in two instances.

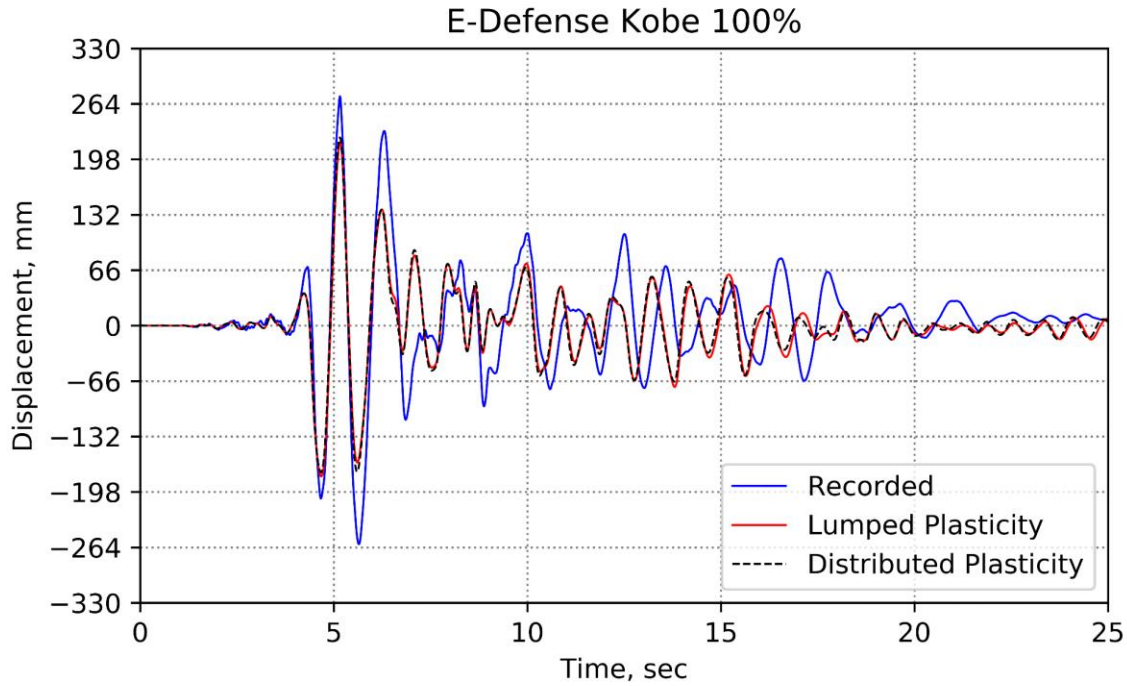


**Figure 38 Plasticity Response History of the E-Defense Structure (Kobe 100%).**

As previously stated, discrepancies between the recorded and numerically generated data may be a result of the repeated loading history in the experimental specimen. Namely, the cracking and resulting loss of stiffness in the experimental specimen from the Kobe 25% and 50% runs are not reflected in the lumped plasticity or distributed plasticity models, resulting in an underprediction of displacement throughout the response history.

#### **4.4 Results of the Validation Tests**

Three separate instrumented buildings were used to validate the Model Builder. General results indicate that the Model Builder is adequate for modelling reinforced concrete frames in terms of overall stiffness, peak system displacements, and overall response history. Issues may arise when utilizing the Model Builder to analyze structures undergo displacements and strains which reside purely in the linear elastic range as hypothesized in the E-Defense Kobe 25% comparison. The simplification of structures into unidirectional systems may also affect the response of small structures where the lateral system in the direction orthogonal to analysis may be adding stiffness to the overall system. Further testing with instrumented buildings can help to continue to validate the response of the Model Builder, specifically with respect to other lateral load resisting systems.

## 5.0 Batch Analysis Time Study

To evaluate the applicability of the Model Builder for regional response simulation, fourteen buildings from an existing structural database were identified and selected for a batch analysis and time study [38]. The purpose of the time study was threefold: (1) demonstrate the batch application of the Model Builder, (2) perform a time study of the required time to log individual buildings into the *Building Information Database*, and (3) to compare the analysis time required for the three MDOF model types (elastic, lumped plasticity, distributed plasticity). The buildings used in the study are summarized in Table 2 and consisted of thirteen concrete moment frames and one steel moment frame ranging in size and scale. These buildings were selected from the Wellington Structural Inventory, which contains general structural information and structural drawings [38].

**Table 2 A Summary of Buildings used in the Time Study.**

Building	Constructed	Stories	Frame Type
1	1973	18	Concrete MF
2	1940	5	Concrete MF
3	1960	8	Concrete MF
4	1961	9	Concrete MF
5	1930	8	Steel Frame
6	1936	8	Concrete MF
7	1955	7	Concrete MF
8	1962	5	Concrete MF
9	1970	11	Concrete MF
10	1958	4	Concrete MF
11	1960	9	Concrete MF
12	1968	13	Concrete MF
13	1981	13	Concrete MF
14	1956	6	Concrete MF

## **5.1 Creation of the Building Index**

Using detailed structural plans, the building information database spread sheets were populated for each of the fourteen buildings. To perform this process, each building was first identified as a suitable candidate for the Model Builder software based on general structural layout. The general building dimensions (number of floors and bays) were then determined and cataloged. A preliminary load takeoff (idealized as the weight of the floor slabs within the building) was calculated, and finally representative column and beam cross sections were determined and cataloged. A total of 116-minutes was required to log all fourteen buildings, which averaged to 8.3 minutes per building. It is worthy to note that the building indexing process decreased in time with experience. The first building indexed took 23 minutes to identify and log, whereas later buildings required an average of five to six minutes to catalog.

## **5.2 Ground Motion Determination**

The buildings were subjected to the Chi-Chi Taiwan ground motion from the FEMA P695 ground motion acceleration history suite [39]. The recorded response spectrum for this motion, as well as the contemporary design spectrum for all structures in this study are shown in Figure 29. The Chi-Chi ground motion was selected because the response spectrum can be easily scaled to match the design spectrum for varying seismic hazards. Here, the recorded response spectra was scaled to three different probabilistic seismic hazards (2% in 50 year, 10% in 50 year, and 10% in 10 year) such that the mean of the spectral acceleration from the recorded response spectrum within the constant acceleration region of the design spectrum was equal to the constant spectral

acceleration in the design spectrum. The scale factors were then applied to the ground motion acceleration history for the batch analyses. The buildings were analyzed for each hazard using the three MDOF approaches, for a total of 126 total building analyses. Note that the three seismic hazards were selected to provide a range of building response within the batch analysis – from mostly elastic to highly non-linear.

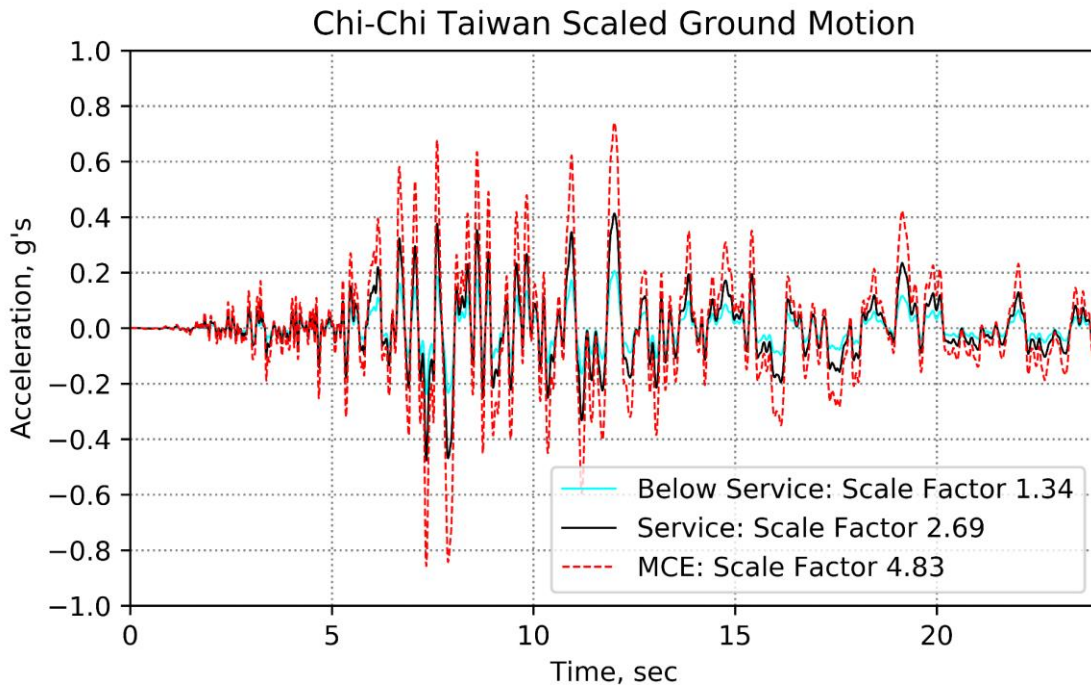


**Figure 39 Chi-Chi Taiwan FEMA P695 121042 Scaled Ground Motion.**

### **5.3 Time Required for Analysis**

A summary of the time required for each analysis is given in Table 3. The distributed plasticity approach was the most computationally demanding, requiring approximately two-hours to analyze all fourteen buildings for a single ground motion. The lumped plasticity approach took an average of 1.3 hours, while the elastic approach averaged 2-minutes. The overall time to

complete all 126 analyses consisting of an equal distribution between model types lasted just over ten hours with the bulk of the time required for the distributed plasticity analyses. All analyses were performed in series using a non-overclocked Intel core i5 7300HQ with a base speed of 2.5GHz with turbo range up to 3.5GHz.

**Table 3. Analysis Times By Ground Motion**

	10% in 10			10% in 50			2% in 50		
Building	E	LP	DP	E	LP	DP	E	LP	DP
Time (min)	2	70	110	2	72	117	2	85	145

#### **5.4 Damage State Characterization**

The damage state of each building in the batch analysis was determined based on the maximum story drift recorded during each response history analysis. The damage states corresponding to the maximum drifts were determined using ATC-58 fragility functions, which were developed for Special Moment Frame (SMF), Intermediate Moment Frame (IMF) and Ordinary Moment Frames (OMF) [40]. For the purposes of this analysis, the OMF damage state fragility function was utilized with 5 damage state break points (Damage State Zero – Damage State Four) as summarized in Table 4. Damage state zero (DS0) is characterized by yielding of reinforcing and a maximum crack width exceeding 0.5mm. This damage state can be repaired through epoxy injection into the cracks and has no structural penalty. Damage state 1 (DS1) is characterized by crack widths in excess of 1.3mm and has a similar repair methodology with epoxy injection. Damage state 2 (DS2) is characterized by the initiation of cover concrete spalling and reinforcing bar slippage. The repair procedure requires patching of spalled concrete. Damage

state 3 (DS3) is characterized by concrete crushing, spalling of cover concrete exceeding 30%, and exposure of longitudinal reinforcing. The repair procedure replacing the spalled concrete. The final damage state, damage state 4 (DS4) is characterized by failure due to beam or column longitudinal steel buckling or loss of anchorage within the member. This damage state is the most severe as it requires full replacement of concrete and steel within the member.

**Table 4 Damage States Related to Maximum Story Drift.**

Maximum % Drift	1.16%	2.0%	2.36%	3.36%	> 3.36%
Damage Level	Damage State 0	Damage State 1	Damage State 2	Damage State 3	Damage State 4
Description of Damage	Yielding; Crack Width < 0.5mm	Crack Width > 1.3mm	Spalling and Bar Slippage	Spalling Exceeding 30%	Longitudinal Steel Buckling

An overview of the estimated damage states of all buildings within the batch study is given in Figure 40. While not the primary focus of the time study, an assessment of the damage reveals several notable features. The damage characteristics and relative damage states remain constant for the elastic, lumped plasticity and distributed plasticity models. Although the estimated damage states were not identical for all model types for a given building, buildings which saw high damage states in an elastic analysis also tended to display high damage states in the lumped plasticity and distributed plasticity analyses. These results suggest elastic modeling may be sufficient in capturing damage state characterization in line with higher levels of analysis. Buildings also tended to be grouped in damage states by fundamental period; buildings with lower periods tended to share the same or relatively similar damage states to structures with similar periods. This agrees with the notion that the alignment of natural ground motion frequency and building frequency is what causes damage. Finally, as expected, overall damage states tended to follow accordingly with scaled ground motions. The damage states seen in structures for the below service scaled

ground motion did not exceed damage state 1, with two notable damage state 3 exceptions. Damage states at service reflect the performance of the structures with most structures in either damage state one or three. Lastly, the maximum considered event (MCE) level event caused DS4 in several buildings.

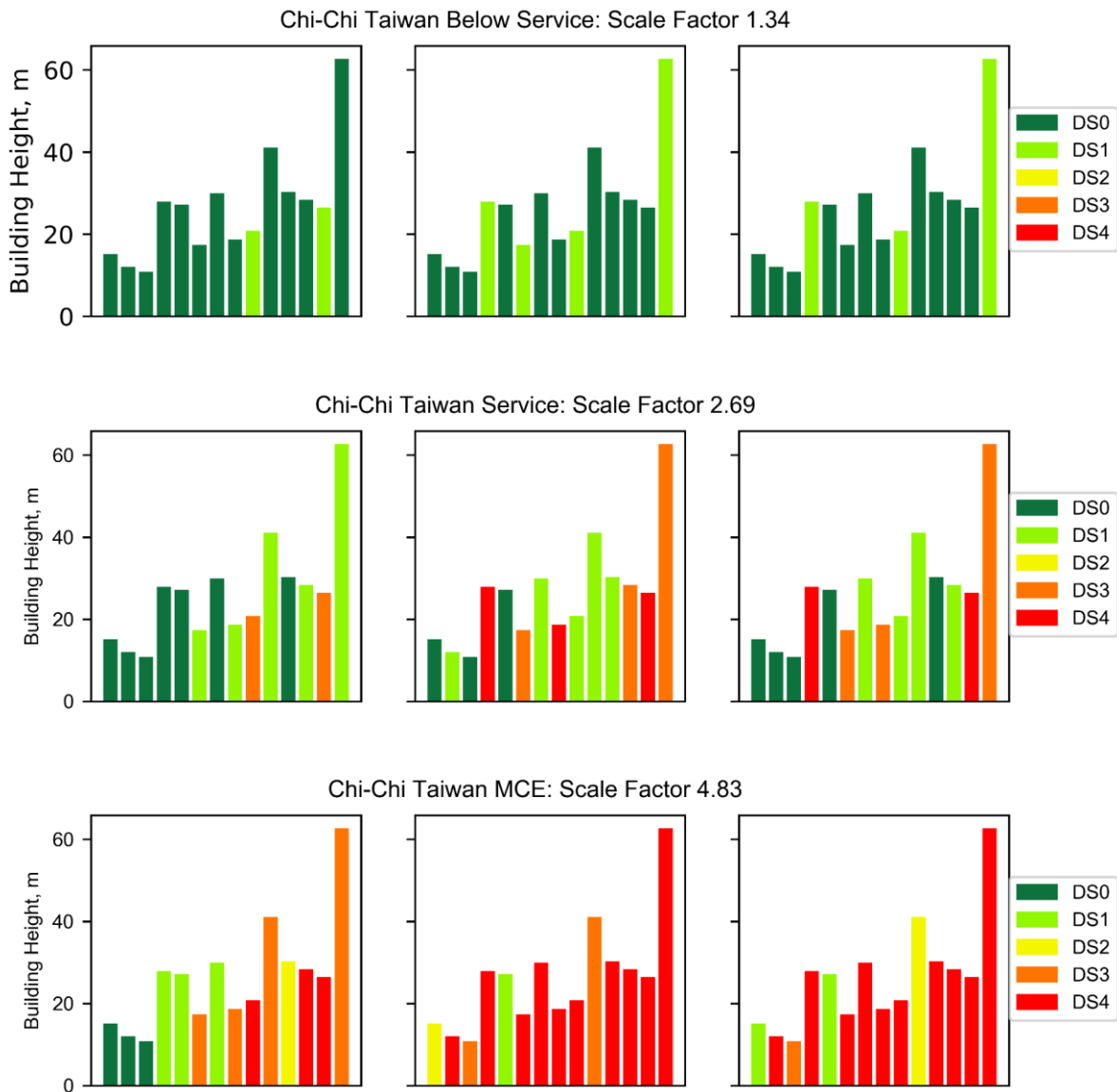


**Figure 40 Time Study Batch Analysis. Left to Right: Elastic, LP Fiber, DP Fiber.**

## 5.5 Methodologies for Real World Application and Optimization

The time study demonstrated several key points regarding the applicability of the Model Builder software for regional structural performance evaluation:

1. If the key buildings in a city have been indexed prior to a ground motion, the Model Builder software provides an avenue for rapid multi-fidelity analyses to determine an inspection priority list.
2. The fidelity of the selected modeling type can be prioritized based on required immediacy of the analysis. For a high impact event, an elastic analysis can be performed to get a rudimentary scope of impacted buildings. This analysis would be followed up with a higher fidelity MDOF analysis. If time permits, a full distributed plasticity analysis can be performed to assess structures to the highest capacity. Secondly, for a medium impact event, a lumped plasticity analysis strikes a balance between computation time and accuracy. Lastly for a low impact event a full distributed plasticity analysis can be performed without the need for an immediate elastic analysis for preliminary results.
3. The demonstration batch analysis here was performed in a series. The time to run the analyses can be improved through several methods. A computer with a high-end CPU with emphasis on single core performance can drastically increase computation time. Analysis times can further be increased through parallel processing, either through application of multiple instances of the Model Builder or through the development of OpenseesMP, a parallelization module for Opensees.py.

## 6.0 Parametric Sensitivity Study

A sensitivity study was conducted on the 2DOF models to (1) ensure that all mass and axial load parameters were incorporated into the models correctly and (2) to determine the parameters which have the largest impact on the efficacy of the output. The Van Nuys Holiday Inn was used for the study as it had the most regular layout of the case-study validation buildings. In addition to being instrumented, the building had a uniform column detail and only two unique beam details.

Several key parameters were identified for the sensitivity study including: (1) the mass and axial load applied to the frame and columns, (2) the beam and column cross section geometries, and (3) variations in the nominal and actual material strengths. Four separate studies were selected to evaluate the sensitivity of the models. First the effects of the mass and corresponding axial load parameters were evaluated. The mass and corresponding axial load parameters were selected because the mass applied to the structure within the model can vary significantly based on how the user indexes the structure. For example, a simple office structure may be adequately modeled by just using the weight of the slab and structural components. A library on the other hand, with floor to ceiling stacks would not generate an accurate result if only the slab and structural components were used. Two comparisons were performed based on the changing of mass: (1) changing the overall floor load by +/- 25% and (2) incorporating the miscellaneous dead loads associated with the structure (e.g. cladding, partition walls). Next, the influence of the interaction of the leaning column was evaluated. This study specifically evaluated the behavior of the structure if the gravity carrying axial load is applied to the frame rather than the leaning column. The next study evaluated the effects of utilizing typical vs atypical cross sections. The Van Nuys Holiday Inn has a standard column cross section for its exterior moment frame; however, the second-floor spandrel

beam is unique as compared to the typical cross section for the rest of the floors in the structure. This comparison looks at the change in response if the typical beam section is used as compared to the second-floor beam cross section. The final study evaluated the influence of the material properties on the overall response – namely the influence of specifying nominal vs. actual properties. While the concrete in the Van Nuys Holiday Inn may be specified as 5ksi, actual material properties are design with an excess of capacity. This may result in a vastly different structural response. The four sensitivity case studies were compared against the recorded data.

## **6.1 Mass and Load**

The first study evaluated the influence of changing the overall floor load by  $\pm 25\%$ . When indexing large numbers of buildings, a user may find that they have incorrectly characterized the mass of the structure. Either by using an atypical slab thickness, or by missing a detail, it could be reasonably estimated that the floor load could be off by 25%. This study evaluated the influence of changing the mass, and resulting axial load, impacted the period and resulting output of the structural response history.

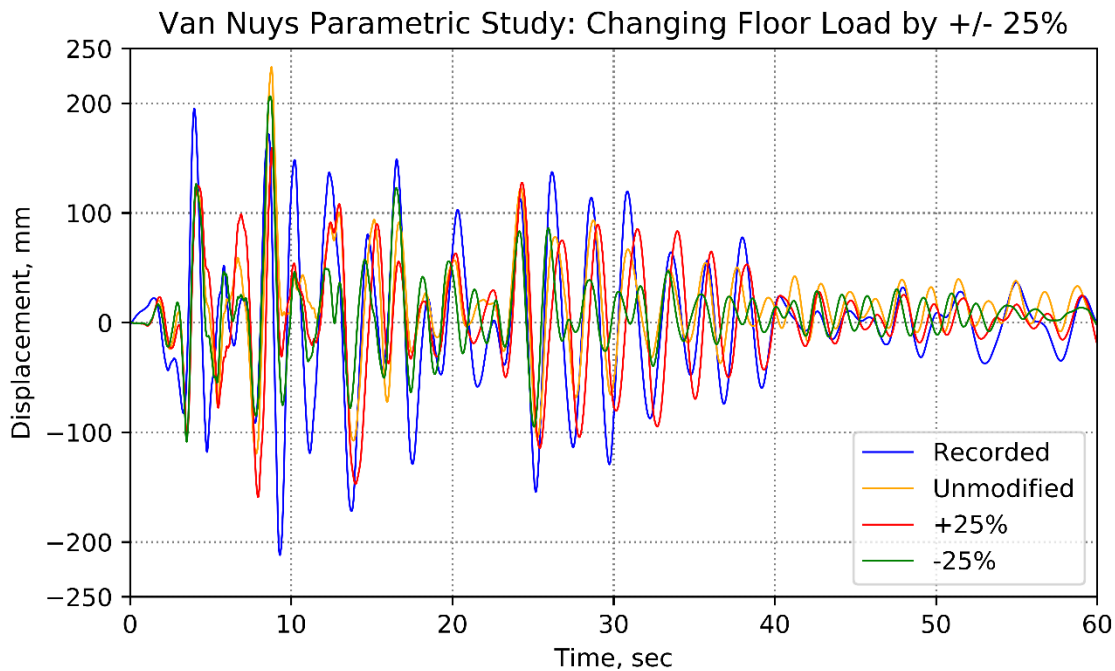


**Figure 41 Van Nuys Parametric Study: Changing Floor Load by  $\pm 25\%$ .**

While the general shape and magnitude of all three response histories seen in Figure 41 is generally agreeable with the recorded data, removing 25% of the mass and load resulted in lower peaks and an overall stiffer response as expected. With less structural mass and load the structure correspondingly displayed lower magnitude displacements throughout the entire response history. The maximum top floor displacement for all three simulated responses occurs at 8.5 seconds as compared to the very distinct opposing peak in the recorded data occurring at 9 seconds. The unmodified data showed the highest peak displacement at 233 millimeters as compared to the 159 and 206 of the models with 25% removed and added respectively. The addition of 25% extra mass and load generated an overall response which most closely aligned with that of the recorded response. The period between 25 and 40 seconds displayed large displacements which was most closely matched with the run that had an additional 25% mass.

## 6.2 Accounting for Miscellaneous Dead Loads

The second study evaluated the influence of accounting for mass from various dead loads that would be found in a typical structure. Using ASCE 7-10 several additional dead loads such as a drop ceiling, miscellaneous partitions, and mechanical allowances were incorporated [26]. The added masses are summarized in Table 5.

**Table 5 Miscellaneous Dead Loads Incorporated.**

Load Categorization	Load	Unit
Permanent Partitions	10	PSF
Finish Allowance	10	PSF
Mechanical Allowance	4	PSF
Drop Ceiling	2	PSF
Total	26	PSF

The addition of these loads resulted in an increase in the general floor loads by 20%, thus the response of the modified model is similar that of the 25% added mass run in the previous study. The overall peak displacement shown in Figure 42 was reduced compared to the unmodified run; however, the overall shape and magnitude of the response history more closely matched the recorded top floor displacement throughout.

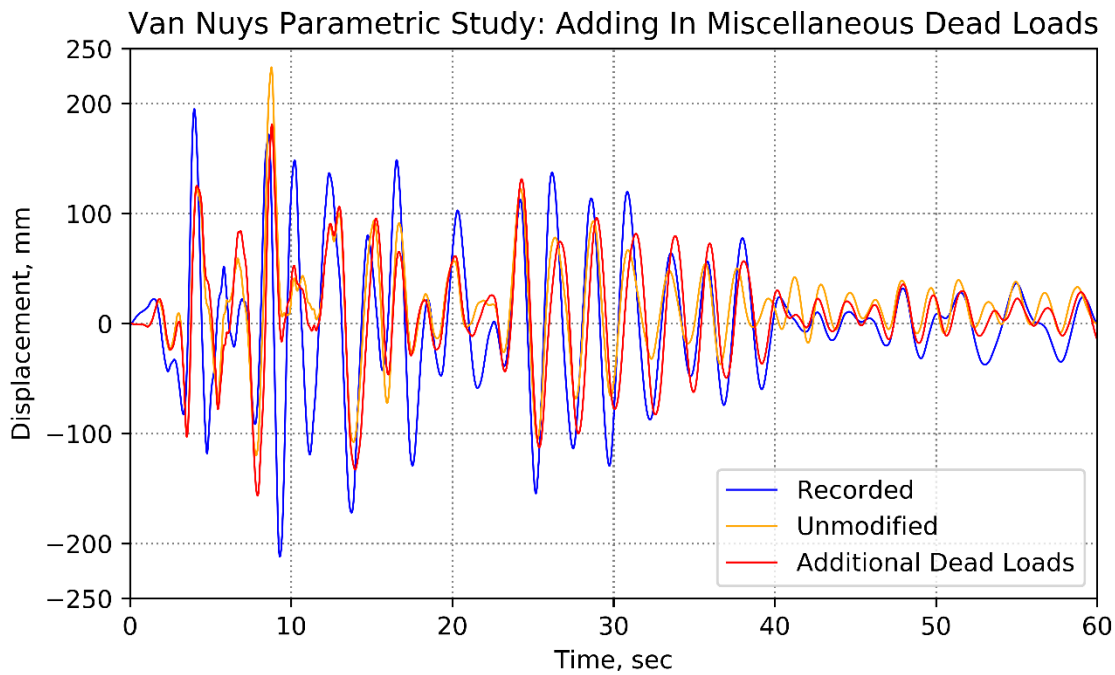


**Figure 42 Parametric Study: Incorporating Miscellaneous Dead Loads.**

### 6.3 Leaning Column Loads

The leaning column is included in the model to incorporate the mass and loads associated with internal gravity-only columns into the response of the structure without artificially increasing column axial loads in the moment frame. This is done in order to capture the P-delta effects that the interior columns have on the lateral load resisting system. While the seismic tributary mass from the structure is assigned to the lateral load resisting frame, only the axial loads within the tributary area of the frame should be applied to the moment frame columns. Thus, all the gravity loads carried by the gravity-only columns are lumped onto the leaning column to capture P-delta effects. In this sensitivity study two separate cases were analyzed: (1) a case where all the interior

gravity loading was placed on the leaning column and (2) a case where all the interior gravity loading was placed on the lateral load resisting frame.

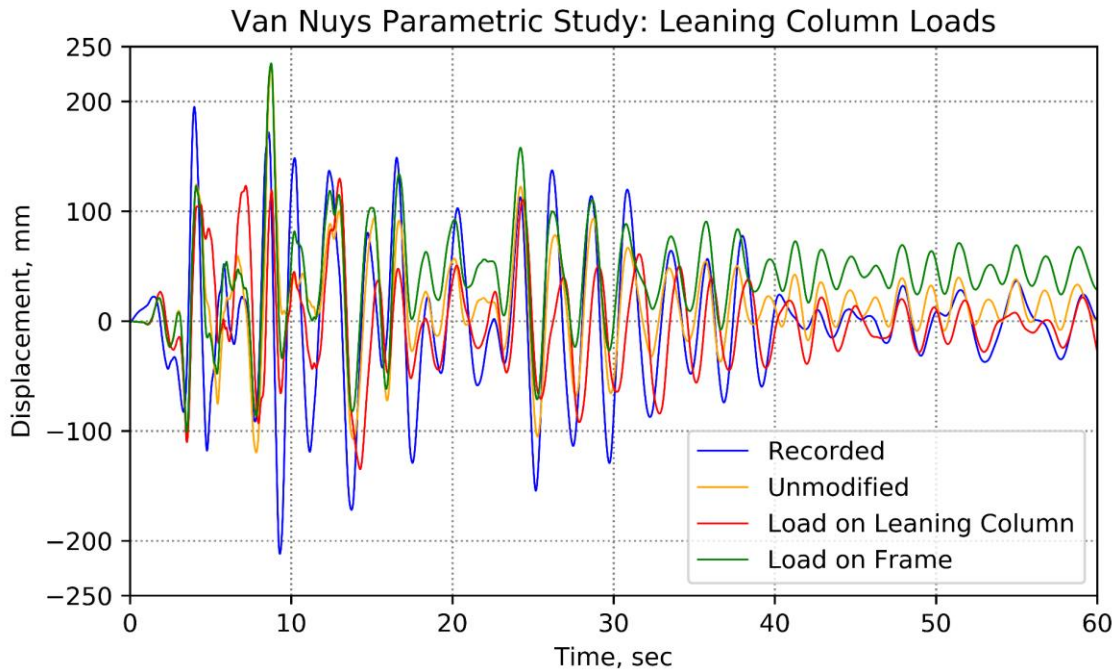


**Figure 43 Parametric study: Placing Loads on the Leaning Column Versus Frame.**

Placing the all gravity loads solely on the leaning column yielded a response that had smaller displacements throughout as compared to the unmodified result as shown in Figure 43. This is expected as the removal of loads from the structural frame to the leaning column alleviates the initial force in all the structural columns, removing the combined bending and axial load condition. Conversely, lumping all interior gravity loads on the lateral load resisting frame resulted in a large amount of residual plastic deformation in the frame. This was expected as the columns were subjected to a combined axial-flexure loading case beyond the design loads.

## 6.4 Cross Sections

As is common in many buildings, the Van Nuys Holiday Inn does not use a single beam and column cross section throughout the entire structure. Most buildings do not have consistent column/beam sections throughout the lateral load resisting system because they are designed based on the seismic and axial loads which decrease with height. Simplifying a structure using typical cross sections is a critical assumption of using the model builder, thus it was important to look at the effect of varying the section details. The Van Nuys Holiday Inn provides a structure which is apt for this study. The column detail is consistent throughout the structure, and the beam detail for the second floor as seen in Figure 44 is larger than the typical section on all the other floors and in the validation analysis the typical section on all the other floors was used.

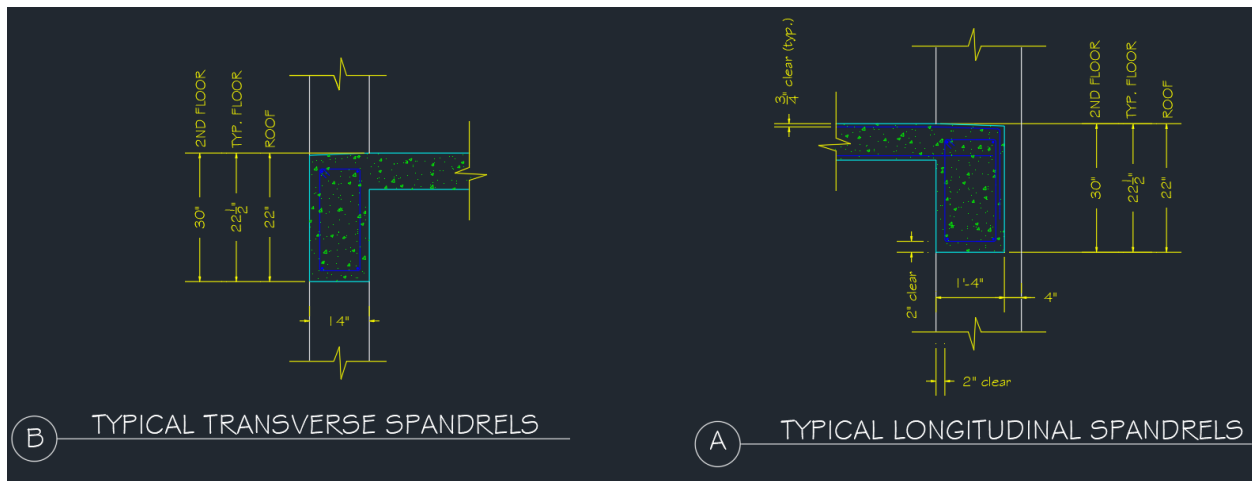


**Figure 44 Beam Cross Section Details for the Van Nuys Holiday Inn.**

The second-floor beam has the same reinforcement as the beams on the other floors however of the depth is 30 inches as opposed to 22.5-inch depth of the spandrel beams for floors 3 - 5. If a user were to analyze the structure using the second-floor beam details as the typical section, the stiffness would be influenced. This purpose of this study was to quantify the relative change in global response that this change in cross section would cause.

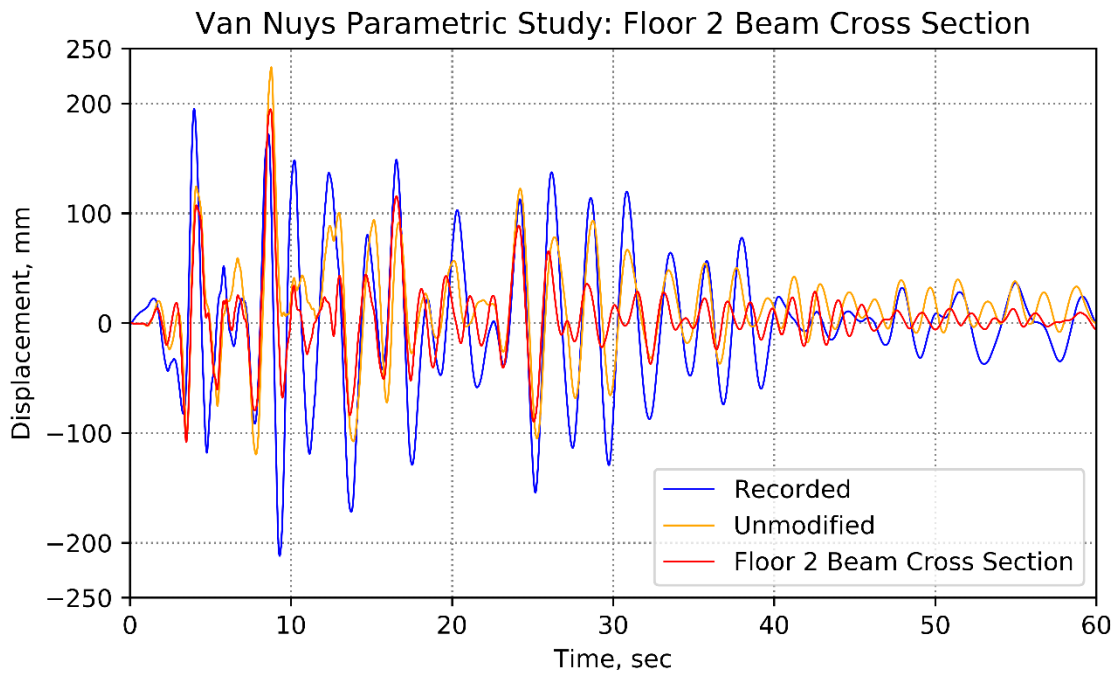


**Figure 45 Parametric Study: Using Non-Typical Cross Sections.**

The change in typical beam cross section resulted in an expected change in response. The overall increase in frame stiffness associated with the change in beam depth yielded smaller top floor displacements as indicated in Figure 45. Using the beam cross section from floors 3-5 resulted in a numerical response that was closer to that of the measured data. The data would suggest that a typical cross section generates a more representative response history. The results from this limited study suggest that in cases where several beam cross sections are apparent, an aggregated cross section which represents the average stiffness of the beams throughout the structure may yield better results than using the bottom floor cross section.

## 6.5 Material Properties

Material properties as specified on engineering documents are conservative by design. When designing concrete, safety factors are built into the mix design such that the actual strength of the concrete exceeds that target strength. This has large implications for the efficacy of a modeled result. Using nominal material properties rather than actual material properties could result in premature yielding or unexpected inelastic behavior which drastically influences the output of the structure's response history. This becomes especially important in cases where elements are capacity designed to resist the strength of adjacent elements.

The Van Nuys Holiday Inn was built using nominally specified 5 ksi concrete and 60 ksi steel in all concrete components [36]. While the slab and gravity columns used a different grade of concrete, these elements are not explicitly incorporated into the model and are therefore not relevant. The actual material properties for the concrete and steel were estimated as 6.2ksi and 75ksi respectively.

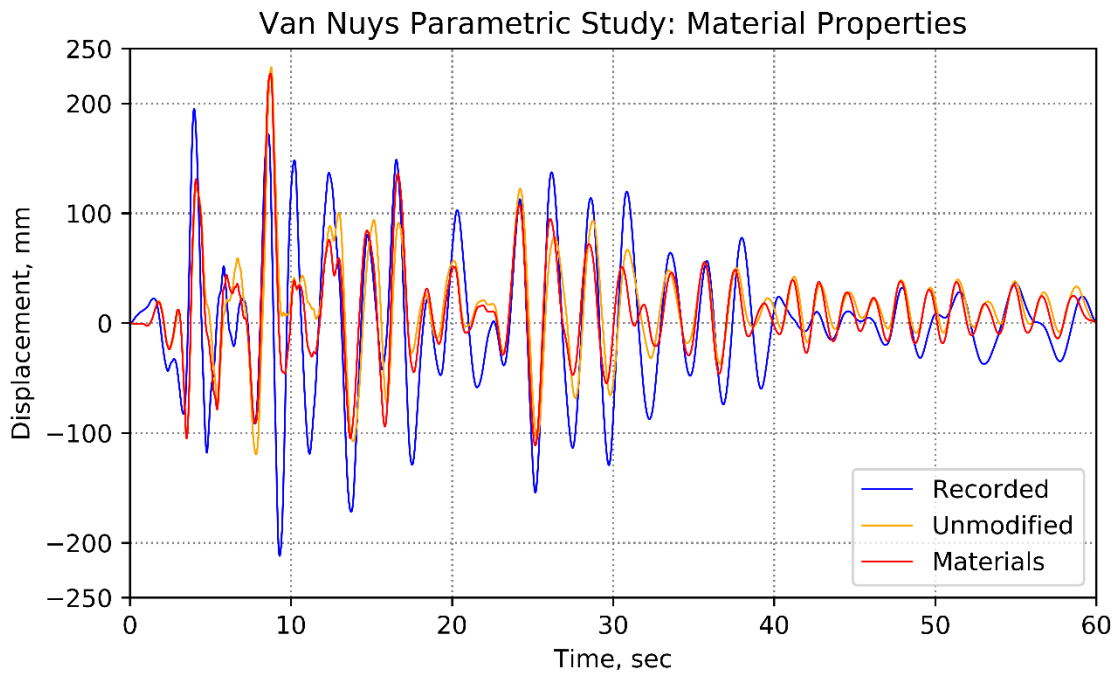


**Figure 46 Parametric Study: Using Projected Actual Material Properties.**

The additional strength provided by the updated material properties displayed a minimal effect on the global response history of the structure as seen in Figure 46. The maximum displacement of the frame was reduced by approximately three percent over the unmodified analysis. This relatively minor change in response could be due to the simulated structure remaining largely elastic throughout the entire response history. It is important to note that if a large amount of plasticity were observed, the changing in material specifications could drastically change the performance of the structure. Further analysis is required to investigate the results of different material models such as Concrete02 which incorporates tensile strength, or Steel01 which represents a bilinear steel material model with a fixed strain hardening ratio.

## 7.0 Summary, Conclusions and Future Work

This paper introduced the Model Builder, a tool which represents a more refined method to generate structural response estimates for seismic performance evaluation. The objective of the Model Builder is to provide an intermediate level of analysis that lies between the general fragility-based analysis and bespoke building models. While currently limited to only 2D systems, the Model Builder was proven to display accurate results across all model types when compared against recorded data for the Wellington Building, the Van Nuys Holiday Inn, and the E-Defense structure. The validation study performed resulted in several key findings:

- Models generated using the Model Builder provide outputs which are of similar shape and magnitude to recorded building responses indicating both that the formulation of models within the Model Builder are not only correct, but also adequate for modeling real world structures.
- While less accurate, the elastic models provide analysis that is orders of magnitude faster than both the lumped plasticity and distributed plasticity models; which could prove invaluable in a post-event disaster relief scenario.
- Both the lumped plasticity and distributed plasticity models displayed results which matched well against both recorded data as well as against each other, inferring that the rigid offset and zero length sections of the lumped plasticity model were implemented correctly.
- Reinforced concrete structures which have response-histories that remain completely linear elastic may require a material model which incorporates the tensile strength of concrete to adequately model displacements and story drifts.

The time study was performed as a validation study of the Model Builder in terms of real-world applications. This study was performed to determine how much time would be required on the user end to index critical infrastructures as well as perform an analysis in a post-event environment. The time study yielded several major conclusions:

- The batch analysis procedure is robust and able to run large libraries models in sequence to generate hundreds of response histories.
- Elastic models are orders of magnitude faster than the lumped plasticity and distributed plasticity models and generate damage states of similar class for a variety of structures.
- Lumped plasticity and distributed plasticity models generated very similar damage state outputs, indicating that the increased fidelity of distributed plasticity models may just be a computational burden as compared to lumped plasticity models when damage is being categorized by damage states.
- If a structural library is created a priori to an event, the Model Builder can be implemented in a time-efficient manner to help characterize damage states in structures and assist in building inspection priority.

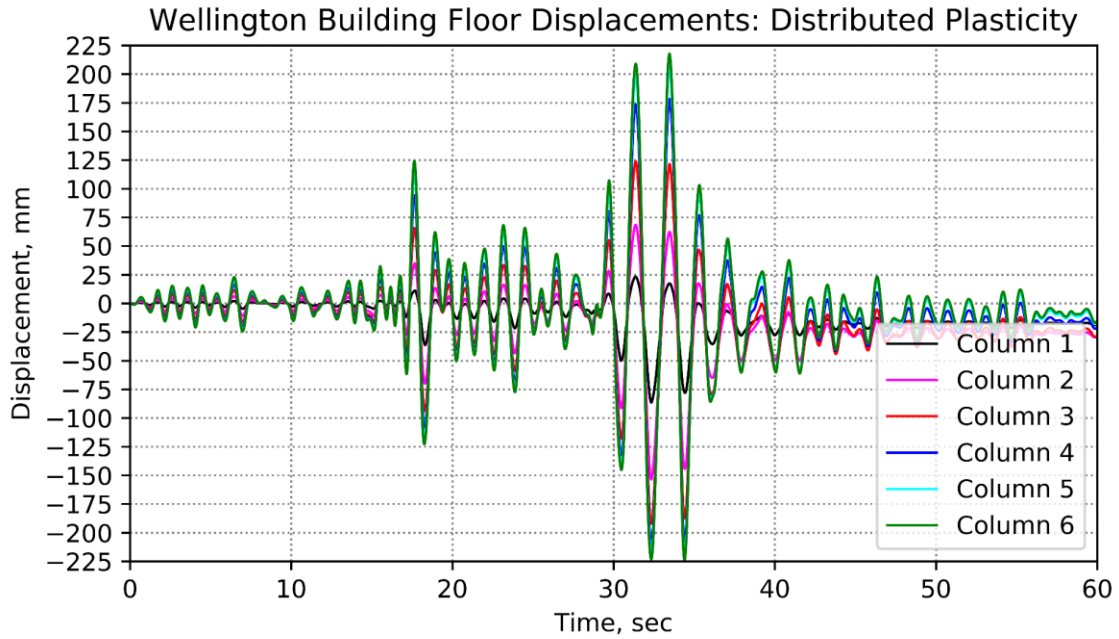
The parametric study was performed to determine the impact of user specified parameters. End users filling out building index forms may generate unique results based on the details they use to fill out the building information sheets. This study was performed to determine how much end user decisions would affect the outputs of structural models generated and which parameters most impacted the outputs. The parametric study yielded several major conclusions:

- Accounting for miscellaneous dead loads can increase overall loading by up to 20%.
- Applying all loads to the lateral load resisting system does not adequately capture building response, thus necessitating the leaning column.
- Accurate tributary area discretization is required in order to properly assign mass and load to the lateral load resisting system and the leaning column individually.
- Specified material strengths are adequate in scenarios where large residual plastic deformations aren't present.

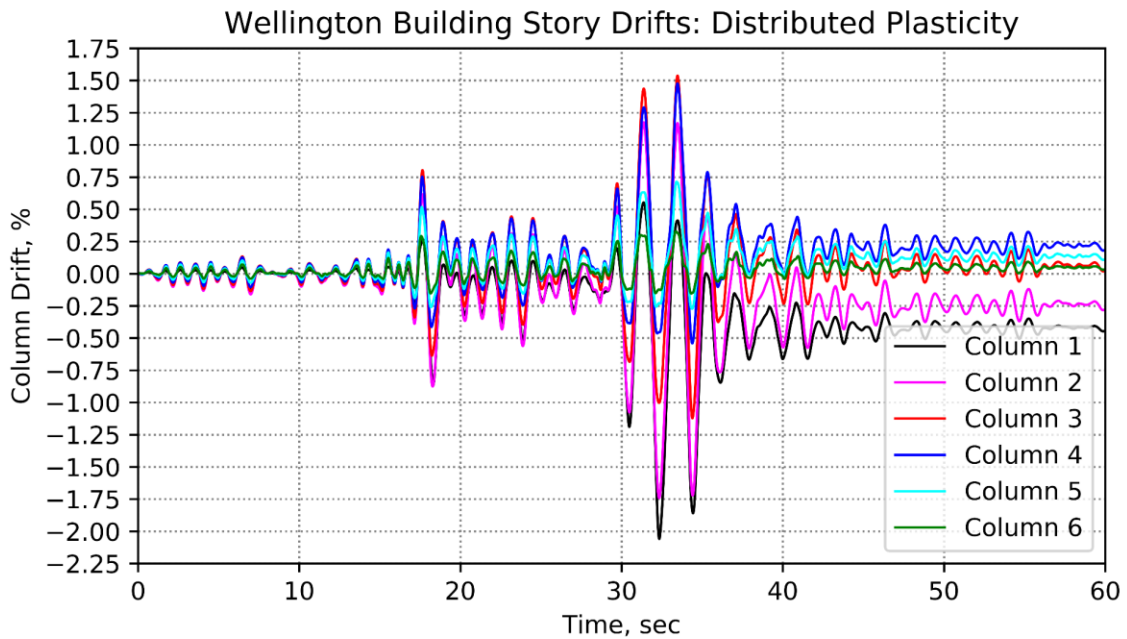
This study introduced a simulation tool capable of rapidly developing multi-fidelity structural models using limited structural information. Based on the results presented here, several recommendations for future work are provided:

- Perform a more in-depth sensitivity study using a Monte Carlo simulation. The sensitivity study presented here was limited, however it identified important parameters can influence the global structural response. These include accurate estimation of structural mass and load, assignment of mass and load to the leaning column, and material properties.
- Expand the capabilities to include addition structural systems such as shear walls, eccentrically braced frames, and specially reinforced moment frames (SMRF's).
- Introduce 3D modeling capabilities.
- Continue to compare numerical results generated using the model builder to recorded data to improve the output and modeling approach.
- Identify and implement strategies to expedite and standardize the input of structural data.

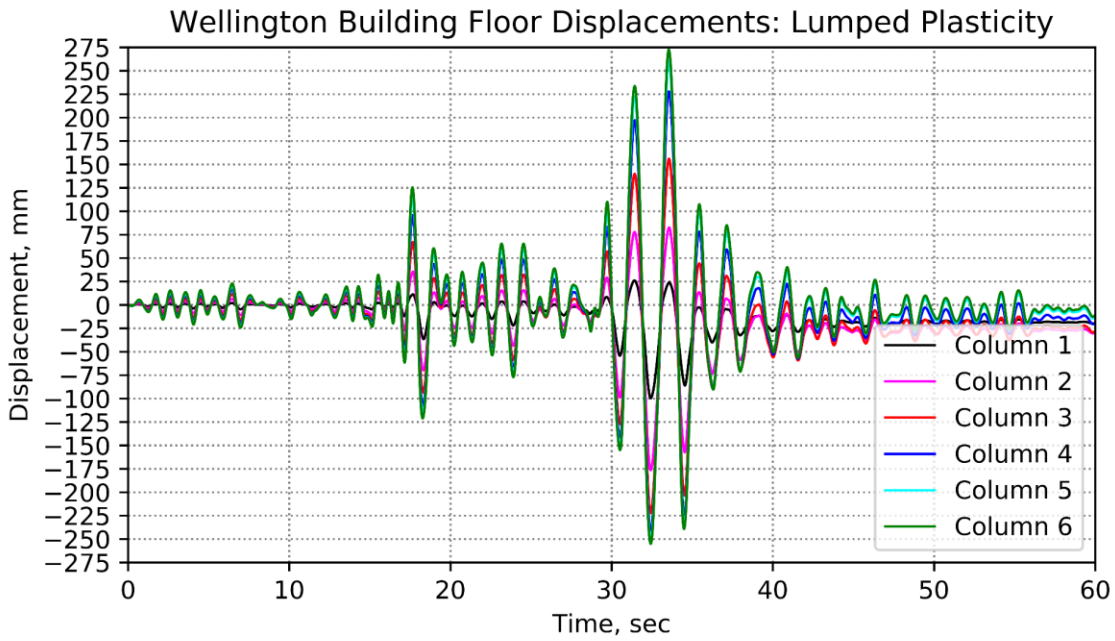
## Appendix A Model Builder Outputs for the Wellington Building



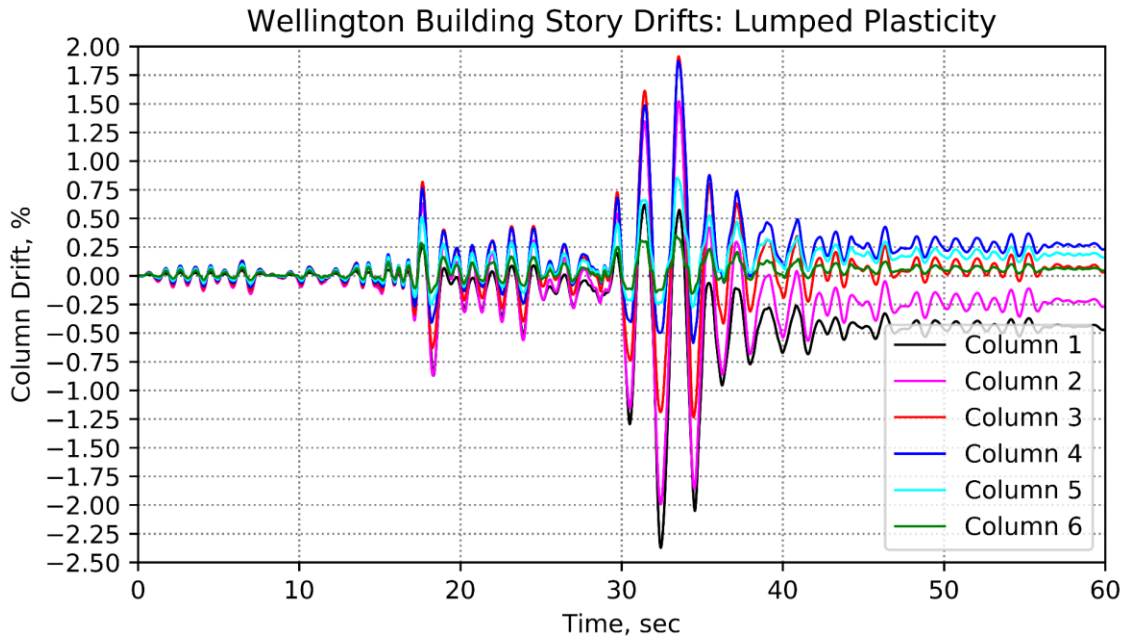
Appendix Figure 1 Wellington Building Floor Displacements: Distributed Plasticity.



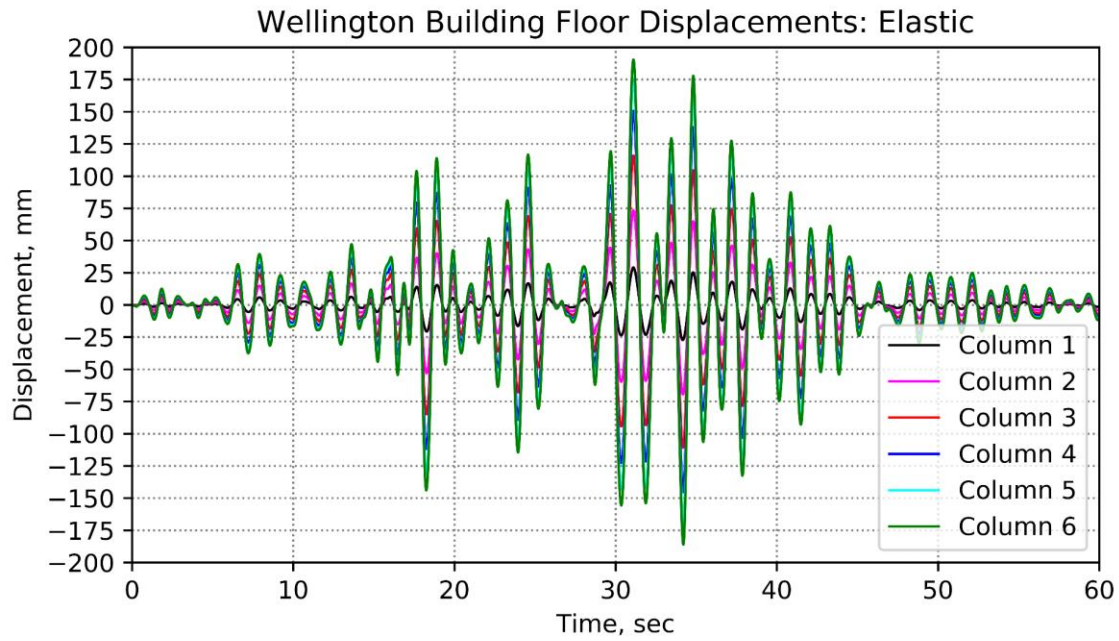
Appendix Figure 2 Wellington Building Story Drifts: Distributed Plasticity.



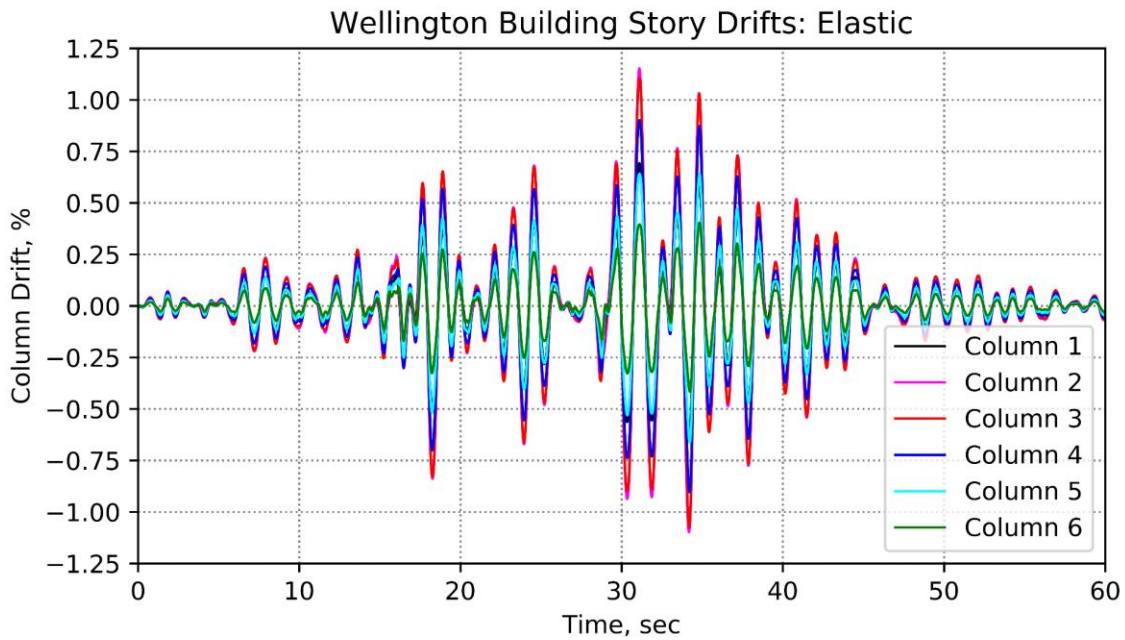
**Appendix Figure 3 Wellington Building Floor Displacements: Lumped Plasticity.**



**Appendix Figure 4 Wellington Building Story Drifts: Lumped Plasticity.**

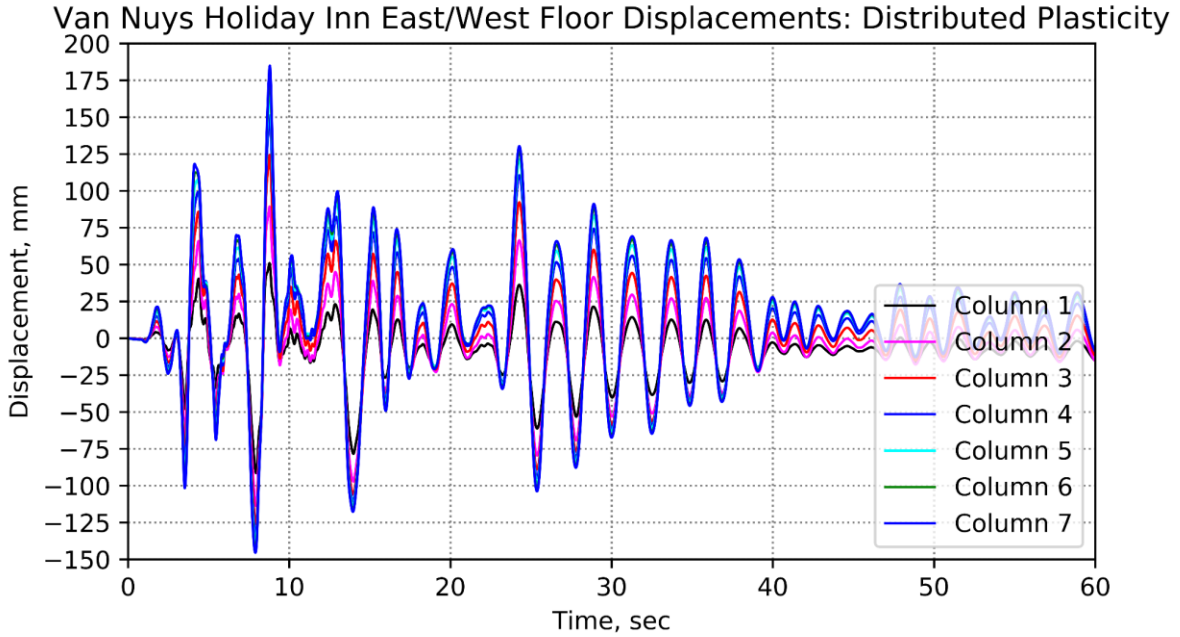


**Appendix Figure 5 Wellington Building Floor Displacements: Elastic.**

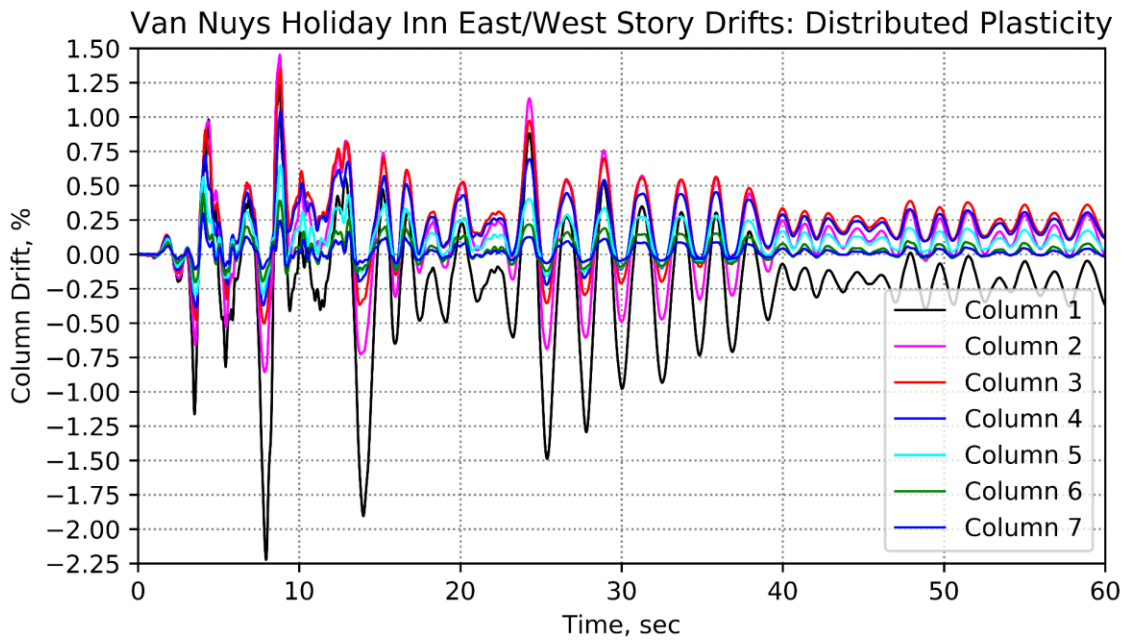


**Appendix Figure 6 Wellington Building Story Drifts: Elastic.**

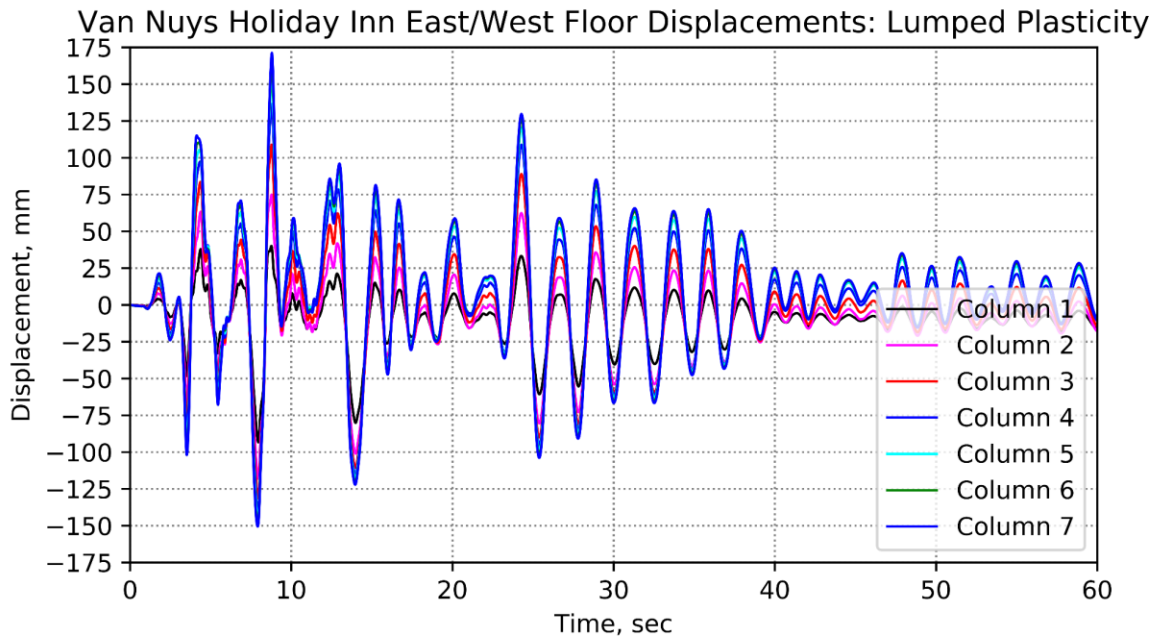
**Appendix B Model Builder Outputs for the Van Nuys Holiday Inn**



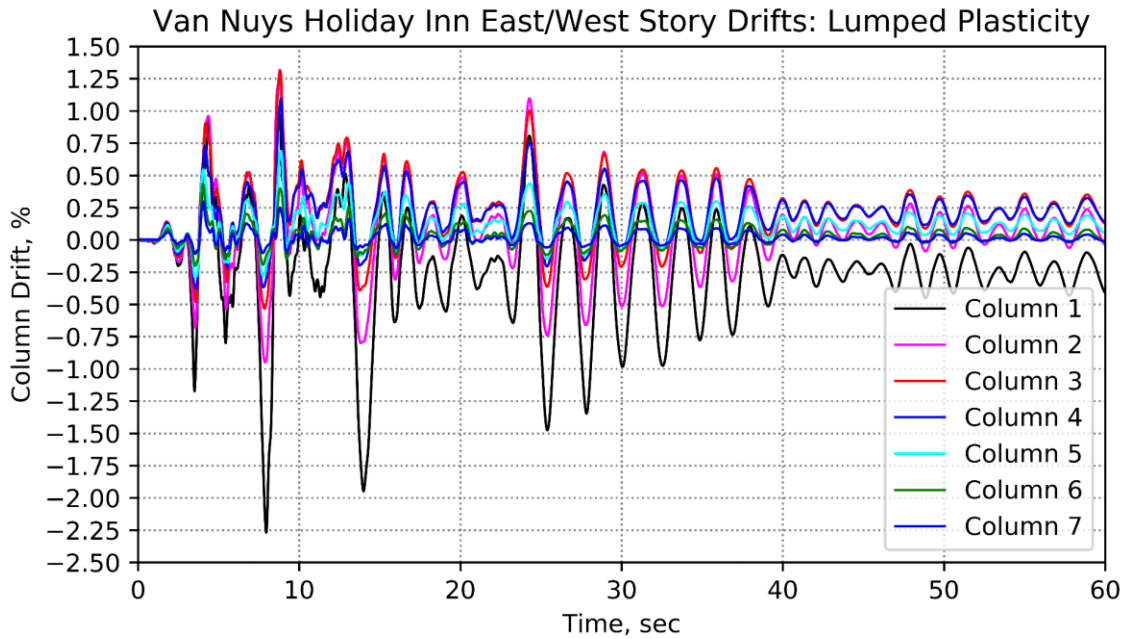
**Appendix Figure 7 Van Nuys E/W Floor Displacements: Distributed Plasticity.**



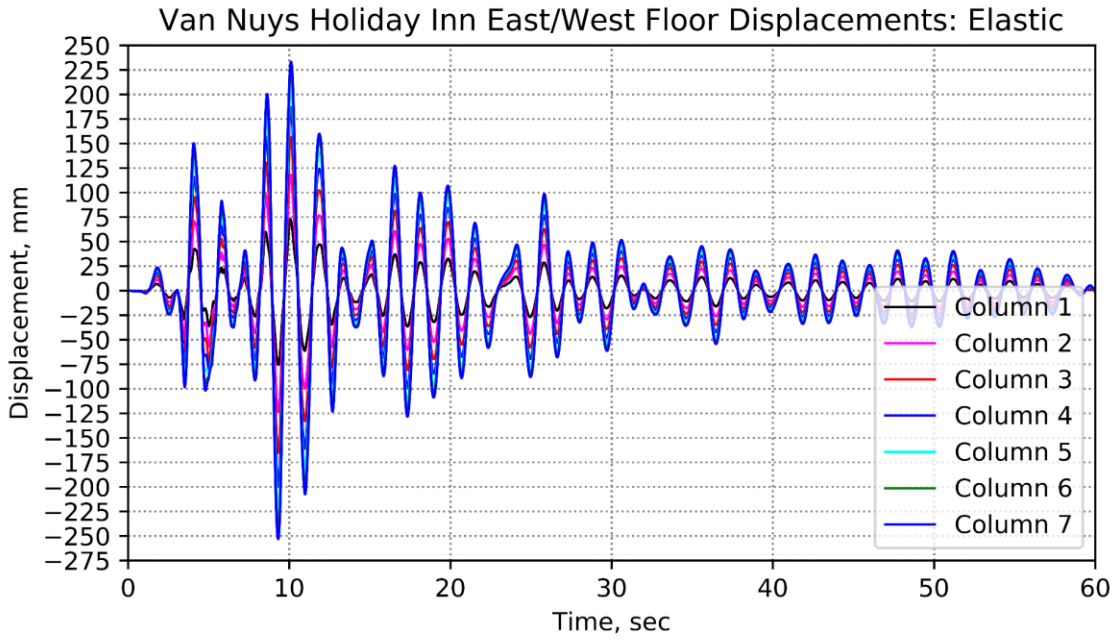
**Appendix Figure 8 Van Nuys E/W Story Drifts: Distributed Plasticity.**



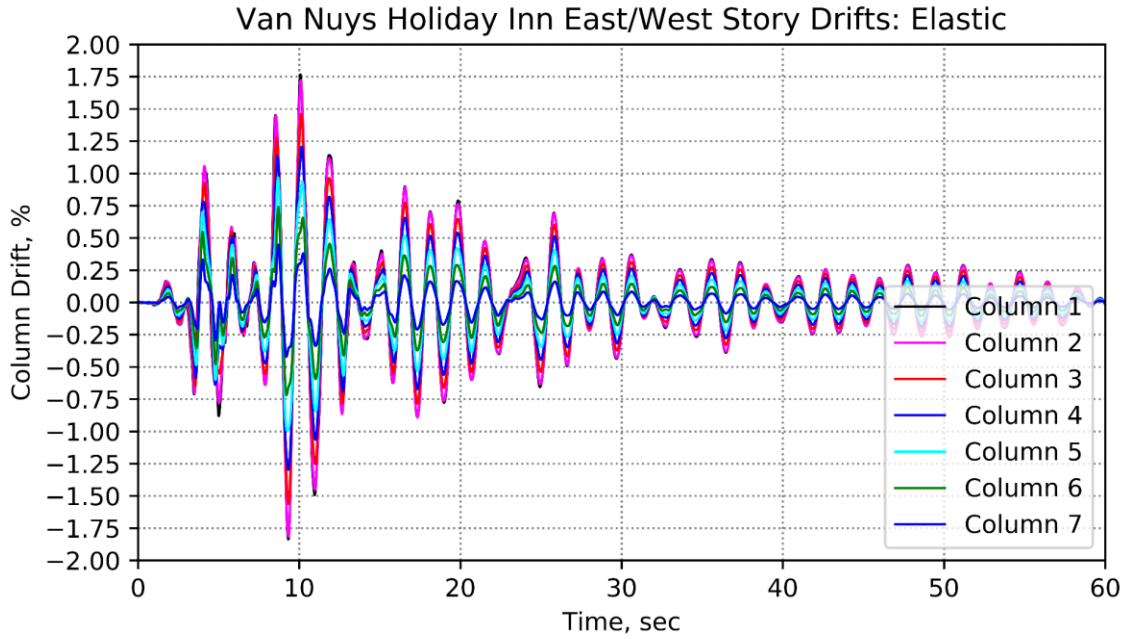
Appendix Figure 9 Van Nuys E/W Floor Displacements: Lumped Plasticity.



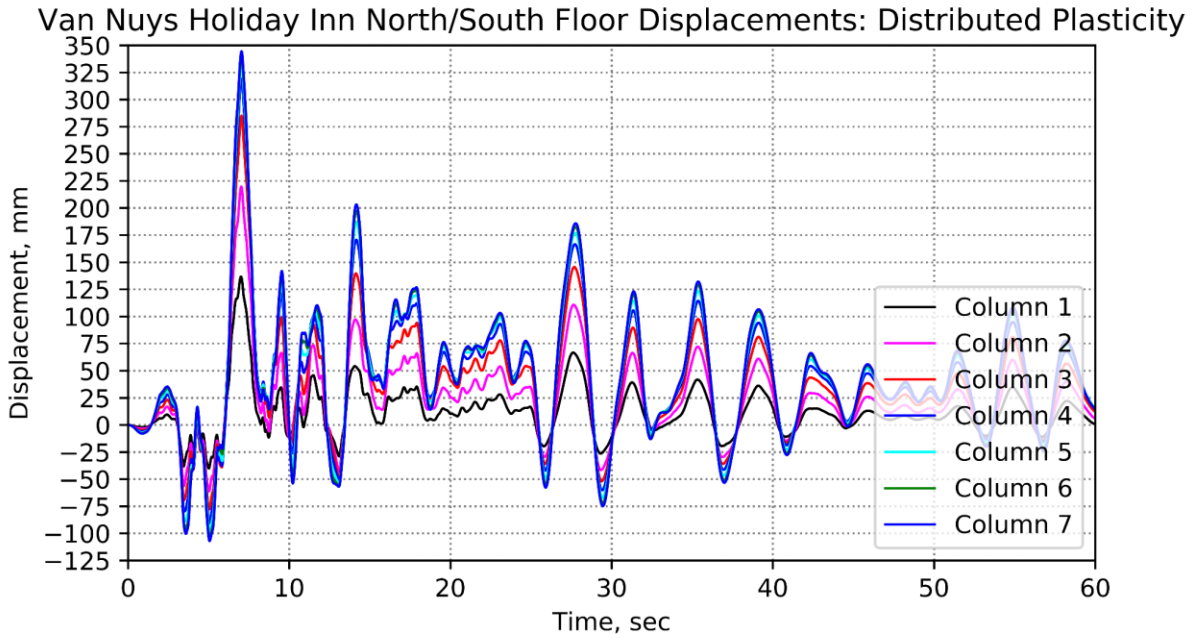
Appendix Figure 10 Van Nuys E/W Story Drifts: Lumped Plasticity.



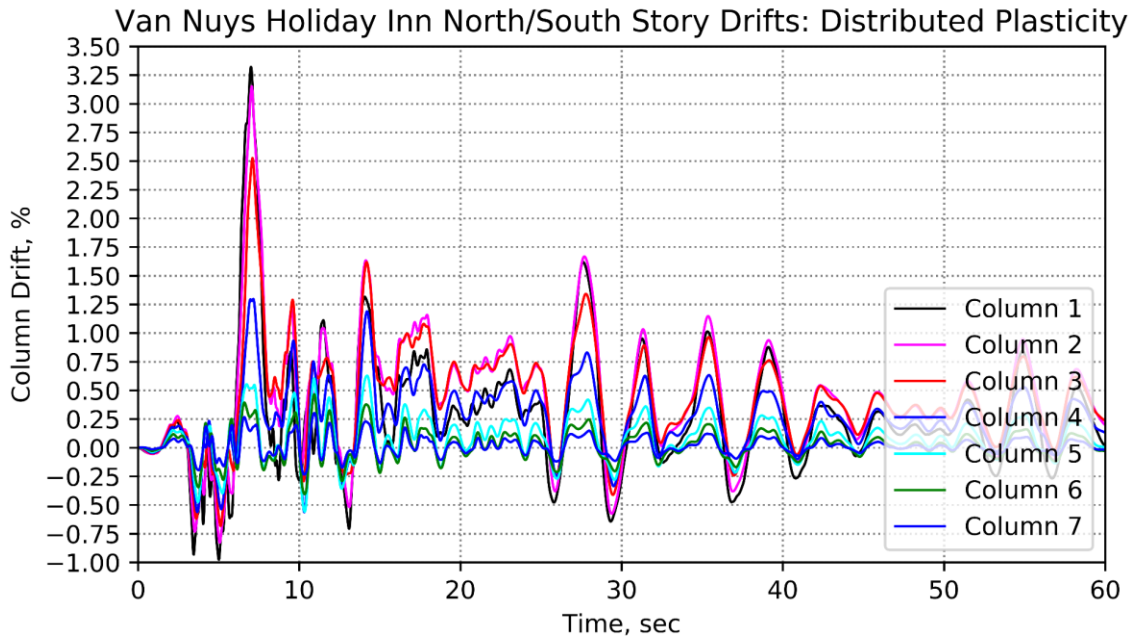
**Appendix Figure 11 Van Nuys E/W Floor Displacements: Elastic.**



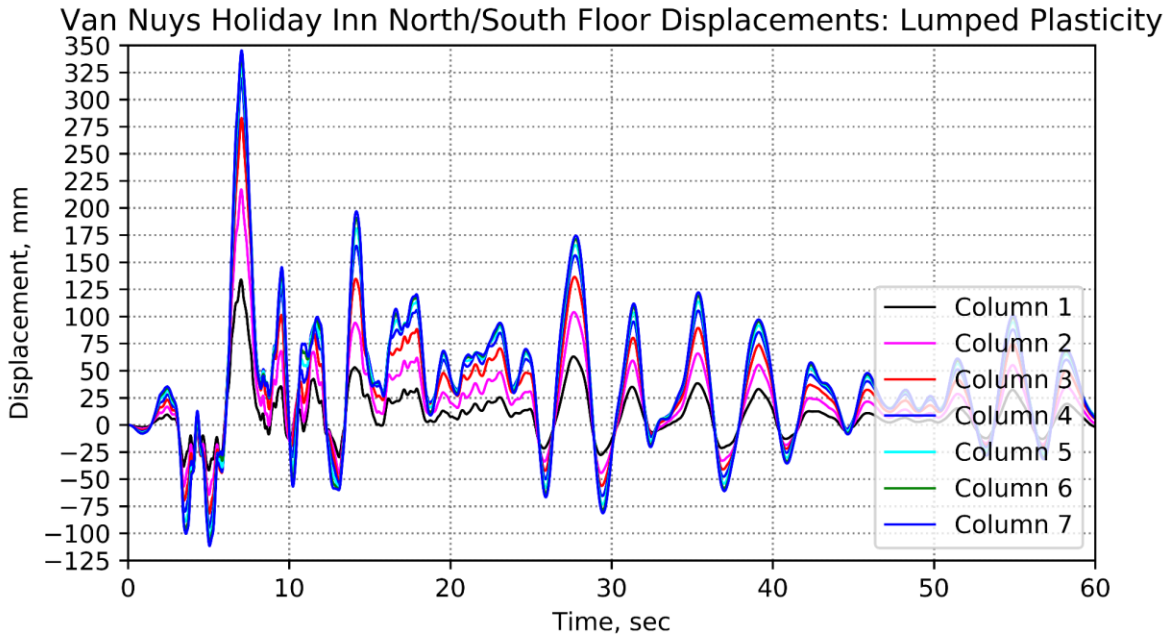
**Appendix Figure 12 Van Nuys E/W Story Drifts: Elastic.**



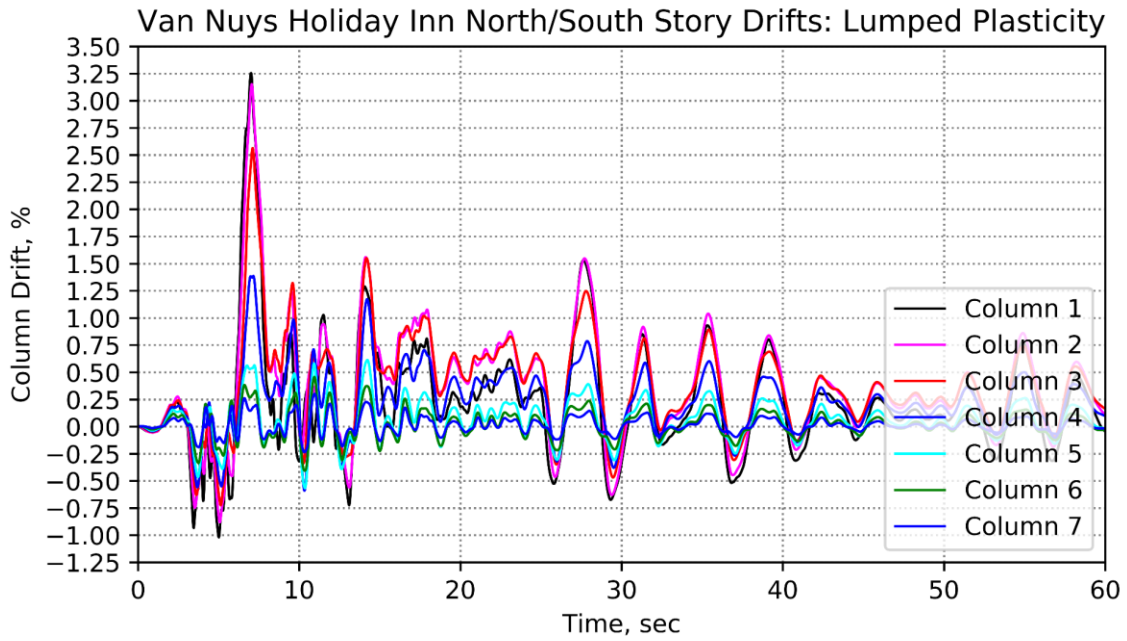
**Appendix Figure 13 Van Nuys N/S Floor Displacements: Distributed Plasticity.**



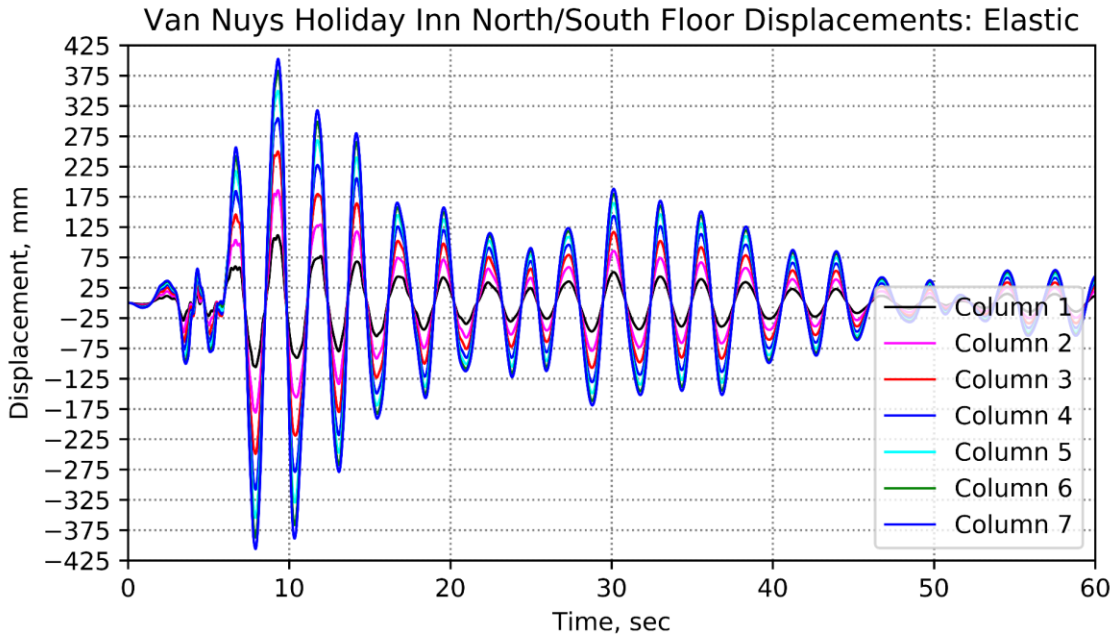
**Appendix Figure 14 Van Nuys N/S Story Drifts: Distributed Plasticity.**



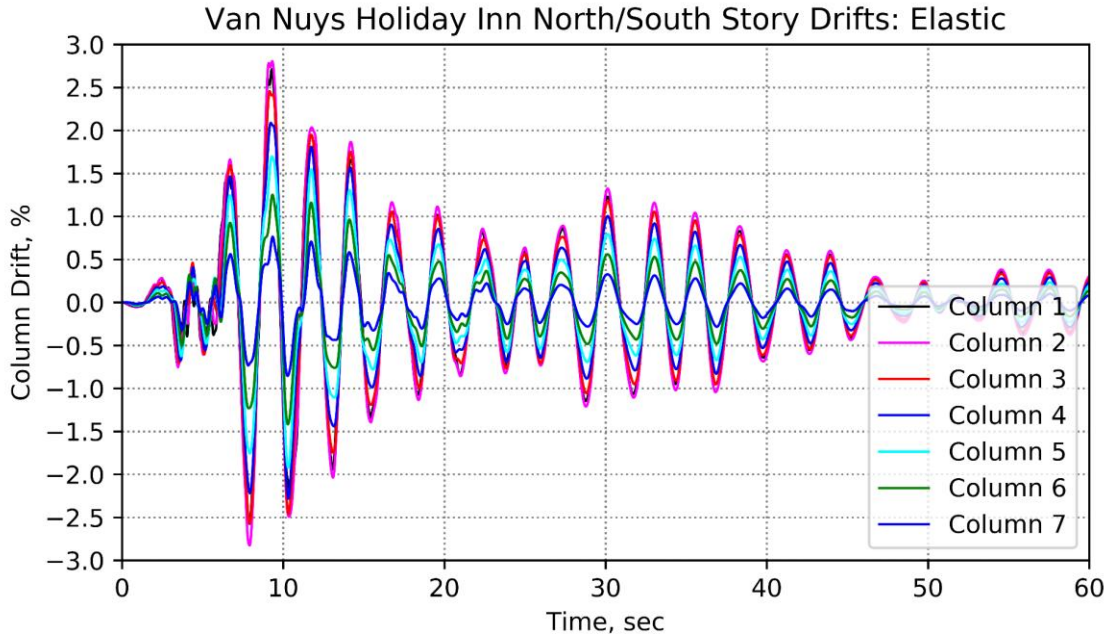
Appendix Figure 15 Van Nuys N/S Floor Displacements: Lumped Plasticity.



Appendix Figure 16 Van Nuys N/S Story Drifts: Lumped Plasticity.

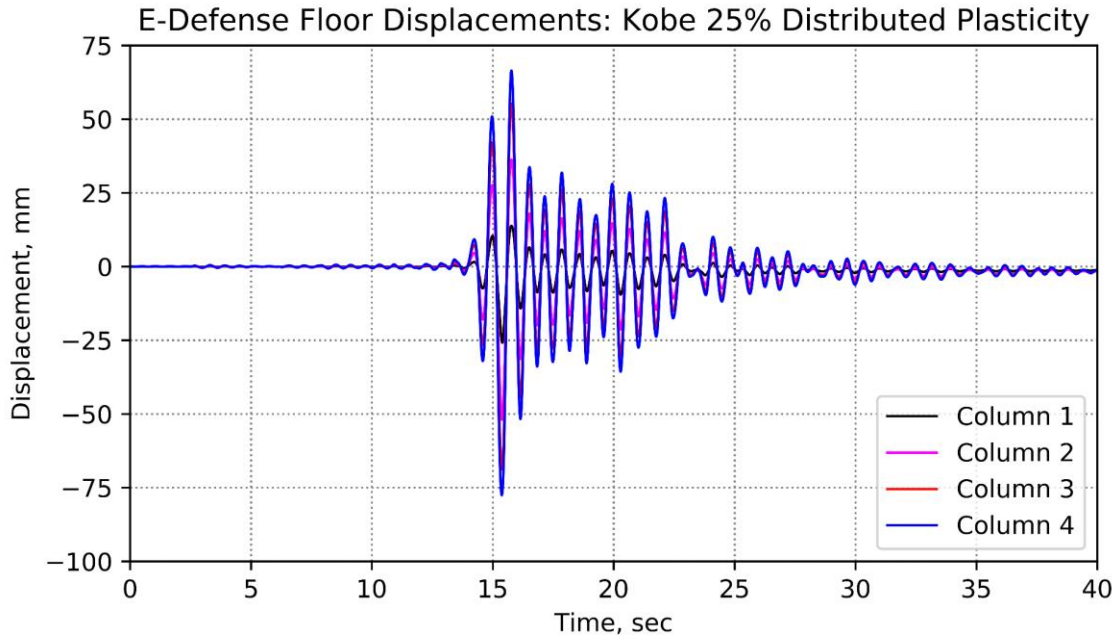


Appendix Figure 17 Van Nuys N/S Floor Displacements: Elastic.

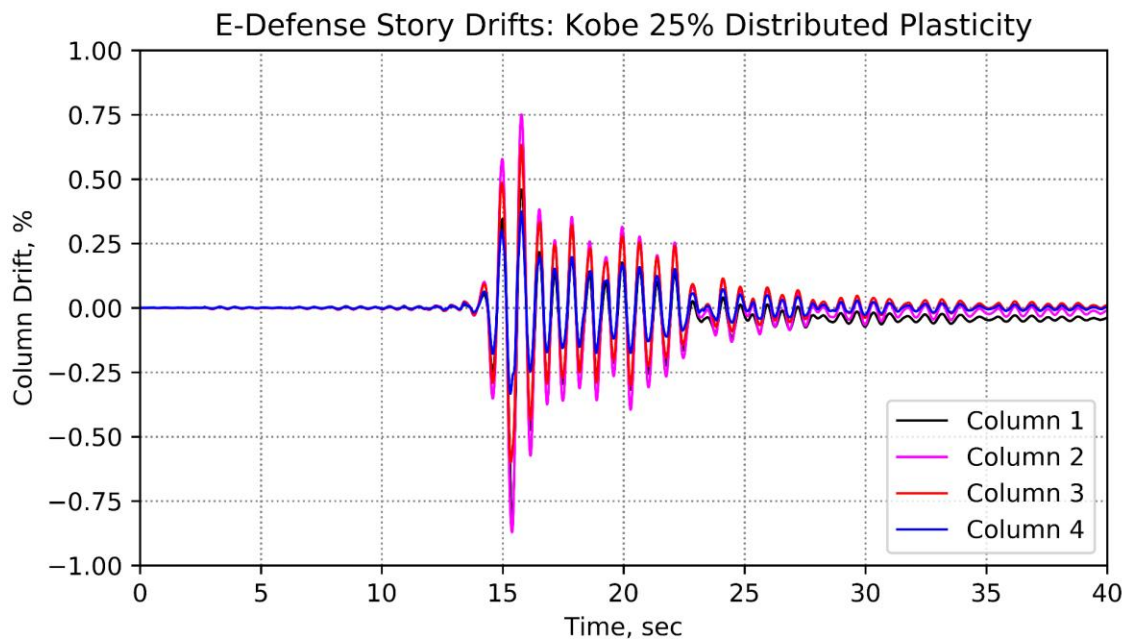


Appendix Figure 18 Van Nuys N/S Story Drifts: Elastic.

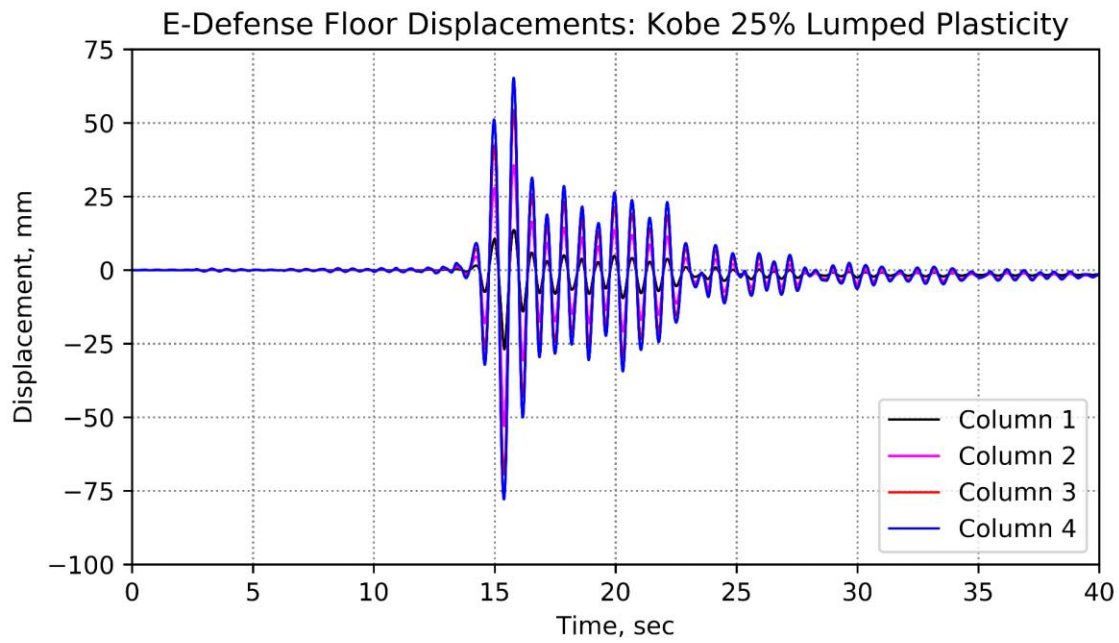
## Appendix C Model Builder Outputs for the E-Defense Structure



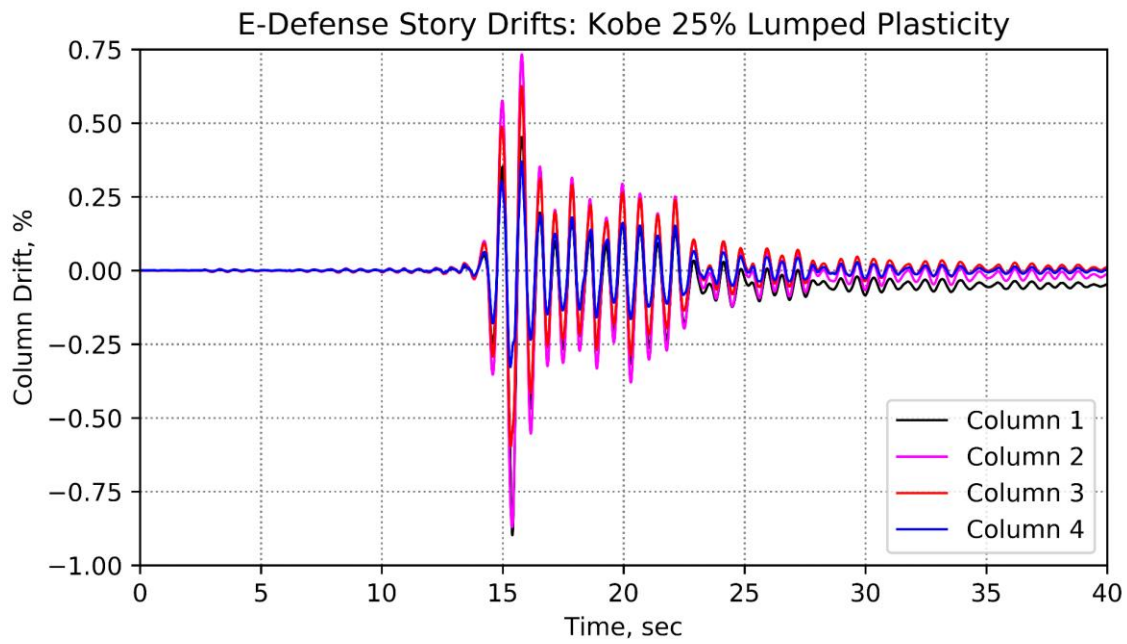
Appendix Figure 19 E-Defense Floor Displacements: Kobe 25% Distributed Plasticity.



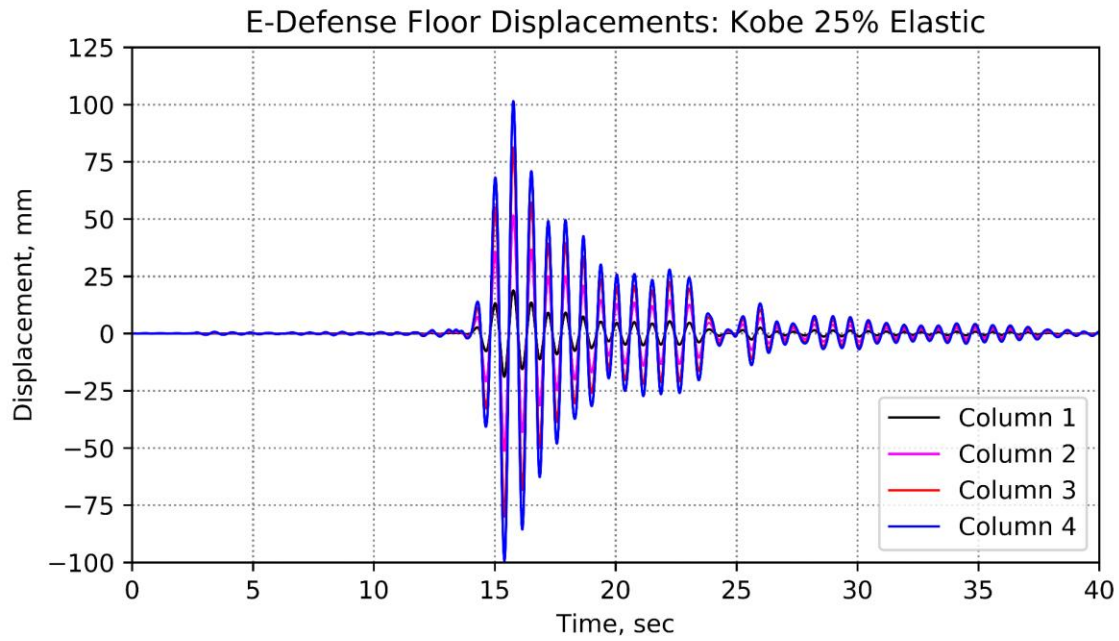
Appendix Figure 20 E-Defense Story Drifts: Kobe 25% Distributed Plasticity.



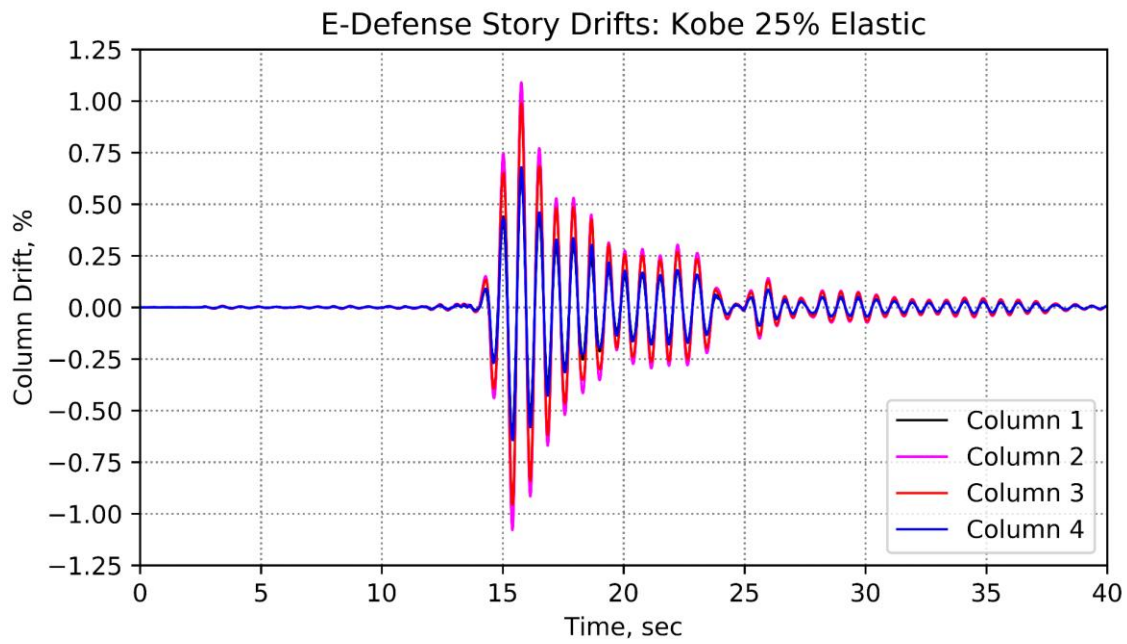
**Appendix Figure 21 E-Defense Floor Displacements: Kobe 25% Lumped Plasticity.**



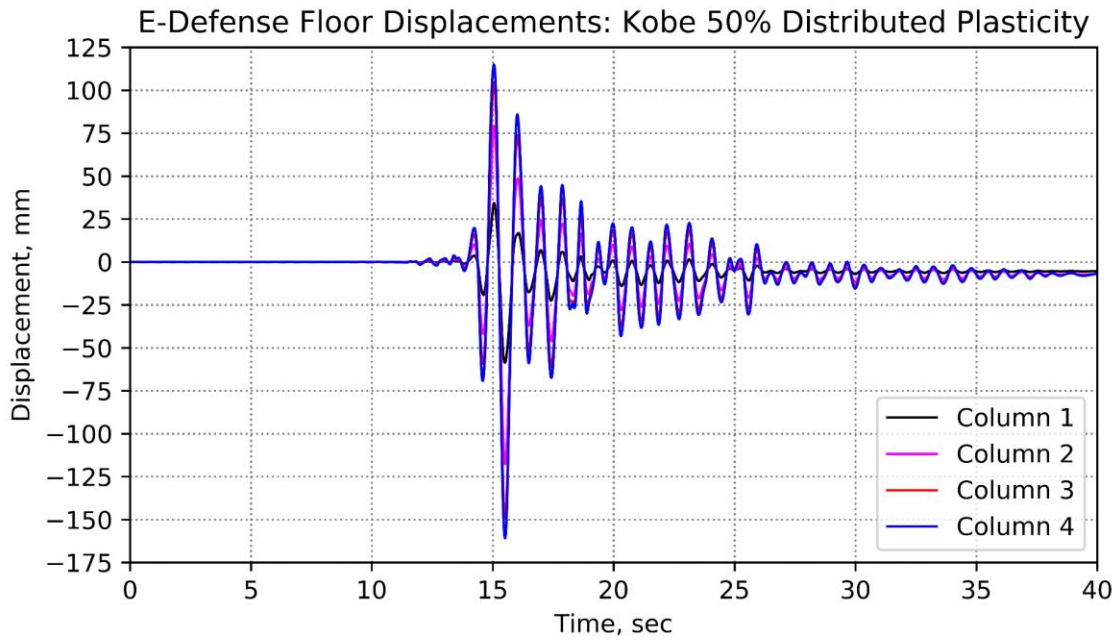
**Appendix Figure 22 E-Defense Story Drifts: Kobe 25% Lumped Plasticity.**



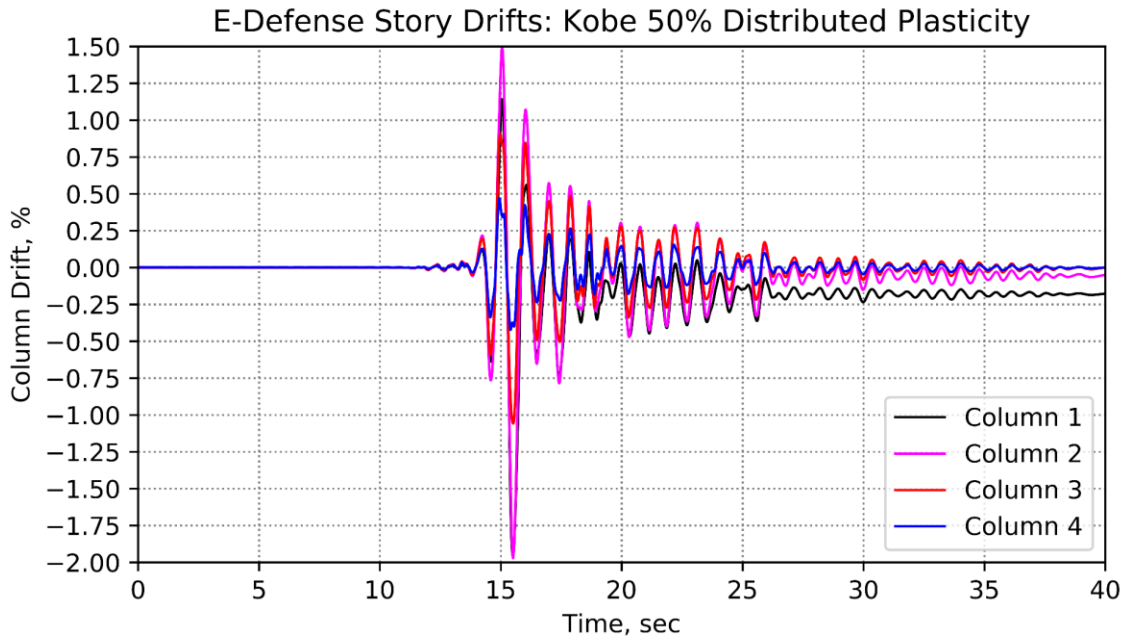
**Appendix Figure 23 E-Defense Floor Displacements: Kobe 25% Elastic.**



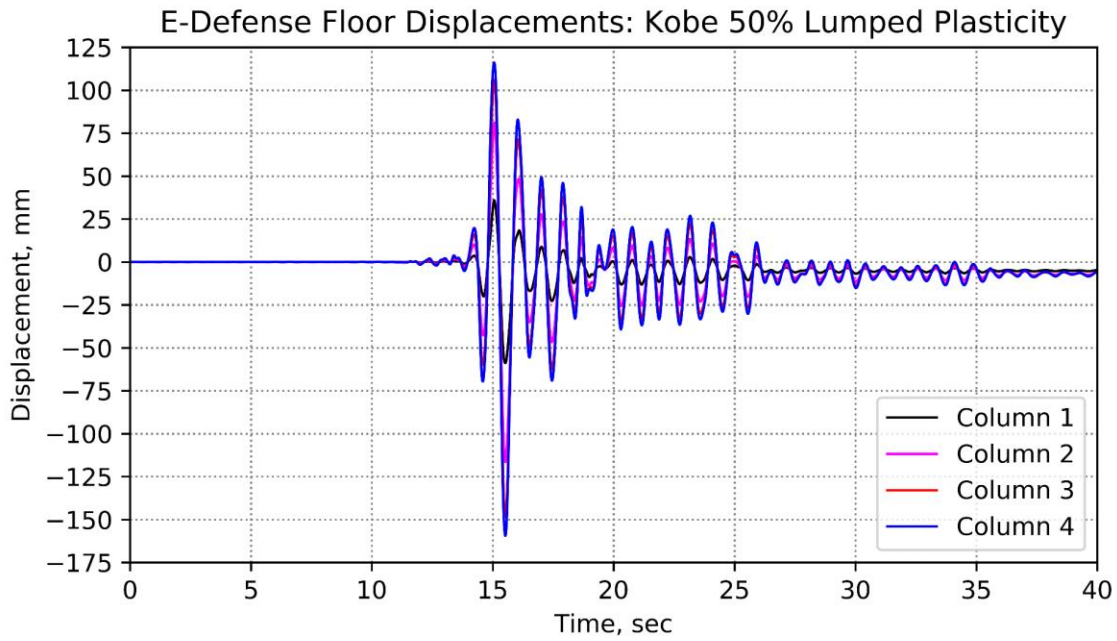
**Appendix Figure 24 E-Defense Story Drifts: Kobe 25% Elastic.**



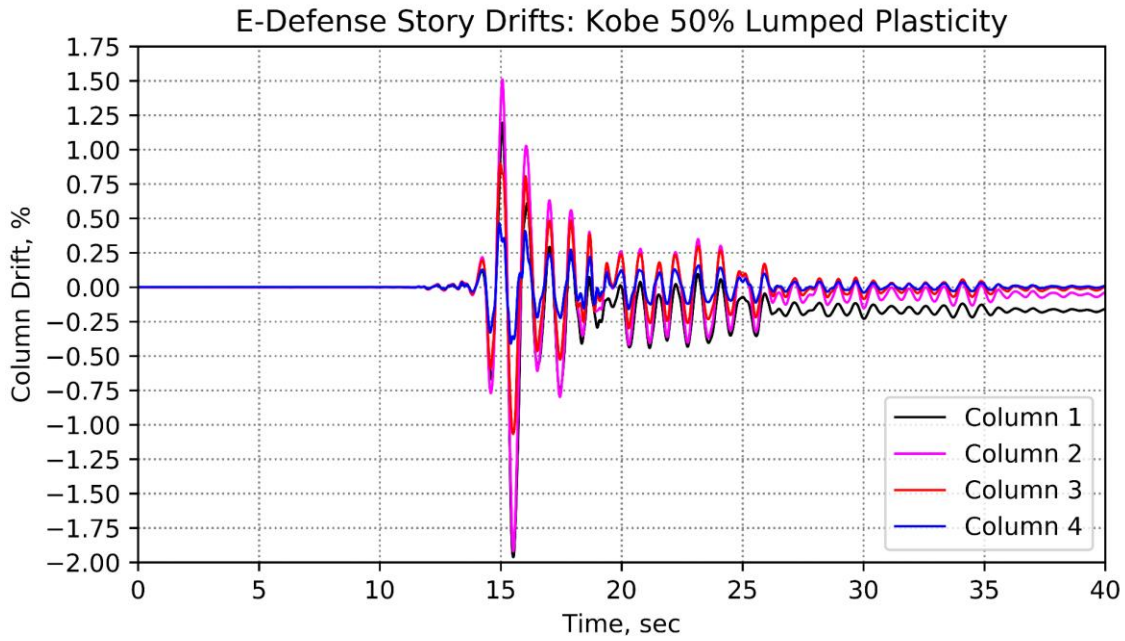
**Appendix Figure 25 E-Defense Floor Displacements: Kobe 50% Distributed Plasticity.**



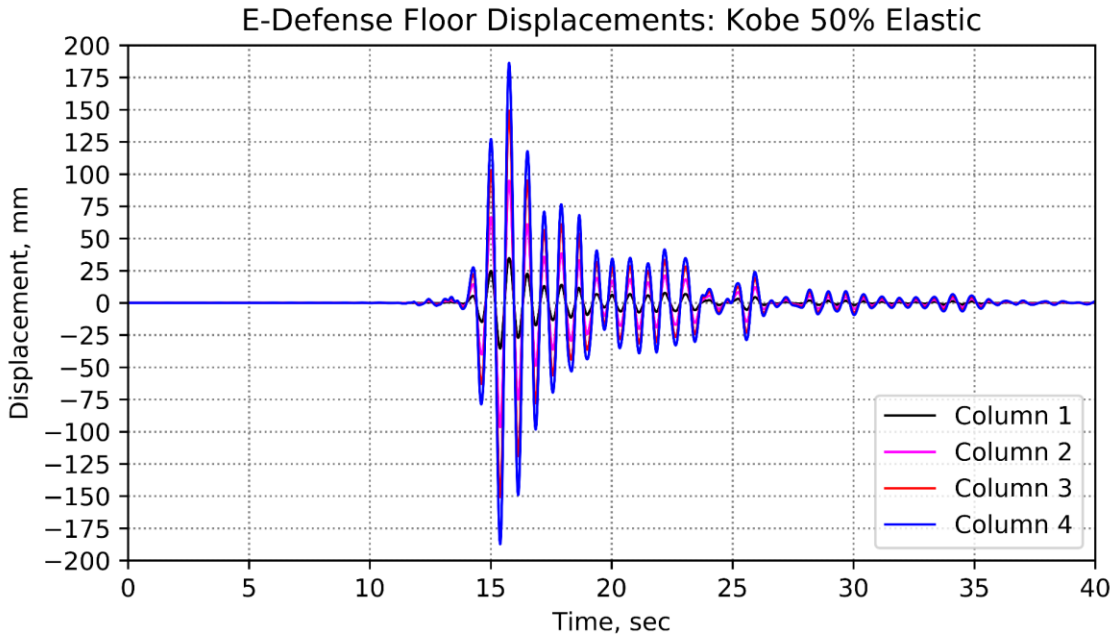
**Appendix Figure 26 E-Defense Story Drifts: Kobe 50% Distributed Plasticity.**



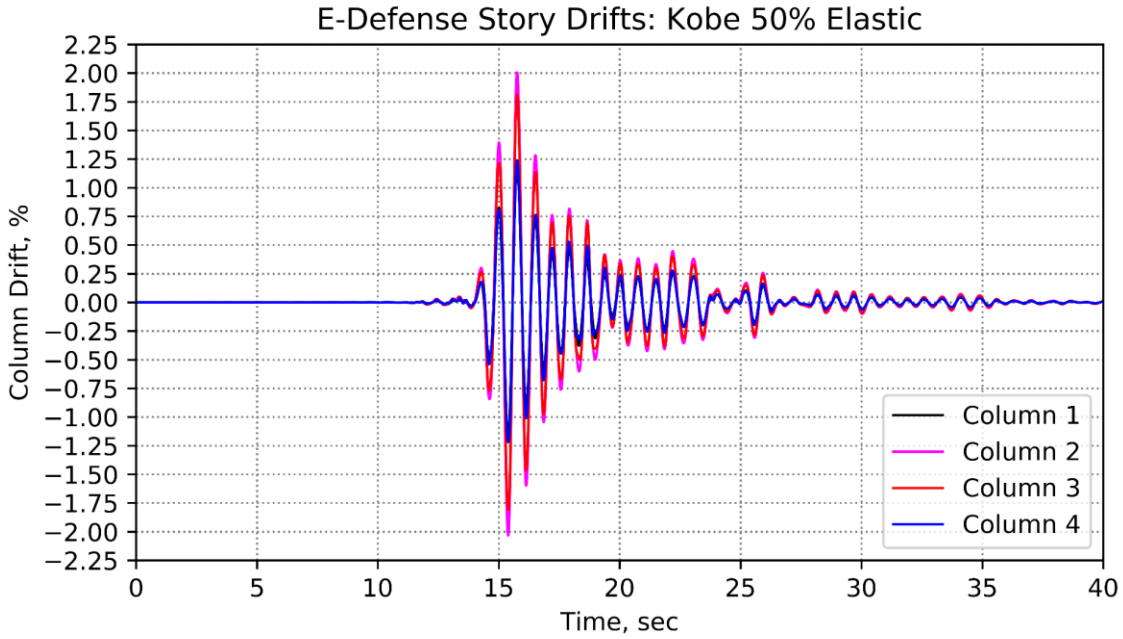
**Appendix Figure 27 E-Defense Floor Displacements: Kobe 50% Lumped Plasticity.**



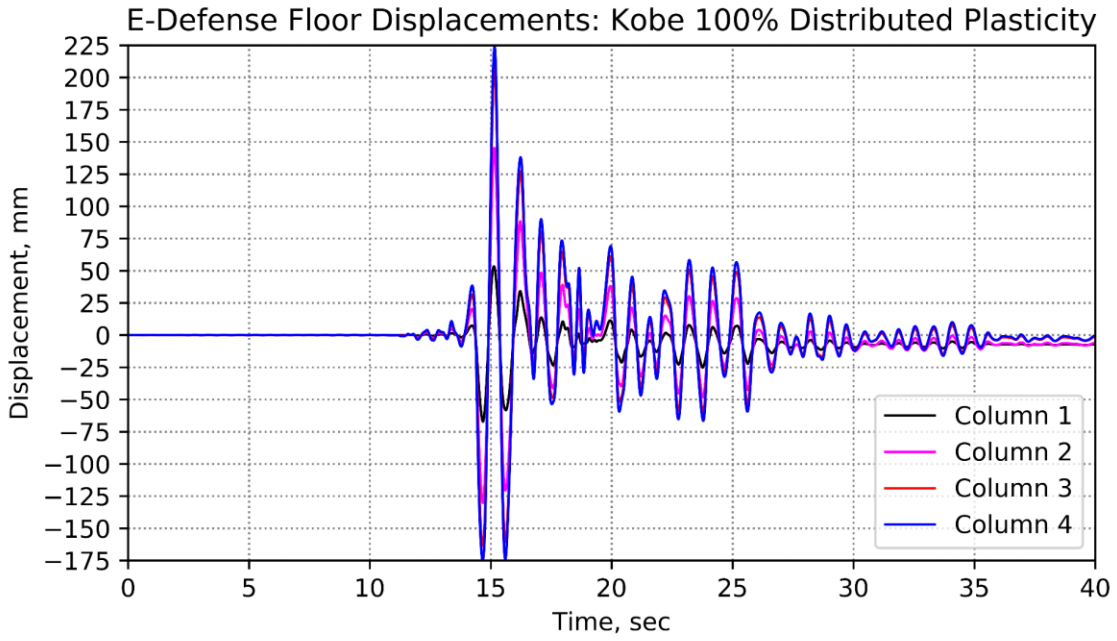
**Appendix Figure 28 E-Defense Story Drifts: Kobe 50% Lumped Plasticity.**



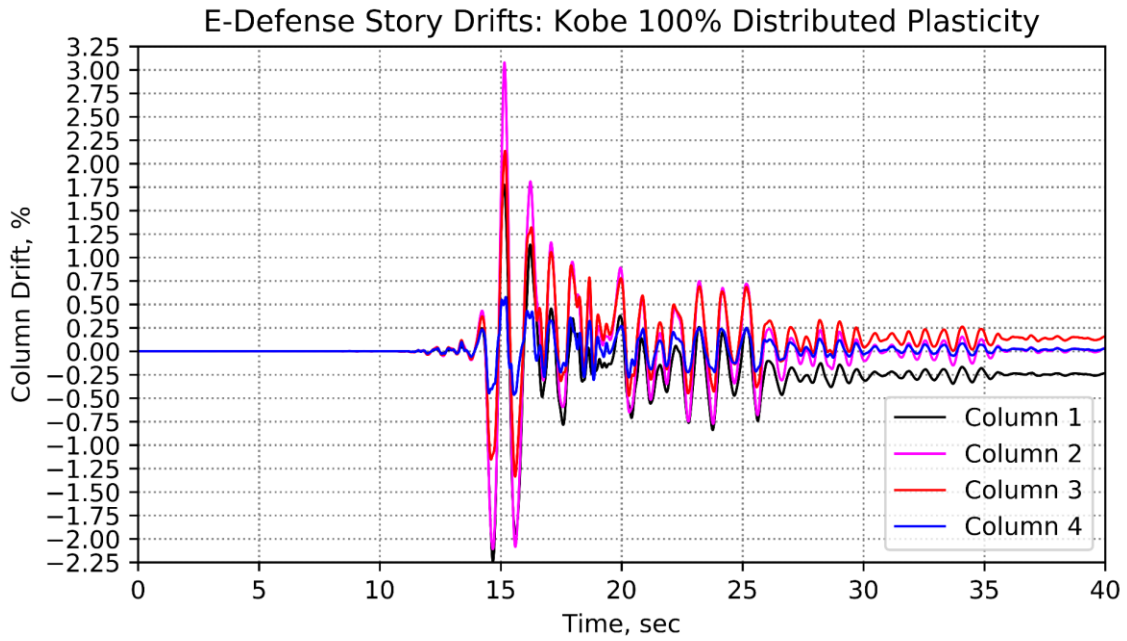
**Appendix Figure 29 E-Defense Floor Displacements: Kobe 50% Elastic.**



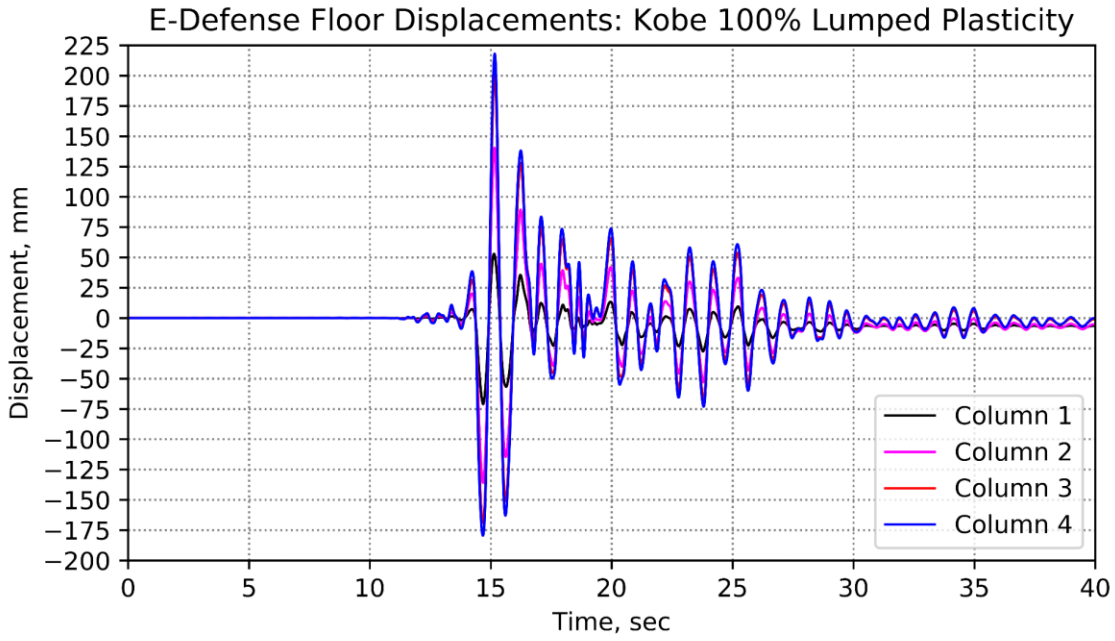
**Appendix Figure 30 E-Defense Story Drifts: Kobe 50% Elastic.**



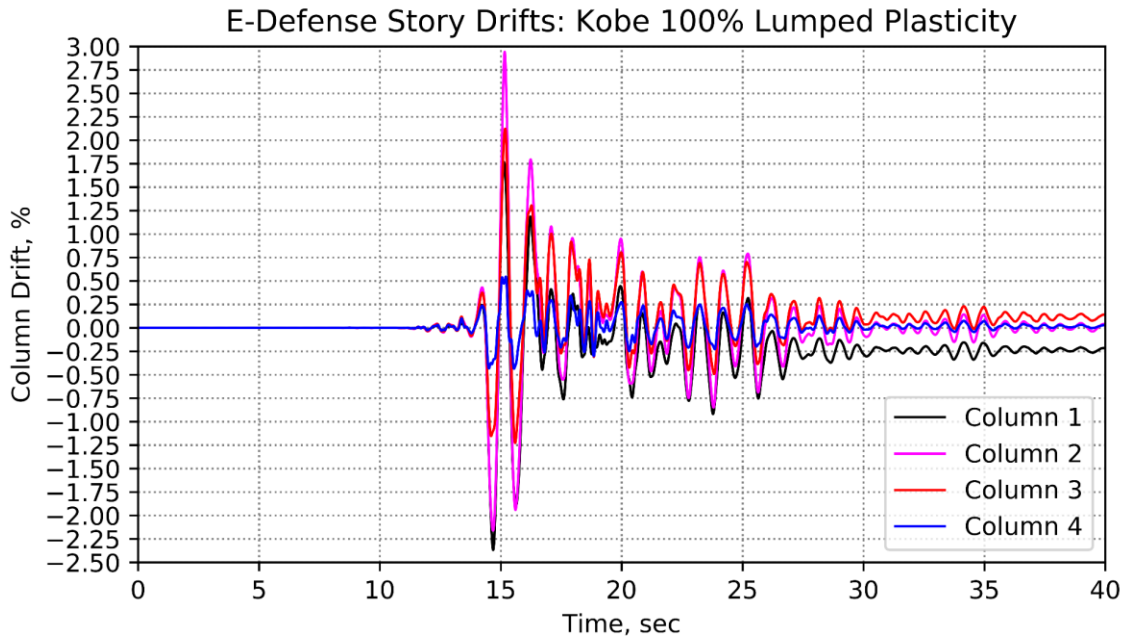
**Appendix Figure 31 E-Defense Floor Displacements: Kobe 100% Distributed Plasticity.**



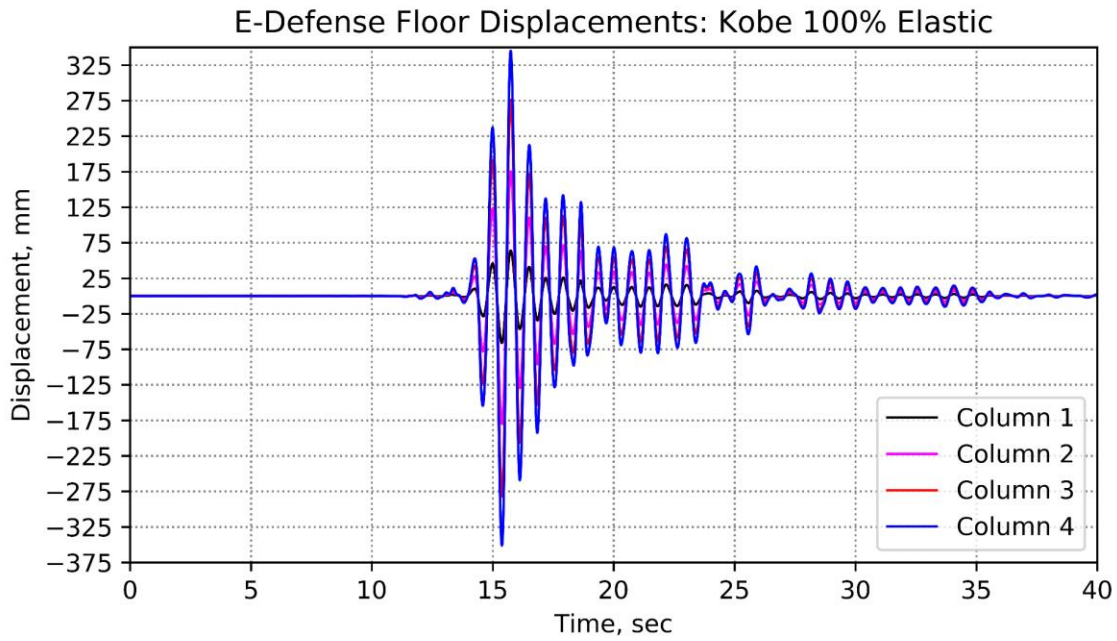
**Appendix Figure 32 E-Defense Story Drifts: Kobe 100% Distributed Plasticity.**



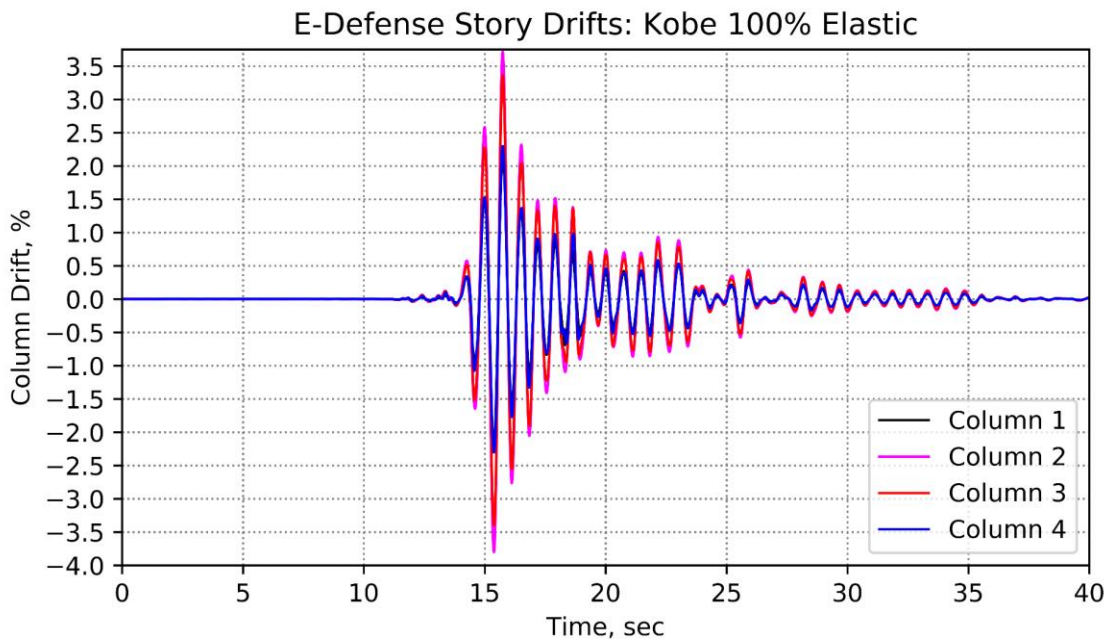
**Appendix Figure 33 E-Defense Floor Displacements: Kobe 100% Lumped Plasticity.**



**Appendix Figure 34 E-Defense Story Drifts: Kobe 100% Lumped Plasticity.**



**Appendix Figure 35 E-Defense Floor Displacements: Kobe 100% Elastic.**



**Appendix Figure 36 E-Defense Story Drifts: Kobe 100% Elastic.**

## Bibliography

- [1] “Estimated number of deaths from earthquakes,” *Our World in Data*. [Online]. Available: <https://ourworldindata.org/grapher/earthquake-deaths>. [Accessed: 21-Oct-2019].
- [2] “Hazus | FEMA.gov.” [Online]. Available: <https://www.fema.gov/hazus>. [Accessed: 01-Sep-2019].
- [3] “Hazus Earthquake Model | FEMA.gov.” [Online]. Available: <https://www.fema.gov/hazus-mh-earthquake-model>. [Accessed: 01-Sep-2019].
- [4] “Presentation: HAZUS-MH Used to Support San Francisco Bay Area Earthquake Exercise | FEMA.gov.” [Online]. Available: <https://www.fema.gov/media-library/assets/documents/19621>. [Accessed: 02-Sep-2019].
- [5] “Hazus® Estimated Annualized Earthquake Losses for the United States | FEMA.gov.” [Online]. Available: <https://www.fema.gov/media-library/assets/documents/132305>. [Accessed: 01-Sep-2019].
- [6] “Hazus User & Technical Manuals | FEMA.gov.” [Online]. Available: <https://www.fema.gov/media-library/assets/documents/24609>. [Accessed: 21-Oct-2019].
- [7] “Hazus Analysis Levels | FEMA.gov.” [Online]. Available: <https://www.fema.gov/hazus-mh-analysis-levels>. [Accessed: 01-Sep-2019].
- [8] “New Madrid Seismic Zone Catastrophic Earthquake Planning | FEMA.gov.” [Online]. Available: <https://www.fema.gov/news-release/2008/11/20/new-madrid-seismic-zone-catastrophic-earthquake-planning>. [Accessed: 02-Sep-2019].
- [9] “PAGER Scientific Background.” [Online]. Available: <https://earthquake.usgs.gov/data/pager/background.php>. [Accessed: 07-Sep-2019].
- [10] “USGS Fact Sheet 2010-3036, PAGER—Rapid Assessment of an Earthquake’s Impact.” [Online]. Available: <https://pubs.usgs.gov/fs/2010/3036/>. [Accessed: 07-Sep-2019].
- [11] “ShakeMap.” [Online]. Available: <https://earthquake.usgs.gov/data/shakemap/>. [Accessed: 07-Sep-2019].
- [12] “Did You Feel It?” [Online]. Available: <https://earthquake.usgs.gov/data/dyfi/>. [Accessed: 07-Sep-2019].
- [13] C. Yeh and C. Loh, *Haz-Taiwan: Earthquake Loss Estimation Methodology*.

- [14]A. King and R. Bell, *Modelling Tool*.
- [15]“About The Project | RiskScape.” [Online]. Available: <https://www.riskscape.org.nz/about-the-project>. [Accessed: 09-Sep-2019].
- [16]“Meshblock (Concept).” [Online]. Available: <http://datainfoplus.stats.govt.nz/Item/nz.govt.stats/011d668f-1fe2-4820-8957-837aae2bf575>. [Accessed: 09-Sep-2019].
- [17]F. McKenna, “OpenSees: A Framework for Earthquake Engineering Simulation,” *Comput. Sci. Eng.*, vol. 13, no. 4, pp. 58–66, Jul. 2011.
- [18]“OpenSeesWiki.” [Online]. Available: [http://opensees.berkeley.edu/wiki/index.php/Main\\_Page](http://opensees.berkeley.edu/wiki/index.php/Main_Page). [Accessed: 14-Sep-2019].
- [19]F. McKenna, “Introduction to OpenSees and Tcl,” p. 14.
- [20]C. del Vecchio, L. di Sarno, O.-S. Kwon, and A. Prota, “VALIDATION OF NUMERICAL MODELS FOR RC COLUMNS SUBJECTED TO CYCLIC LOAD,” in *Proceedings of the 4th International Conference on Computational Methods in Structural Dynamics and Earthquake Engineering (COMPADYN 2013)*, Kos Island, Greece, 2014, pp. 1958–1974.
- [21]M. P. Berry and M. O. Eberhard, “Performance Modeling Strategies for Modern Reinforced Concrete Bridge Columns,” p. 210.
- [22]“Wall Modelling with Beams.” .
- [23]V. Terzic, “Force-based Element vs. Displacement-based Element,” p. 25.
- [24]“Welcome to Python.org,” *Python.org*. [Online]. Available: <https://www.python.org/>. [Accessed: 28-Sep-2019].
- [25]“The OpenSeesPy Library — OpenSeesPy 0.4.2019.7 documentation.” [Online]. Available: <https://openseespydoc.readthedocs.io/en/latest/>. [Accessed: 28-Sep-2019].
- [26]“ASCE 7 | ASCE.” [Online]. Available: <https://www.asce.org/asce-7/>. [Accessed: 28-Sep-2019].
- [27] null null, *Minimum Design Loads for Buildings and Other Structures*, ASCE/SEI 7-10. American Society of Civil Engineers, 2013.
- [28]“Concrete01 Material -- Zero Tensile Strength.” [Online]. Available: <http://opensees.berkeley.edu/OpenSees/manuals/usermanual/164.htm>. [Accessed: 29-Sep-2019].

- [29]“Steel02 Material -- Giuffré-Menegotto-Pinto Model with Isotropic Strain Hardening - OpenSeesWiki.” [Online]. Available: [http://opensees.berkeley.edu/wiki/index.php/Steel02\\_Material\\_--\\_Giuffr%C3%A9-Menegotto-Pinto\\_Model\\_with\\_Isotropic\\_Strain\\_Hardening](http://opensees.berkeley.edu/wiki/index.php/Steel02_Material_--_Giuffr%C3%A9-Menegotto-Pinto_Model_with_Isotropic_Strain_Hardening). [Accessed: 29-Sep-2019].
- [30]“318-14: Building Code Requirements for Structural Concrete and Commentary.” [Online]. Available: <https://www.concrete.org/store/productdetail.aspx?ItemID=318U14&Language=English>. [Accessed: 28-Sep-2019].
- [31]D. C. Kent and R. Park, “FLEXURAL MEMBERS WITH CONFINED CONCRETE,” *J. Struct. Div.*, Jul. 1971.
- [32]“Effects of Bond Deterioration on Hysteretic Behavior of Reinforced Concrete Joints.” .
- [33]“Pushover Analysis of 2-Story Moment Frame - OpenSeesWiki.” [Online]. Available: [http://opensees.berkeley.edu/wiki/index.php/Pushover\\_Analysis\\_of\\_2-Story\\_Moment\\_Frame](http://opensees.berkeley.edu/wiki/index.php/Pushover_Analysis_of_2-Story_Moment_Frame). [Accessed: 28-Sep-2019].
- [34]“Newton Algorithm - OpenSeesWiki.” [Online]. Available: [http://opensees.berkeley.edu/wiki/index.php/Newton\\_Algorithm](http://opensees.berkeley.edu/wiki/index.php/Newton_Algorithm). [Accessed: 28-Sep-2019].
- [35]S. R. Uma and GNS Science (N.Z.), *Seismic instrumentation in BNZ building, Wellington*. Lower Hutt, N.Z.: GNS Science, 2010.
- [36]Y. R. Li and J. O. Jirsa, “Nonlinear Analyses of an Instrumented Structure Damaged in the 1994 Northridge Earthquake,” *Earthq. Spectra*, vol. 14, no. 2, pp. 265–283, May 1998.
- [37]J. Wallace, “U.S. Instrumentation and Data Processing for the 4-Story RC and Post-Tensioned E-Defense Building Tests (NEES-2011-1005),” 2017.
- [38]A. Puranam *et al.*, “A Snapshot of the Inventory of Medium to High-Rise Buildings in Wellington’s Central Business District,” *Bull. N. Z. Soc. Earthq. Eng.*, vol. Accepted for Publication.
- [39]FEMA, “Quantification of Building Seismic Performance Factors,” p. 421.
- [40]L. N. Lowes and J. Li, “Fragility Curves for Reinforced Concrete Moment Frames,” in *Improving the Seismic Performance of Existing Buildings and Other Structures*, San Francisco, California, United States, 2009, pp. 403–414.